Structure, Gating, and Regulation of the CFTR Anion Channel

László Csanády[1,2,*], Paola Vergani[3], David C. Gadsby[4]

[1]Semmelweis University, Department of Medical Biochemistry, Budapest, Hungary

[2]MTA-SE Ion Channel Research Group, Budapest, Hungary

[3]Department of Neuroscience, Physiology and Pharmacology, University College London, London, UK

[4]Laboratory of Cardiac/Membrane Physiology, The Rockefeller University, New York, NY,USA

*Correspondance:

László Csanády

E-mail: csanady.laszlo@med.semmelweis-univ.hu

Competing interests statement: no competing interests.

Table of Contents

Abstract

The Cystic Fibrosis Transmembrane Conductance Regulator (CFTR) belongs to the ATP Binding Cassette (ABC) transporter superfamily but functions as an anion channel crucial for salt- and water transport across epithelial cells. CFTR dysfunction, due to mutations, causes cystic fibrosis (CF). The anion-selective pore of the CFTR protein is formed by its two transmembrane domains (TMDs) and regulated by its cytosolic domains: two nucleotide binding domains (NBDs) and a regulatory (R) domain. Channel activation requires phosphorylation of the R domain by cyclic AMP-dependent protein kinase (PKA), and pore opening and closing (gating) of phosphorylated channels is driven by ATP binding and hydrolysis at the NBDs. This review summarizes available information on structure and mechanism of the CFTR protein, with a particular focus on atomic-level insight gained from recent cryo-electronmicroscopic structures, and on the molecular mechanisms of channel gating and its regulation. The pharmacological mechanisms of small molecules targeting CFTR's ion channel function, aimed at treating patients suffering from CF and other diseases, are briefly discussed.

I. Introduction

A. CFTR and cystic fibrosis

Cystic fibrosis (CF) is the most common life threatening inherited monogenic disorder among Caucasian populations: it affects one in ~2500 newborns in Europe, and one in ~3500 newborns in the United States. CF is a multiorgan disorder, with symptoms including airway blockage by thickened mucus leading to chronic lung infections, inflammation and bronchiectasis, blockage of pancreatic ducts and consequent pancreatic insufficiency, bowel obstruction in newborns, male infertility due to obstruction of the vas deferens, and a characteristic high-salt sweat, diagnostic of the disease. Although at present efficient causative treatment is still restricted to a small subset of CF patients, in the past decades improvements in patient care and symptomatic treatment have greatly prolonged the life expectancy of people born with CF, from ~1 year in 1950 to ~40 years at present (171).

The primary defect in CF patients is a reduction in chloride (190, 259) and bicarbonate (208) transport capacity across the apical membrane of epithelial cells. In 1989 the gene mutated in CF patients was identified on chromosome 7 by positional cloning (201), and the protein product was named the Cystic Fibrosis Transmembrane Conductance Regulator (CFTR), to reflect its presumed involvement in the regulation of other anion transport proteins. Purification of the CFTR protein and its functional reconstitution in lipid bilayers soon provided proof that CFTR is itself the anion channel responsible for cyclic AMP-dependent anion transport across epithelial surfaces (16).

B. The ATP Binding Cassette protein superfamily

CFTR is a member of the large superfamily of tens of thousands of ATP Binding Cassette (ABC) proteins that are found in all kingdoms of life (147), and that serve to transport a large variety of substrates into and out of cells at the expense of ATP hydrolysis. ABC proteins share a conserved general architecture, based on the modular assembly of four canonical domains: two transmembrane domains (TMDs) and two cytosolic nucleotide binding domains (NBDs). The number of polypeptide chains that this "core" functional unit comprises is variable. In prokaryotes the four domains are often expressed as four individual polypeptides, or as two TMD-NBD "halftransporters" that coassemble

posttranslationally. The human genome encodes 48 ABC proteins which have been grouped into seven subfamilies (ABCA through ABCG) (69). Except for the E and F subfamilies, which contain no TMDs, the human ABC proteins consist either of halftransporters that homo- or heterodimerize, or of full transporters in which the four canonical domains are linked in a single polypeptide chain. The ABCC subfamily to which CFTR (ABCC7) belongs falls into the latter class. In CFTR each TMD contains six transmembrane (TM) helices, and the two homologous TMD-NBD halves (TMD1-NBD1 and TMD2-NBD2) are linked by a contiguous, unique, cytosolic regulatory (R) domain (201) (Fig. 1A). At the sequence level CFTR's two homologous halves display a marked asymmetry, a general feature of ABCC subfamily proteins (187). Within the entire ABC superfamily CFTR is the only protein shown to form a transmembrane ion channel pore, in contrast to the vast majority of its homologs that serve as active transporters. The only other exceptions among human ABC proteins are the soluble E and F subfamily members that are not involved in transmembrane transport, and CFTR's close relatives SUR1 (ABCC8) and SUR2 (ABCC9) that serve as regulatory subunits of ATP-sensitive potassium channels (69).

C. Basic functional properties of the CFTR anion channel

Opening and closing (gating) of the CFTR anion pore is largely regulated by two processes. First, for a CFTR channel to become activated, its cytosolic R domain must be phosphorylated by cyclic AMP dependent protein kinase (PKA) (20, 48, 183, 225). Second, gating of a phosphorylated CFTR channel is driven by binding of ATP to its cytosolic NBDs (9). In single-channel recordings CFTR channel activity displays typical bursting behaviour, with brief ("intraburst") closures interrupting longer periods of channel opening, yielding open bursts that are separated by long ("interburst") closures (32, 95, 261). Gating kinetics are relatively slow, the duration of a burst+interburst cycle is on a seconds timescale (0.1-2 seconds, depending on species, phosphorylation level, and temperature) rather than the milliseconds timescale of voltage-gated channels. Moreover, except for the kinetics of intraburst closures which little affect channel open probability (30), CFTR gating is largely voltage-independent (20). Anion permeation through the open pore follows simple ohmic behaviour: in symmetrical 140 mM chloride the unitary current-voltage relationship is relatively

linear (20); cf., (30)), with a slope conductance of ~10 pS at 35-37^{o}C (20), or ~7-8 pS at 20-25^{o}C (227). These basic biophysical properties serve as a fingerprint which allows reliable identification of CFTR currents both in native tissues and in heterologous expression systems.

D. Root cause of CF disease symptoms

To date more than 2000 CFTR mutations have been identified in CF patients (http://www.genet.sickkids.on.ca), a remarkable number for a 1480-residue protein, although a subset of these variations is likely to have no functional consequence. The roughly 200 mutations that are known to cause CF are traditionally classified (68, 282) based on how they affect the encoded protein: that is, whether they abolish or reduce the production of the full-length CFTR polypeptide (truncation mutations, Class I; alternative splicing, Class V), impair protein trafficking/maturation (Class II), impair regulation of channel gating (Class III), or anion permeation through the open channel pore (Class IV), or affect the lifetime of the channel protein in the apical membrane (Class VI). Despite the large number of identified CFTR mutations, a single mutation, deletion of phenylalanine 508, is responsible for the majority of CF cases worldwide. The ΔF508 allele represents ~70% of all CF-associated alleles; thus, given the recessive inheritance of the disease, >90% of CF patients carry at least one ΔF508 allele. The ΔF508 mutation belongs to several classes. Due to a severe folding defect, resulting in degradation of most of the protein translated at the endoplasmic reticulum (Class II) (42, 148), coupled with thermal instability and an increased rate of degradation once at the plasma membrane (Class VI) (173, 251), the amount of mature, fully glycosylated ΔF508 CFTR protein in the plasma membrane is estimated to be only ~2% of that of WT (239). In addition, the small amount of ΔF508 CFTR present in the plasma membrane is phosphorylated by PKA at a diminished rate (246), and even fully phosphorylated channels display a severe gating defect (Class III) characterized by a >40-fold reduction in channel open probability, due to a lower rate of pore opening (66, 125, 161).

A reduction of CFTR anion permeability is undoubtedly one of the root causes of abnormal lung secretions that lead to the ultimately lethal CF lung symptoms. However, CF airway epithelia also show enhanced amiloride-sensitive transepithelial potentials and short-circuit currents (28, 121, 122). Loss of an inhibitory effect of WT CFTR on the amiloride-sensitive epithelial Na^{+} channel (ENaC),

and consequent ENaC overactivation, was thought to underlie this observation, and increased Na^+ absorption together with the loss of Cl^- secretion was suggested to cause dehydration of the airway surface liquid, impairing mucociliary clearance and increasing susceptibility to infection (27). Although initial electrophysiological studies coexpressing CFTR and ENaC in *Xenopus* oocytes, did not detect any inhibitory effect of CFTR on ENaC (165), studies in more native systems do support this hypothesis. In primary nasal epithelia, a Na^+-permeant channel had a higher open probability in cells obtained from CF patients than in those from normal individuals (44). Biochemical studies demonstrated that WT CFTR could protect ENaC from protease-dependent activation in airway epithelial cells, but ΔF508-CFTR failed to do so (89, 128). This consistent picture was questioned, however, when CF pigs (both -/- and homozygous ΔF508) were developed by the Welsh lab. These, like humans, developed lung disease and showed increased susceptibility to bacterial infection when newborn. A reduced pH of the airway surface liquid was found to be crucial in developing the disease (181) (see section III.C), but increased Na^+ absorbtion was not detected (39, 110), suggesting that amiloride-sensitive changes in epithelial properties might be secondary to reduced apical Cl^- permeability. However, using a biophysical model of transepithelial ion fluxes, alterations in bioelectric properties of CF epithelia were found to be too large to be accounted for by electrical coupling alone (170). Thus, a more complex interpretation of CF pathogenesis might be required before decades of controversy can be finally laid to rest.

II. CFTR domain topology and structure

A. Domain boundaries

Cloning of the CFTR sequence revealed its domain organization (Fig. 1A) and allowed a rough prediction of transmembrane topology and domain boundaries (201). That suggested topology has stood the test of time, except for some small adjustments of helical boundaries (e.g., (86, 255)). However, the originally predicted N- and C-termini of NBD1 and 2 turned out to be quite inaccurate. Exploiting ABC transporter modular architecture, co-expression of complementary CFTR segments was used to provide a functional definition of NBD1 boundaries (33): this approach extended the NBD1 C-terminus from amino acid position (a.a.) 586 to 633, but left its N-terminus uncorrected. The crystal structure of mouse CFTR NBD1 (130) finally assigned correct NBD1 N- and C-terminal boundaries to ~a.a. 390 and ~670, respectively, although residues distal from ~a.a. 645 form a helix that is not conserved among ABC proteins and contains two consensus serines (S660, S670) phosphorylated by PKA, suggesting that it might be considered part of the R domain. For NBD2 the crystal structure of a fusion protein of human CFTR NBD2 with the Regulatory domain of *E. coli* MalK (3GD7) allowed adjustment of NBD2 N- and C-terminal boundaries to a.a. 1208 and ~1427, respectively, largely confirmed (1207-1436) by the first atomic structure of full-length human CFTR (145). Given that much of the R domain of CFTR is unstructured (145, 177), its exact N- and C-terminal boundaries are still uncertain and might be assigned to ~ a.a. 645(670?) and ~845, respectively, largely based on the boundaries of its bracketing domains (NBD1 and TMD2; see Fig. 1A), as well as on the locations of consensus sites for PKA phosphorylation.

B. The ATP Binding Cassettes

NBD1 and NBD2 are CFTR's ATP Binding Cassettes, the highly conserved (both at a sequence and 3-D structure level) ATPase subunits characteristic of ABC proteins (Fig. 1B). ABC NBD structures consist of two subdomains. The nucleotide binding core subdomain (the "head") comprises an F1-like parallel β sheet (Fig. 1B, *light green*) which is stabilized by α helices (Fig. 1B, *dark green*) and contains the conserved Walker A (consensus GXXXXGKS/T; Fig. 1B, *red*) and B (consensus

ΦΦΦΦDE, Φ hydrophobic; Fig. 1B, *marine*) motifs important for MgATP binding (245), and is completed by an ABC-specific three-stranded antiparallel β sheet (Fig. 1B, *cyan*). The two β sheets surround a central α helix preceded by the P loop, which is formed by residues of the Walker A motif (Fig. 1B, *dark green helix and red loop*). The NBD α-helical subdomain (the "tail"; Fig. 1B, *orange*) contains the highly conserved ABC-specific "signature sequence" (consensus LSGGQ; Fig. 1B, *magenta*). In nucleotide-bound high-resolution NBD structures the P-loop is seen to coordinate the phosphate chain, with the conserved Walker-A lysine (K464 and K1250 in CFTR; Fig. 1B, *red sticks*) playing a dominant role by coordinating all three phosphates of ATP. The antiparallel β sheet provides a conserved aromatic residue which stacks against the adenine base of the bound nucleotide (W401 and Y1219 in CFTR; Fig. 1B, *blue sticks*). The Walker B motif ends in a conserved aspartate (D572 and D1370 in CFTR; Fig. 1B, *marine sticks*) important for Mg^{2+} coordination, and is followed by a conserved glutamate (E1371 in NBD2 of CFTR; Fig. 1B, *salmon sticks*) which acts as the general base that polarizes the attacking water molecule during the ATP hydrolysis reaction (162, 174, 175). A conserved glutamine (Q493 and Q1291 in CFTR; Fig. 1B; *orange sticks*) in the loop which links the head and tail subdomains (the "Q loop") acts as the γ-phosphate sensor and plays a key role in an induced fit conformational change elicited by ATP binding: an ~15^{o} rotation of the tail subdomain towards the core subdomain in ATP- compared to ADP-bound, or apo, structures (115, 268). These key catalytic residues are held together by the conserved "switch histidine" (H1402 in NBD2 of CFTR; Fig. 1B, *light magenta sticks*), also called the "linchpin" (174, 269). In CFTR there is substantial asymmetry between NBD1 and NBD2 regarding the key consensus motifs. In NBD1 the post-Walker B glutamate and the switch histidine are replaced by serines (S573 and S605, respectively), whereas in NBD2 the signature sequence is atypical (LSHGH). In addition, CFTR's NBD1 contains two unique sequence segments (130): an ~30-residue unstructured segment (aa. 406-436) inserted into the antiparallel β-sheet (regulatory insertion; RI), and an ~30-residue helical extension (aa. 641-670; regulatory extension; RE). Both segments contain consensus serines phosphorylated by PKA (S422 and S660, S670, respectively), and both are unstructured in full-length CFTR (Fig. 1B; *light magenta dotted lines*).

In the presence of ATP, but under conditions that preclude ATP hydrolysis, isolated ABC NBDs form head-to-tail dimers that occlude two molecules of ATP at the dimer interfaces. Such NBD dimerization can be observed both for isolated soluble NBD domains (e.g., (38, 215, 269)), or in the context of full-length ABC proteins (e.g., (46, 67, 256)) including CFTR ((99, 159, 207, 274); Fig. 1C). In both composite nucleotide binding sites, an ATP is sandwiched between the Walker motifs of one NBD (Fig. 1C, Walker A, *red*) and the signature sequence of the other NBD (Fig. 1C, *magenta*). This arrangement explains the crucial role the signature sequence plays in catalysis, despite its distance from the bound nucleotide within an NBD monomer (Fig. 1B). Furthermore, in CFTR the head-to-tail arrangement of the NBD dimer collects all non-canonical substitutions into a single composite binding site, formed by the head of NBD1 and the tail of NBD2 ("site 1"; Fig. 1D, *upper site*): in this "degenerate" site the catalytic glutamate and the switch histidine are ablated by mutation, and the signature sequence is aberrant. In contrast, in the composite binding site formed by the head of NBD2 and the tail of NBD1 ("site 2"; Fig. 1D, *lower site*) all key residues are canonical. A similar asymmetrical distribution of consensus vs. atypical residues is found throughout the entire ABCC subfamily, as well as in many other prokaryotic and eukaryotic heterodimeric ABC proteins (101, 187).

C. Structural organization of full-length CFTR

The overall 3-dimensional arrangement of full-length CFTR was resolved in a series of recent atomic resolution structures obtained by cryo-electron microscopy (cryo-EM), two from zebrafish CFTR (273, 274) and one from the human protein (145). Although at present no functional information is available on zebrafish CFTR, which is only ~55% identical in sequence to the human protein, the structures of the two orthologs in their dephosphorylated apo-states are virtually identical (root-mean-square deviation ~1.9Å across the entire protein), suggesting that structural information obtained from the zebrafish ortholog is largely relevant to the human protein.

The global arrangement of the CFTR protein (Fig. 1E-F), resembles that of other ABC exporters (46, 67, 212, 256), as had been predicted by extensive crosslinking studies (99, 159, 207). The membrane spanning components are formed by the twelve transmembrane helices, six from TMD1 (Fig. 1E-F, *light gray*) and six from TMD2 (Fig. 1E-F, *dark gray*), which also extend deep into the

cytosol. TMD-NBD interactions occur via four short "coupling helices" (CH1-4; Fig. 1E-F, *magenta*) formed by intracellular loops 1 (CH1, aa. 168-174) and 2 (CH2, aa. 269-275) of TMD1, and the analogous intracellular loops 3 (CH3, aa. 961-966) and 4 (CH4, aa. 1062-1068) of TMD2. As for other ABC exporters, TMD1 and TMD2 do not form distinct, separate bundles of transmembrane helices but are closely intertwined, with each other as well as with the NBDs. In particular, a unit formed by TM4-CH2-TM5 reaches out from TMD1 and contacts NBD2, and in a similar fashion, TM10-CH4-TM11 extends from TMD2 towards NBD1 (“domain swap”, (67)). Thus the full length CFTR molecule can be seen to be formed by two structural halves (TM helices 1, 2, 3, 6 + 10, 11 with NBD1 and TM helices 7, 8, 9, 12 + 4, 5 with NBD2 (274), Fig. 1E). The coupling helices run roughly parallel with the plane of the membrane and fit into corresponding clefts on the NBD surfaces, forming ball-and-socket-like joints that are the transmission interfaces for communications between the NBDs and the TMDs. Due to deletion of a short helix from NBD1, the "socket" on the NBD1 surface that accepts CH4 is shallower than the NBD2-socket that accepts CH2 (compare sockets in Fig. 1B), rendering the NBD1-CH4 interface more sensitive to deleterious effects of mutations. This explains the severe structural destabilization caused by deletion (or mutations) of phenylalanine 508 (Fig. 1B, NBD1, *purple sticks*), which contributes a hydrophobic side chain to formation of the shallow NBD1 socket (273).

Experimentally observed conformations of ABC proteins fall into two major classes. First, in most structures solved in the absence of nucleotide (apo-structures) the TMDs adopt an inward-facing conformation in which the extracellular ends of the TM helices are tightly bundled whereas their cytosolic extensions, including the coupling helices, are spread apart, and the NBDs are separated (8, 101, 212, 256). Among the many solved inward-facing structures of ABC proteins the observed degree of separation between NBD interfaces is highly variable. In the structure of dephosphorylated apo-CFTR (both zebrafish (273) and human (145)) the NBD interface separation is relatively large (>17Å; Fig. 1E). Second, in nucleotide-bound ABC exporter structures solved under conditions that preclude ATP hydrolysis, the TMDs typically adopt an outward-facing orientation in which the cytosolic ends of the TM helices are tightly bundled, the coupling helices approach each other, and the NBDs are tightly dimerized. In such structures a variable degree of separation is observed between the extracellular ends of the TM helices, ranging from widely splayed extracellular loops (67, 256) to more compact bundling

(46). The structure of phosphorylated, ATP-bound zebrafish CFTR is in an outward-facing conformation (274) resembling the latter, tighter extracellular bundling arrangement, with the TM helices largely parallel to each other (Fig. 1F; see also (52)).

In addition to these – mostly expected – general ABC protein characteristics, the recent CFTR structures revealed several unpredicted features. The N-terminal ~60 residues, conserved throughout the ABCC subfamily, and unique to it, form a "lasso motif" (Fig. 1E-F, *red*). The lasso contains two α-helices, the first of which is partly inserted in the membrane, packed against TMD2. The second, amphipathic, helix which runs parallel to the membrane and exposes a highly charged surface to the aqueous environment has been implicated in both channel trafficking and gating regulation (166, 167). Further unique features of CFTR's TMDs are likely essential for its ion channel function. The pseudosymmetry of the TM helices is disrupted by a discontinuity of TM helix 8 (TM8 (51)), which makes two sharp breaks within the membrane (Fig. 1F, *right*; TM8 external segment and helical breaks are highlighted in *cyan*), thereby displacing TM7 from its ABC-typical location (Fig. 1F, *right, pale green*). As a consequence, the central ion pore is mostly lined by TM1 and 6 of TMD1, but by TM8 and 12 of TMD2, consistent with earlier accessibility studies (12, 85, 88, 188, 254, 255, 271). In ABC transporters, access to the substrate translocation pathway is gated at both ends: the external gate is open in the outward-facing TMD conformation, whereas the internal gate opens in the inward-facing state. In contrast, in the CFTR channel the open pore provides a continuous aqueous transmembrane pathway permeable to anions. Given that the open CFTR pore corresponds to an outward-facing TMD conformation, an aqueous pathway must exist that bypasses the closed internal ABC transporter gate. Consistent with results of functional (76, 77) and modeling (52, 163) studies, in the corresponding CFTR structure (274) that pathway is formed by a lateral opening (Fig. 1F, *red arrow*) between TM4 (Fig. 1F, *yellow*) and 6 (Fig. 1F, *orange*) that connects the cytosolic environment with the internal vestibule of the pore.

D. Structural information on the Regulatory domain

The entirely unique amino acid sequence of the R domain is a consequence of its evolutionary origin from an intronic DNA sequence (205). Although early CD spectra of an R-domain peptide,

based on the originally suggested domain boundaries (a.a. 595-831), reported some α-helical content, to a degree influenced by phosphorylation, and identified an N-terminal "subdomain" with high sequence conservation among CFTR orthologs (residues 587-672) (72), the latter segment in fact largely belongs to NBD1. In contrast, CD spectra of an R-domain peptide encompassing a.a. 708-831 predicted this domain to be largely unstructured (177), consistent with its origin from non-coding sequence. Nevertheless, biochemical pull-down assays and NMR studies with isolated peptides suggested that the R-domain interacts with other parts of the channel in a phosphorylation-dependent manner (29, 36, 249). In the dephosphorylated closed apo-structures of both zebrafish (273) and human (145) CFTR a large amorphous density corresponding to the R domain is seen wedged between the two CFTR halves, interacting with NBD1 and the cytosolic ends of the TM helices; in the dephosphorylated human structure a part of the density which interacts with the TM helices can be modeled as an α-helix (Fig. 1E, *yellow surface plot*) and likely corresponds to the C-terminal end of the R-domain (aa. 825-843). Such an intercalated arrangement of the dephosphorylated R domain is sterically incompatible with NBD dimerization or with an outward-facing conformation of the TMDs: correspondingly, in the phosphorylated ATP-bound outward-facing zebrafish CFTR structure ((274); Fig. 1F) no density corresponding to the R domain is observed, indicating that this region does not adopt a common conformation in most of the analyzed particles, but instead becomes disordered.

III. The CFTR anion permeation pathway

A. Structural segments lining the pore

Long before the availability of high-resolution structural information, several of CFTR's helices had been probed for their contributions to the ion permeation pathway by use of the substituted cysteine accessibility method (SCAM). Such studies identified TM helices 1 (85, 88, 254), 5 (271), 6 (11, 75, 88), 11 (78, 255), and 12 (17, 78, 188) as pore lining. The accessibility patterns were generally consistent with helical structures, with each 3rd-to-4th substituted residue being accessible from the ion permeation pathway; and the patterns even predicted some symmetry break by suggesting that TM7 does not participate in forming the pore (255, 271). A lateral portal serving as the cytosolic entrance of

the pore vestibule, between the cytosolic extensions of TM4 and 6, was hypothesized (52, 163) and later experimentally confirmed. It is lined by a number of positively charged amino acid side chains which play a role in attracting cytoplasmic chloride ions to the inner mouth of the pore ((76, 77); some of the corresponding residues in zebrafish CFTR are highlighted as *blue spheres* in Fig. 1F, *right*). Except for the unanticipated helical break observed in TM8 (Fig. 1F *right*, *cyan*), the recent cryo-EM structures largely confirmed the predictions of these functional studies and revealed that the entire inner surface of the pore is lined by positively charged residues, as expected for an anion channel (273).

B. Location of the channel gate

A deep and wide intracellular (12, 141, 211, 221, 279), and a shallower extracellular (169, 218), vestibule predicted from the voltage dependence of pore block by various large organic anions suggested an asymmetric hour-glass shape for the CFTR pore. This shape positioned the gate, corresponding to a narrow constriction in the permeation pathway (with a functional diameter of ~5.3A (106, 144) in the open conformation), close to the extracellular membrane surface, at the level of TM6 residues 338-341 (63, 75, 87). Consistent with a gate located at the extracellular end of the pore, binding of large organic anion pore blockers (59) or ATP (219) in the intracellular vestibule does not prevent gate closure. In the inward-facing structures of zebrafish (273) and human ((145); Fig. 1E) CFTR the funnel-shaped intracellular vestibule indeed tapers down to a narrow tunnel at the predicted location of the gate, consistent with those structures representing closed CFTR channels. Interestingly however, in the outward-facing structure of phosphoryated ATP-bound zebrafish CFTR (274), although this gate constriction between TM6, TM1 and TM11 widens as expected, access to the pore from the extracellular space is nevertheless prevented by the extracellular segments of TM helices 8 and 12 (Fig. 1F, right, *cyan* and *dark cyan*); this results from a local reorientation of these two secondary structure elements with respect to the rest of the half-molecule. A structure of the CFTR pore in its fully conductive conformation remains to be captured.

C. Mechanism of anion selectivity

The CFTR pore shows high anion vs. cation selectivity (the relative permeability of Na^+ compared to Cl^-, p_{Na}/p_{Cl}, is ~0.03; (226)), but poorly selects among anions. Experimentally obtained anion *permeability* sequences (which report relative ease of ion entry into the pore) are consistent with a lyotropic selection mechanism: relative permeability of a given anion is inversely proportional to its energy of dehydration (140, 157, 216). For instance, compared to chloride, large anions like SCN^- and nitrate, which more easily shed their hydration shell, display higher permeability through CFTR (e.g., $p_{SCN}/p_{Cl}>2.4$; (140, 157)). On the other hand, these high permeability large anions also typically bind very tightly within the pore, resulting in a low throughput rate, operationally defined by measuring relative *conductance* (e.g., the relative conductance for SCN^- compared to Cl^-, g_{SCN}/g_{Cl}, is <0.2; (135, 157)). Thus, evolution seems to have optimized the CFTR pore to provide maximal conductance for the physiologically most relevant anion, chloride (135). Besides chloride, the other physiologically relevant ion permeant through CFTR is bicarbonate. CFTR's relative permeability (p_{HCO3-}/p_{Cl-}) and relative conductance (g_{HCO3-}/g_{Cl-}) for bicarbonate are both ~0.25 (144, 184). Low permeability ratios were initially found also in isolated pancreatic ducts (91), and CFTR's role in bicarbonate secretion was thought to be indirect, mediated by regulation of Cl^-/HCO_3^- exchangers of the SLC26A family (reviewed in (129)). However, several studies have raised the possibility that direct HCO_3^- permeation through CFTR might become important, especially in some physiological conditions (108), and that CFTR anion permeability might be dynamically regulated (178, 198). Regardless of the exact mechanism, CFTR-dependent bicarbonate secretion clearly plays an important physiological role in controlling the pH of the fluid layers that line various epithelial surfaces (189, 202), including the lung (181, 210), as demonstrated by the correlations seen between levels of CFTR, bicarbonate fluxes and strength of lung host defence defects (209).

The region responsible for CFTR's lyotropic selectivity, i.e. the region that provides sites of interaction for permeating anions, corresponds to the narrow region of the pore, as evidenced by changes in anion selectivity sequences upon mutation of residues F337, T338, S341, S1118, or T1134 (90, 135, 140, 157, 158, 275). In addition, the large number of positively charged residues that line the entire internal surface of the pore (in particular residue K95 in the internal vestibule; (137, 139)), or

flank the cytoplasmic lateral opening ((76, 77); cf., Fig. 1F, right, *blue spheres*), contribute to enhancing chloride conductance by attracting chloride ions to the pore (139). Thus, it has been suggested that the anion selectivity characteristics of CFTR might result from at least two distinct "selectivity filters" operating in series; interactions between permeant anions and the pore constriction around F337 being largely responsible for determining the selectivity of permeability, while anion-pore interactions in the inner vestibule and around the entrance of the lateral portal determine anion over cation selectivity and boost anion conductance (139). Some evidence suggests that overall high conductance and tight pore binding of CFTR might result from simultaneous, multiple interactions of permeating anions along the permeation pathway (138). Channel pores with multiple ion binding sites often show a non-linear dependence of unitary conductance on the mole fractions of two types of permeant ion that are simultaneously present. In the case of CFTR such "anomalous mole fraction behavior" has been reported for the anion pairs Cl^-/SCN^- (136, 139) and Cl^-/SO_4^{2-} (60).

By stabilizing the open-pore structure, anion-pore interactions contribute to the energetic stability, and therefore the life time, of the open-channel state. Thus, anion replacement affects not only permeation properties, but also the kinetics of gating transitions: nitrate and bromide, which bind more tightly than chloride, delay, whereas formate, which binds less tightly than chloride, accelerates, pore closure (219, 266). These effects of tight-binding permeating ions to retard the closing of the CFTR gate might be analogous to the influence exerted by a substrate bound to an outward-facing exporter: extracellular release of the substrate favours closing of the extracellular gate, and thus restoration of the inward-facing conformation (see Section IV. G) [see also (266)].

D. Pore blockers

Many large organic anions block the CFTR pore when applied from the intracellular side. The resulting brief closed events ("flickery block") reflect the brief residence time of the blocker at its binding site in the pore. Pore block is more pronounced at hyperpolarized (more negative) membrane potentials that drive the negatively charged blocker into the intracellular pore vestibule, but is alleviated at depolarized (more positive) membrane potentials. The steepness of this voltage dependence allows estimation of how deep the blocker binding site is, i.e., what fraction (θ) of the

membrane electrical field the blocker traverses before reaching its binding site. Similar voltage dependences suggest a common binding site for a structurally diverse group of blockers including diphenylamine-2-carboxylate (DPC), flufenamic acid (FFA) (θ~0.41 for both, (156)), glibenclamide (θ~0.45-0.48, (211, 279)), 5-nitro-2-(3-phenylpropylamino)benzoate (NPPB) (θ~0.5, (59)), 3-(N-morpholino)propanesulfonic acid (MOPS) (θ~0.5, (59, 109)), and anthracene-9-carboxylic acid (9-AC) (θ~0.5, (1)). In line with the notion of a common binding site, glibenclamide and isethionate (279), or NPPB and MOPS (60), were shown to compete for pore block. Mutagenesis studies highlighted how the positively charged side chain of the pore-lining residue K95 plays an important role in interacting not only with permeant anions, but also with blockers (137). In the atomic structure of human CFTR, K95 is located at a position where the intracellular vestibule tapers down to the narrow tunnel believed to comprise the gate (145). Of note, an intrahelical salt bridge between the side chains of K95 and E92 was recently noted in the cryo-EM structure of human CFTR and proposed to play a role in anion-pore and blocker-pore interactions (104). Consistent with the binding site for diverse blockers being located intracellular to the channel gate, the presence of NPPB or MOPS in the pore does not delay gate closure (59). More modest voltage dependences reported for block by the disulphonic stilbenes 4,4' diisothiocyanostilbene-2,2'-disulphonic acid (DIDS) and 4,4'-dinitrostilbene-2,2'-disulphonic acid (DNDS) (θ~0.16 and θ~0.34, respectively, (141)) suggest that a more superficial blocker binding site might also exist.

Whereas the above compounds block from the cytosolic side and show low affinity for the CFTR pore (K_d in the hundreds-of-micromolar to millimolar range at 0 mV membrane potential), high-throughput screening has led to the discovery of a higher-affinity pore blocker that acts from the extracellular side: N-(2-naphthalenyl)-[(3,5-dibromo-2,4-dihydroxyphenyl)methylene]glycine hydrazide (GlyH-101) blocks CFTR currents with a K_d of ~4 μM at 0 mV membrane potential, and shows the inverse voltage dependence expected for an anionic blocker that binds in the extracellular vestibule (164). The electrical distance of the GlyH-101 binding site (θ=0.35), and strong reductions in apparent affinity by mutation R334C (62), or upon covalent modification of a cysteine engineered into position 338 (169), suggest that GlyH-101 binds at the bottom of the shallow extracellular vestibule, just above the constriction that forms the channel gate (169).

E. Intraburst ("flickery") closures

Under all experimental conditions, gating of single CFTR channels shows clear bursting behavior: groups of open events interrupted by brief (~1-3 ms at 37^{o}C, ~10 ms at 25^{o}C) "flickery" closed events form "bursts" which are separated from each other by long (~0.1-0.2 s at 37^{o}C, ~0.4-2 s at 25^{o}C) "interburst" closed events. Some of the brief intraburst closures represent block by large cytosolic anions (278) or by anionic buffer molecules present in the recording solution that bathes the cytosolic membrane surface (109); indeed, even cytosolic ATP causes low-affinity pore block (219). But not all intraburst closures may be accounted for by such a mechanism, because flickery closures can be observed for locked-open channels long after ATP has been washed away, even in a cytosolic solution buffered with a cationic buffer (279), and also when channel currents are studied at positive voltages (243), which deter cytosolic anion entry. Thus, at least a fraction of the observed flickery closures must represent a gating mechanism intrinsic to the channel protein.

Several studies have addressed the dependence of intraburst gating kinetics on a variety of factors, including voltage, pH, or the concentration of ATP used for channel activation. Both the frequency and the duration of flickery closures increases at positive membrane potentials, reporting a weak voltage dependence of intraburst gating (30). Acidification of the bath solution to pH=6.3 prolongs the average duration of flickers by ~2-fold (40). In contrast, neither the frequency nor the duration of intraburst closures is sensitive to the concentration of applied ATP (243, 261). Finally, mean flickery closed time is prolonged by catalytic site mutations that disrupt ATP hydrolysis (243), due to the appearance of a second population of intraburst closed events with an average life time of ~50-100 ms (25, 61). As a result, intraburst closures lasting up to several hundred milliseconds may be observed during long locked-open bursts, and have been dubbed "gating" in some reports (172). Although temperature dependence of intraburst kinetics has not yet been addressed systematically, comparison of studies conducted at room temperature (20-25^{o}C) and those obtained at 37^{o}C suggests ~3-5-fold briefer flickers at the higher temperature (e.g., (243) vs. (30)).

Two alternative kinetic mechanisms, $C_{slow} \leftrightarrow C_{fast} \leftrightarrow O$ and $C_{slow} \leftrightarrow O \leftrightarrow C_{fast}$, with C_{slow} and C_{fast} denoting the interburst and intraburst closed states, respectively, have been used to model CFTR

bursting behavior. Because these two schemes cannot be distinguished by steady-state recordings, all data available to date may be explained equally well by either scheme. In such situations it is customary to prefer the scheme which requires adjustment of the smaller number of parameters to describe two data sets obtained under two different experimental conditions. However, even that "parsimony argument" has been of no help so far, as for either model only one rate was found to be sensitive to ATP concentration (243, 261), but several to both voltage (30) and intracellular pH (40).

The physical mechanism underlying flickery closures is still elusive. The "slow" and "fast *gates*" that cause inter- and intraburst closures, respectively, may or may not be formed by two physically distinct protein regions. But "slow" and "fast *gating*" certainly reflect two distinct types of TMD conformational change: slow gating (i.e., entering and exiting a burst) likely represents flipping between TMD conformations that are analogous to inward- and outward-facing conformations of ABC exporters, respectively (146, 242), whereas fast gating (i.e., intraburst flickering) is likely caused by a smaller scale, more localized conformational change. One possibility is that the outward-facing occluded structure seen for phosphorylated zebrafish CFTR (274), in which the pathway is blocked by a local distortion of the outer segments of TM helices 8 and 12, represents the flickery closed state. As described above, in that conformation the "gate" constriction is widened, but the external extremity of the ion conduction pathway is blocked by a localized conformational change of the outer-leaflet segments of TM helices 8 and 12 (Fig. 1F, *right*, *cyan* and *dark cyan*). However, given that the (human) CFTR channel dwells in the flickery closed state only for a small fraction of the total duration of a burst, capturing this conformation in a cryo-EM structure is unlikely, unless it is stabilized by some factor specific to the cryo-EM conditions (e.g., species difference, low temperature). Thus, an alternative interpretation of the outward-facing occluded zebrafish CFTR structure is that it represents an intraburst closed state with a high occupancy probability, but a life time too short (~1 μs) to be resolved in limited-bandwidth electrophysiological recordings: in that case, the experimentally measured unitary conductance of 7-10 pS would reflect the full conductance multiplied by the fraction of time the pore is truly open within a burst (274). Molecular dynamics simulations, encompassing 1.5 μs, highlight the relative stability of the outward-occluded conformation seen in the ATP-bound zebrafish structure (51), disfavoring the latter scenario. Nevertheless, it remains possible that for both

interburst and conventional flickery closures the ion conduction pathway is interrupted by a similar conformation of the narrow constriction between TM helices 1, 6, 8, and 12, observed at the height of TM6 residues 338-341 (the "gate"; (273)).

IV. Regulation of CFTR gating through nucleotide interactions at the Nucleotide Binding Domains

Because phosphorylation and ATP regulate slow gating, in the following sections channel "opening" and "closing" will be used synonymously with entering and exiting a burst.

A. ATP hydrolysis at one of two non-equivalent composite ATP binding sites

The catalytic turnover rate of CFTR ATPase activity (0.5-1 s^{-1}), estimated for phosphorylated human CFTR protein purified to homogeneity (131, 145), falls into the range of channel gating (bursting) rates. An early hint that ATPase activity might be coupled to pore gating was provided by the observation that lowering free Mg^{2+} to 4 nM, or adding Na-azide, inhibited both processes (131). The catalytic activity of the CFTR protein must originate from composite site 2 of the NBDs, because mutation of the Walker A lysine in site 2, but not that in site 1, abolishes ATPase activity (192). Indeed, photocrosslinking experiments revealed that site 1 retains ATP bound and unhydrolyzed for up to tens of minutes (7, 14). The presence of canonical consensus motifs in site 2, but non-canonical residues in site 1 (Fig. 1D) readily explains such functional asymmetry between CFTR's two composite ATP binding sites, and is likely a shared feature of heterodimeric ABC proteins (102, 186, 235) (including the entire human ABCC subfamily, as well as many prokaryotic homologs (187)).

B. Coupling of pore opening/closure to formation/disruption of a head-to-tail NBD heterodimer

Decades of experimental work gathering information on both CFTR and related ABC proteins have clarified the basic mechanism by which ATP binding and hydrolysis at the NBDs drives pore gating in CFTR. Early studies demonstrated that preventing (or attenuating) ATP hydrolysis in site 2, by mutations of the Walker A lysine (K1250A/G/M/T) or the catalytic glutamate (E1371Q/S) in NBD2

554 (Fig. 1B, *right*; Fig. 1D), locks channels in the open bursting state (32, 96, 242, 243) for time intervals
555 at least two orders of magnitude longer than the mean burst duration of WT CFTR. These results
556 clearly demonstrated that site 2 ATP hydrolysis is required for normal (fast) termination of a burst.
557 Mixtures of ATP either with non-hydrolyzable ATP analogs, such as 5'-adenylyl-imidodiphosphate
558 (AMPPNP), adenosine 5'-(gamma-thiotriphosphate) (ATPγS), or with pyrophosphate (PP_i), also lock
559 channels open (95, 103), suggesting that these analogs prevent closure by binding at site 2. A similar
560 lock-open effect of mixtures of ATP with the inorganic phosphate (P_i) analog orthovanadate (V_i) is
561 believed to reflect formation of a stable ADP:V_i complex that resembles the pentacovalent transition
562 state of the ATP hydrolysis reaction in site 2 (15, 95). Formation of such complexes by the hydrolysis
563 product ADP and a P_i analog that binds tightly in place of the released P_i has been observed in atomic
564 structures of ABC proteins (174).
565 Contrary to early conclusions obtained mostly on single CFTR channels (9, 103, 203), non-
566 hydrolyzable ATP analogs such as AMPPNP, ATPγS, β,γ-methyleneadenosine 5′-triphosphate
567 (AMPPCP) (4, 243), or PP_i (234) alone are capable of opening CFTR channels, although the nucleotide
568 analogs are poor substitutes for ATP, supporting a maximal opening rate only ~5% of that observed in
569 saturating ATP (243). Although the hydrolysis-abolishing K1250A mutation was found to reduce not
570 only closing but also channel opening rate (32, 192), the latter effect was later shown to be largely due
571 to a reduced ATP binding affinity in site 2 (243). Indeed, another site-2 mutation expected to disrupt
572 hydrolysis, E1371S, does not impair channel opening (243). Thus, pore opening requires nucleotide
573 binding, but – in contrast to channel closure – not hydrolysis.
574 By what mechanism is ATP binding at the NBDs translated into pore opening? The hyperbolic
575 dependence of channel opening rate (i.e., the rate of entering a burst) on ATP concentration ($K_{1/2}$~50
576 μM; (55, 241, 243, 270)) indicates a rate limiting step for pore opening other than ATP binding. That
577 step is Mg^{2+} dependent (71, 131), and must follow ATP binding because its rate is sensitive to
578 nucleotide structure: maximal opening rates supported by 8-azido-ATP (14) or AMPPNP (243) are
579 much lower than that observed in ATP. Furthermore, ATP binding must have happened at least at the
580 NBD2 head before the pore opens, because mutations of the Walker A lysine (K1250A, *red*), the
581 Walker B aspartate (D1370N, *marine*), or the stacking aromatic residue (Y1219G, *blue*) in NBD2 (Fig.

1B, *right*), all of which destabilize ATP binding there, dramatically reduce the apparent affinity for ATP to open the pore (243, 281). In contrast, prior ATP binding to the NBD1 head (Fig. 1B, *left*) seems less essential for channel opening as the apparent potency of ATP in opening the pore is decreased by some mutations that impair ATP binding (K464A, removal of the Walker A lysine side chain, *red*; (243)), but not by others (W401G, removal of the stacking aromatic side chain; (281)). The observation of tight NBD dimers in ABC proteins in the presence of ATP, and the suggestion that NBD dimer formation/dissociation might underlie the coupling of ATPase cycles to vectorial transport of substrates by ABC transporters (162), prompted the proposal that CFTR and transporters might share a common mechanism. Thus, in CFTR the rate limiting step for pore opening (to a burst) would reflect formation of a tight head-to-tail NBD1/NBD2 heterodimer, while closure (from a burst) would occur upon disruption of that heterodimer (Fig. 2E; (243)).

A first formal proof of that hypothesis was provided by the demonstration that two residues on opposing surfaces of composite site 2 – arginine 555 just downstream of the NBD1 signature sequence and threonine 1246 in the NBD2 Walker A motif – become energetically coupled upon channel opening, but not upon binding of ATP (which occurs on closed channels, see above) (242). For steric reasons, a hydrogen bond observed between the side chains of the corresponding residues in dimeric ABC NBD structures (38, 215) is expected to form either between an arginine-threonine (R-T) pair, as found in the sequence of CFTR and a subset of ABC proteins, or between a lysine-asparagine (K-N) pair, as present in a smaller subset of the ABC superfamily (Fig. 2A), but not between R-N or K-T pairs (which are poorly represented in naturally occurring ABC sequences). A large reduction in channel opening rate (i.e., an increase in interburst duration, τ_{ib}) observed when introducing the R555K or T1246N mutations in the WT CFTR background (Fig. 2C, *blue* and *red bars* vs. *black bar*) was not seen when introducing the same mutations into a background already mutated at the other position (Fig. 2C, *purple bar* vs. *blue* or *red bar*). This suggests that formation of the R555-T1246 hydrogen bond in WT CFTR facilitates channel opening, and that the hydrogen bond is disrupted in each single mutant, but restored in the double mutant. These mutation-induced changes in opening rate report mutational effects on the stability of the transition state for opening ($T^{\ddagger}$) relative to the closed state ($\Delta\Delta G^{\ddagger}_{T\text{-}C}$; numbers next to arrows in Fig. 2D). The R555K mutation destabilizes the transition state when a

610 threonine is present at position 1246 (Fig. 2D, *left vertical arrow*), but stabilizes it when the residue at
611 position 1246 is an asparagine (Fig. 2D, *right vertical arrow*). The difference between $\Delta\Delta G^{\ddagger}_{T\text{-}C}$ values
612 along two parallel sides of the mutant cycle quantifies the change in interaction energy between the
613 native side chains upon entering the transition state from the closed state ($\Delta\Delta G_{int(opening)}$), and is of a
614 magnitude and sign consistent with formation of a hydrogen bond. A similar mutant cycle built on the
615 closed-open equilibrium constant of a hydrolysis deficient mutant, in which gating is reduced to
616 reversible $C_1 \leftrightarrow O_1$ transitions, confirmed the presence of the R555-T1246 hydrogen bond also in the
617 open ground state (242). Chemical crosslinking experiments (159) later confirmed the canonical head-
618 to-tail NBD dimer arrangement seen in all dimeric ABC NBD structures (Fig. 1C-D) to be present in
619 full-length, gating CFTR channels in their native environment.

620 Thus, the rate-limiting step for channel opening (Fig. 2E, step $C_1 \rightarrow O_1$) consists of tight
621 dimerization of ATP-bound NBDs, coupled to TMD rearrangements that open up a transmembrane
622 pathway for anions. Demonstration of salt bridge formation between cytosolic TMD loops in the open
623 state (252) but between extracellular TMD loops in the closed state (64, 107), as well as a proposed
624 narrowing of the intracellular vestibule in open channels (12), all suggested that upon pore opening
625 CFTR's TMDs undergo a conformational change similar to the flipping of ABC transporter TMDs
626 from an inward- to an outward-facing conformation. All these predictions, based on functional studies,
627 were largely confirmed by the recent cryo-EM structures of dephosphorylated apo- and phosphorylated
628 ATP-bound CFTR (Fig. 1E-F; (145, 273, 274)).
629

630 **C. Thermodynamics and timing of the pore opening transition**

631 Among the steps that a phosphorylated WT CFTR channel follows around its gating cycle (Fig.
632 2E) the pore opening transition (Fig. 2E, step $C_1 \rightarrow O_1$) is the slowest (~0.5-2 s^{-1} at 25^{o}C, ~5-8 s^{-1} at
633 37^{o}C), reflecting a high energetic barrier, characterized by an unstable, high free-energy transition
634 state. The most common CF mutation, deletion of phenylalanine 508, further slows this step by >40-
635 fold (125, 161). What is the nature of this transition state, and what causes its high free energy? The
636 steep temperature dependence of WT CFTR opening rate signifies a large activation enthalpy ($\Delta H^{\ddagger}_{T\text{-}C}$
637 ~100-150 kJ/mol, (6, 57, 155)) suggesting molecular strain. On the other hand, the discrepancy

between $\Delta G^{\ddagger}_{T\text{-}C}$ and $\Delta H^{\ddagger}_{T\text{-}C}$ signals a large entropy increase in the transition state ($T\Delta S^{\ddagger}_{T\text{-}C} \geq 40$ kJ/mol, (57)). Given that the NBD interface is already tightened around ATP site 2 in the transition state (Fig. 2A-D; (242)), the large activation entropy has been interpreted to reflect the dispersal of the layers of ordered water molecules that cover the interfacial NBD surfaces when the NBDs are separated and the interface is open and accessible to solvent (57).

The relative timing of motions in different regions of a channel protein during the sub-microsecond process of pore opening (transition from state C to O) can be determined by studying the kinetic consequences of structural perturbations, typically point mutations, introduced into various protein regions. If the perturbation-induced change in the transition-state free energy linearly interpolates the difference, $\Delta\Delta G^{o}$, between the free energy changes of the C and O ground states ($\Delta\Delta G^{o} = \Delta G^{o}_{O} - \Delta G^{o}_{C}$) (94, 153), then the free energy of the transition state for opening, $T^{\ddagger}$, will change by $\Phi\Delta\Delta G^{o}$ ($0 \leq \Phi \leq 1$). A larger Φ value indicates earlier, and a smaller Φ value later, movement of the target position during pore opening. In particular, $\Phi \sim 1$ indicates that, in the transition state, the target position is already near its open-state conformation, whereas $\Phi \sim 0$ suggests it has not yet moved much from its closed conformation (10, 277). Because the perturbation will change the logarithm of the opening rate constant (k_{CO}) by $-\Phi\Delta\Delta G^{o}/(RT)$, but the logarithm of the equilibrium constant (K_{eq}) by $-\Delta\Delta G^{o}/(RT)$, Φ can be estimated from the slope of a REFER (Rate-Equilibrium Free Energy Relationship) plot of $\log k_{CO}$ versus $\log K_{eq}$ for a series of mutations at the target position. Importantly, because the REFER approach assumes equilibrium gating, with opening and closure reflecting reversible transitions along a single kinetic pathway (53), this approach cannot be applied to address the dynamics of the ATP-dependent slow gating process of WT CFTR channels (5, 204), which obey a non-equilibrium cyclic gating mechanism (Fig. 2E). However, the technique may be adapted to studying the pore opening step (Fig. 2E, step $C_1 \rightarrow O_1$), by employing a background mutation that disrupts ATP hydrolysis in site 2, thereby reducing gating to reversible $C_1 \leftrightarrow O_1$ transitions. REFER analysis in such a non-hydrolytic background (NBD2 Walker B aspartate mutant D1370N) revealed a clear spatial Φ-value gradient along the protein's longitudinal axis, from cytoplasm to cell exterior (219, 220): Φ was close to ~1 for both faces of composite ATP site 2 (positions 555 and 1246; Fig. 3A, *left*, *red spacefill*, Fig. 3A, *right*, *red numbers*), ~0.5-0.6 for positions in each of the four coupling

helices (positions 172, 275, 961, and 1068, respectively; Fig. 3A, *purple spacefill* and *numbers*), but ~0.2 for the centrally located pore residue M348 in TM6, and ~0 for position 117 in the first extracellular loop (Fig. 3A, *blue spacefill* and *numbers*). This clear Φ-value gradient suggests that a spreading conformational wave is initiated at the site-2 NBD interface and propagates towards the pore (Fig. 3B, *vertical colored arrow*). In particular, it suggests that in the transition state the site-2 interface is already tightly dimerized, but the pore is still closed (Fig. 3B, *center*). Thus, the high enthalpy of the opening transition state ($\Delta H^{\ddagger}_{T\text{-}C}$~100-150 kJ/mol) might reflect strain at the NBD-TMD interface ((219); cf., (57)), which includes the disease hotspot position 508. Indeed, a Φ value of ~0.5 for position 508 suggests that this NBD position moves synchronously with nearby TMD coupling helix 4 (220). Interestingly, a low-intermediate Φ value of ~0.4 was found for both faces of degenerate site 1 (positions 460 and 1348; Fig. 3A, *orange spacefill* and *numbers*), reporting delayed movement here with respect to site 2, and suggesting that site 1 residues are still on the move in the transition state for channel opening. However, because such pronounced asymmetry cannot be detected at the level of the four coupling helices, it seems likely that the movements completed in site 1 between the transition state and the open state are localized movements, confined to the site-1 NBD interface (220).

D. Strictness of coupling between pore opening events and NBD dimerization

Strict coupling between NBD dimerization and pore opening in CFTR has been called into question because a construct lacking NBD2 (ΔNBD2, truncated after residue 1197) displays low-probability ATP-independent openings following phosphorylation by PKA (65, 248). Based on that observation, spontaneous openings in the absence of ATP, also seen occasionally in WT CFTR (25, 224) but robustly promoted by mutations at TMD positions 978 (ICL3; (253)) or 355 (TM6; (257)), were interpreted as reflecting pore openings in the absence of NBD dimerization. Furthermore, a resemblance was noted between CFTR and classical ligand-gated channels, such as the nicotinic acetylcholine receptor, in that phosphorylation (248), TMD mutations (253, 257), various drugs (112, 248), and ATP analogs (172) all had strongly correlated effects on spontaneous (ATP-independent), and on ATP-dependent, channel activity, and the effects of such "allosteric modulators" were energetically additive (172, 257). These analogies led to CFTR gating being modeled as an equilibrium

loop mechanism in which the ligand (ATP) can bind and unbind in both the closed-pore and the open-pore conformation, and closed-open ("isomerization") transitions can occur whether or not ligand is bound. In that model, due to the thermodynamic principle of detailed balance, which constrains the product of the equilibrium constants around a kinetic cycle to be unity, higher affinity binding of the ligand in the open-channel conformation would shift the closed-open equilibrium of liganded channels towards the open state ((120); cf., (92)). An essential feature of such an allosteric loop model (also key to the proposed "reentry" mechanism (113) discussed in Section IV. E, below) is the postulate that in the ATP-free spontaneous open state the NBDs are disengaged, and the dimer interface is therefore accessible for ATP binding. Studying the accessibility of site 2 in ATP-free open channels is not straightforward, but exploiting the enhanced spontaneous activity of the K978C/P355A double mutant, which allows quantitation of spontaneous gating parameters in microscopic patches, this question was recently addressed (160). In K978C/P355A channels gating in the absence of ATP, just as in WT channels gating in the presence of ATP (242) (Section IV. B), energetic coupling between site-2 residues R555 (NBD1 face) and T1246 (NBD2 face) was found to change in a state-dependent manner: spontaneous open probability of the background construct is reduced by both the R555K and the T1246N single mutation, but restored in the double mutant (Fig. 4A-B), reporting energetic coupling between these residues in the open state (Fig. 4C). Thus, the two side chains on opposing faces of composite site 2 form a hydrogen bond in the open-pore, but not in the closed-pore conformation, indicating the presence of a tightly dimerized site-2 NBD interface in the spontaneous open-channel state (Fig. 4D), just as during normal, ATP-dependent openings (Fig. 2E). Because a tightly dimerized NBD interface does not allow ATP binding/unbinding in the open-pore conformation, CFTR gating must be driven by principles fundamentally different from the allosteric mechanisms that underlie gating of ligand-gated channels. Thus, strict coupling between "slow gating" and NBD dimerization/dissociation seems to be an intrinsic property of the CFTR protein: ATP binding alters the energetics, but not the basic structural organization of the open- and closed-pore conformations. The similar structural architecture of ATP-free, and ATP-bound, open states also readily explains correlated and additive effects on spontaneous and ATP-driven channel activity of the various "allosteric modulators" mentioned above – R-domain phosphorylation, TMD mutations, or drug binding to TMDs

(253) – through energetic stabilization or destabilization of the inherent open-state structure. A similarity between ATP-free and ATP-bound open channel structures is also consistent with inhibition of opening of disease mutant G551D CFTR by ATP binding at site 2, interpreted to reflect electrostatic repulsion between the negative charge of the aspartate in the site-2 signature sequence and that of the γ-phosphate of ATP bound to the site-2 Walker motifs (133). Because electrostatic interactions are very short-range in water, such an interaction would not be expected to occur if the site-2 interfacial NBD surfaces did not approach each other and become dehydrated, i.e., if the dimer interface did not close, in the G551D mutant upon pore opening, but is plausible if pore openings remain strictly coupled to NBD dimerization. Indeed, the aspartate side chain in position 551 does not sterically interfere with closure of the dimer interface, because introduction of large uncharged (serine) or positive (lysine) side chains are tolerated here (133). Although infrequent ATP-independent pore openings of ΔNBD2 CFTR (248) can clearly not be linked to NBD dimerization, it seems likely that upon pore opening its remaining NBD-TMD coupling machinery undergoes movements similar to those that accompany NBD dimerization in full-length CFTR.

E. Strictness of coupling between open burst termination and ATP hydrolysis

How strictly CFTR gating is coupled to ATP hydrolysis has been a matter of longstanding debate. The first hint implying a non-equilibrium gating cycle came from the observation of time-asymmetric changes in permeation properties in patch-clamp records of individual gating CFTR channels (96). The kinetics of pore block of WT CFTR by the anionic buffer MOPS changes within each burst, a phenomenon that can be made evident by the presence, at small recording bandwidth, of two distinct conductance states (one low, one high) (109). The sequence of occurrence of these conductance states shows clear time-asymmetry: the ratio between resolvable low-to-high (L→H) and high-to-low (H→L) transitions is ~16:1 (96), with the majority of time during each burst spent in the initial low-conductance state. Such time-asymmetry is a clear violation of microscopic reversibility, and indicated strong coupling between pore gating and a free-energy releasing process, here most likely ATP hydrolysis. Indeed, the L→H transition itself was suggested to coincide with ATP hydrolysis, because it was absent under non-hydrolytic conditions (96). In apparent conflict with that conclusion of

750 strong coupling, mutation of the NBD1 Walker A lysine (K464A) reduced ATPase activity of purified
751 CFTR protein by ~10-fold but little affected channel gating, interpreted to suggest loose coupling
752 between gating and catalytic activity in CFTR (192).

753 In single-channel records transitions among closed-channel states or among open-channel states
754 remain undetected. However, such invisible transitions contribute to determining the shapes of the
755 open- and closed-dwelltime distributions (which consist of mixtures of exponential components),
756 making it possible to estimate their rates through maximum likelihood fitting (50). For equilibrium
757 processes the fractional amplitude of each exponential component is necessarily positive, and the
758 distributions are therefore monotonically decaying (117). In contrast, for WT CFTR the distribution of
759 open burst durations is clearly peaked (Fig. 5A). This experimental observation thus reveals an
760 underlying non-equilibrium gating mechanism, with most open events involving two sequential steps: a
761 slow step with a rate of ~4 s^{-1} followed by a fast step with a rate of ~50 s^{-1} (at room temperature) (61).
762 These two sequential steps were interpreted to reflect slow ATP hydrolysis (Fig. 2E, step $O_1 \rightarrow O_2$, rate
763 k_1) followed by fast disruption of the posthydrolytic NBD dimer (Fig. 2E, step $O_2 \rightarrow C_2$, rate k_2). Indeed,
764 the rate-limiting step for WT CFTR channel closure is strongly temperature dependent, with an
765 estimated activation enthalpy $\Delta H^{\ddagger}$~70-90 kJ/mol ((57, 155) but, cf., (6)); and the similar values for $\Delta G^{\ddagger}$
766 and $\Delta H^{\ddagger}$ report no decrease in entropy (57). Such an isolated positive enthalpy change, unaccompanied
767 by a change in entropy, is consistent with strain in a single chemical bond, without accompanying
768 changes in interface accessibility to solvent molecules. These observations suggest that the ATP
769 hydrolysis step ($O_1 \rightarrow O_2$) is rate limiting for channel closure: the transition state for this step would
770 include a still tightly dimerized composite site 2, but a strained bond between the β and γ phosphates of
771 the occluded ATP.

772 Because in WT CFTR the rate of non-hydrolytic closure (Fig. 2E, step $O_1 \rightarrow C_1$, rate k_{-1}) is likely
773 very slow, estimated between ~0.03-0.2 s^{-1} based on the slow closing rates of various non-hydrolytic
774 mutants, >95% of pore opening events must terminate through ATP hydrolysis, consistent with the
775 conclusions of Gunderson and Kopito (1995) (94%). In contrast, the burst distribution of the non-
776 hydrolytic D1370N mutant lacks a negative exponential component and is monotonically decaying
777 (Fig. 5B), reflecting a gating cycle truncated to reversible $C_1 \leftrightarrow O_1$ transitions (61), with rate k_{-1} (~0.5 s^{-}

778 [1]) accelerated by this mutation which removes a side chain involved in Mg^{2+} coordination (269). On the
779 other hand, fitting the burst distribution of the site-1 mutant K464A (Fig. 5C) suggested an ~4-fold
780 reduction in rate k_1, i.e., allosteric slowing of ATP hydrolysis in site 2, and a >10-fold acceleration of
781 rate k_{-1} (61)), consistent with the effect of this mutation on macroscopic closing rates in various non-
782 hydrolytic mutant backgrounds (56, 61, 185, 243). Thus, the "coupling ratio" that quantifies the
783 proportion of pore opening (burst) events that result in ATP hydrolysis (given by $k_1/(k_1+k_{-1})$ for the
784 scheme in Fig. 2E, i.e. the ratio of the rate of hydrolysis over the sum of all rates out of the
785 prehydrolytic open state) may be lowered by mutations that slow ATP hydrolysis and/or accelerate
786 non-hydrolytic dissociation of the NBD dimer: it is >0.95 for WT CFTR (strong coupling), but only
787 ~0.2 for K464A (loose coupling), and 0 for non-hydrolytic mutants (no coupling) (Fig. 5D, *colored*
788 *arrows*). Such an interpretation is consistent with the ATPase measurements of Ramjeesingh and
789 colleagues (1999), on both WT CFTR and the two Walker A lysine mutants.
790 More recently, time-asymmetric subconductance patterns (low-to-high: L→H) for single CFTR
791 channels have been observed in the presence of the blocker 3-nitrobenzoate (60), as well as in mutants
792 in which the native charge distribution of the intracellular pore vestibule is perturbed (113, 272).
793 Intriguingly, for the latter mutants, multiple L→H subconductance transitions could be observed in
794 ~10-20% of the bursts. On the assumption that L→H transitions reflect ATP hydrolysis events,
795 L→H→L→H type bursts were interpreted to reflect two ATP hydrolysis events occurring within a
796 single burst, i.e., a "coupling ratio" >1 ("super-coupling"). The phenomenon was explained by a model
797 which postulates that the hydrolysis products ADP+P_i may be released, and a novel ATP molecule may
798 bind, at site 2, returning the channel to the prehydrolytic open state without an intervening pore closure
799 (113). The existence of such a "reentry" pathway, which implies separation of the NBD dimer interface
800 around site 2 uncoupled from pore closure, seemed consistent with the earlier finding that a brief, 1-
801 second, exposure of open CFTR channels to PP_i or AMPPNP in the presence of ATP, or immediately
802 after ATP removal, can lock CFTR channels into a long-lasting burst without an intervening long
803 closure. It also seemed consistent with the modest [ATP]-dependence of steady-state single-channel
804 burst durations observed for W401F (but not for WT) CFTR (114). Moreover, the CFTR potentiator
805 drug VX-770 (ivacaftor) was shown to increase the frequency of L→H→L→H type bursts, and to

prolong CFTR burst durations in a weakly [ATP]-dependent manner, prompting the interpretation that the drug acts by stabilizing the posthydrolytic O_2 state and thus promoting the "reentry" pathway (112).

A major shortcoming of the reentry model is that it predicts a dissociation between the steady-state mean burst duration (τ_b) and the time constant of macroscopic current relaxation following sudden nucleotide removal (τ_{relax}). This is because the latter reflects average survival time in the open burst state at zero nucleotide concentration, i.e., in the certain absence of reentry events. Thus, for a channel which gates at steady state, the average number of site-2 nucleotide occlusion events within a single burst is given by the ratio τ_b/τ_{relax}; and that number was found to be ~1 under most, if not all, conditions tested, including WT CFTR and various mutants gated by either ATP or N^6-(2-phenylethyl)-ATP (P-ATP) (56, 233), and even for WT CFTR stimulated by VX-770 (112). On the other hand, both [ATP]-dependence of τ_b and the existence of L→H→L→H type bursts might be accounted for by alternative explanations. First, τ_b dependence on [ATP] might arise from a differential contribution to channel activity of “spontaneous” openings. CFTR channels are known to open with ATP bound at only one composite site (25, 26, 185), and occasionally even in the complete absence of nucleotide (25, 160, 224, 253). Such monoliganded and unliganded ("spontaneous") openings are briefer than normal "diliganded" openings (160, 257), and their fractional contribution, which shortens mean burst duration, is expected to be stronger at low [ATP]. While for WT CFTR this effect is too subtle to be measurable in most studies ((24, 112, 243); but cf., (270)), it might be accentuated by mutations that perturb ATP binding at either site (114), or by drugs that increase the frequency of spontaneous openings, such as VX-770 (112). Second, how might L→H→L→H type bursts arise? L→H subconductance transitions are believed to coincide with ATP hydrolysis because only the L state is readily observed under non-hydrolytic conditions, e.g., in the absence of Mg^{2+}, in the site-2 mutants D1370N, K1250A, and E1371S, or for WT channels locked open by ATP+PP_i or ATP+AMPPNP (96, 113). However, in ABC proteins, splitting of the ATP β-γ bond is a multi-step process, as evidenced by multiple intermediate states distinguishable by blocking the hydrolysis reaction using ATPγS, V_i, fluoroaluminate, beryllium fluoride, or different catalytic site mutations (213, 222, 236). Which of these partial steps coincides with the L→H transition is as yet unclear: some of these might be reversible, and so repeated L→H transitions might reflect multiple attempts to complete the bond

834 splitting reaction. Alternatively, the entire ATP hydrolysis process (step $O_1 \rightarrow O_2$; Fig. 2E) might well
835 be reversible: although the ATP hydrolysis reaction with reagents and products in aqueous solution is
836 highly exergonic, in a multi-step enzymatic process, which starts with binding of $ATP_{(aq)}$ from the bulk
837 solution and ends with the release of products ($ADP_{(aq)} + P_{i(aq)}$) into solution, the step associated with
838 the largest negative ΔG^o need not be the bond-splitting step itself: thus, ΔG^o for the reaction
839 CFTR•ATP + $H_2O \rightarrow$ CFTR•ADP•P, in which reagents and products are bound within the catalytic
840 site, might not be highly negative (cf., ATP- and ADP•P-bound states of the F1-ATPase β subunit are
841 in equilibrium (264)). Of note, reversibility of step $O_1 \rightarrow O_2$ (Fig. 2E) would not alter the shape of the
842 burst dwell-time distributions (61). As a third possibility, coupling between conductance state and
843 hydrolytic state might be only probabilistic, such that the prehydrolytic state (O_1, Fig. 2E) only *favours*
844 (but is not strictly linked to) the lower-conductance (L), while the posthydrolytic state (O_2, Fig. 2E)
845 *favours* (but is not strictly linked to) the higher-conductance (H) pore conformation. None of these
846 possible alternatives has been excluded to date.

847 Where this has been studied, both ATP-dependent (242) and ATP independent (160) open
848 channels have been found to have tightly dimerized NBDs, with ATP at site 2 occluded (see Section IV
849 D). Given this evidence, and the considerations above on our uncertainty on how to precisely link the
850 conductance changes to events at the catalytic site, the conformational changes underlying the L→H
851 transition are more easily interpreted as changes in the TMDs that do not alter tight NBD dimerization.
852 As described above (Section II. C), structures for a number of ABC transporters have been obtained in
853 outward-facing conformations (46, 67, 256), in which the extracellular portions of the TMDs,
854 corresponding to the regions involved in forming CFTR's permeation pathway, assume diverse
855 arrangements, while the NBDs remain tightly dimerized. Thus, CFTR's low conductance state might
856 represent a conformation in which, like in the phosphorylated ATP-bound zebrafish CFTR structure
857 (274) or the McjD transporter (46), the extracellular ends of the TM helices are arranged in a largely
858 parallel orientation, while the high conductance conformation reached at the end of the burst might be
859 somewhat more similar to the Sav1866 structure (67), in which the extracellular ends of the TM helices
860 further diverge. Of note, the position corresponding to R352 in human CFTR, mutations at which
861 appear to differentially affect conductance in the O_1 and O_2 state (113), is positioned at a constriction of

862 the permeation pathway in Sav1866-based homology models (52, 163), but in the wider intracellular
863 vestibule in the outward-facing zebrafish CFTR structure (274) and in models based on McjD (52).
864
865 **F. Role of the degenerate ATP binding site in channel gating**
866 Photocrosslinking experiments using [α^{32}P]8-azido-ATP to label the two ATP sites, and various
867 unlabeled nucleotides to compete that labeling, identified site 1 as a high-affinity binding site with a K_d
868 for MgATP in the low micromolar range (7, 14). Furthermore, labeling of site 1 by [γ^{32}P]8-azido-ATP,
869 without crosslinking, was shown to survive several minutes of extensive washing with nucleotide-free
870 solution at 30^{o}C, demonstrating poor or absent catalytic activity at the degenerate site (14). Given that
871 the cycle time for channel gating is on the order of ~1 s, these biochemical findings suggested that site
872 1 must retain ATP bound and unhydrolyzed throughout many gating cycles, in contrast to site 2 which
873 hydrolyzes ATP within each channel burst event. Indeed, such an asymmetry between the kinetics of
874 nucleotide exchange in the two sites was supported by ligand exchange experiments in which ATP and
875 the high-affinity analog P-ATP were intermittently applied to inside-out patches. Gating of CFTR
876 channels in P-ATP is characterized by ~2-fold prolonged bursts (slower closing) and ~2-fold shortened
877 interbursts (faster opening), as compared to gating in ATP. However, whereas the effect on opening
878 rate – attributed to the nucleotide bound in site 2 – is observed instantaneously upon exchange of the
879 bath nucleotide, the effect on closing rate – attributed to the nucleotide bound in site 1 – appears with a
880 delay of ~50 s (233).
881 What is the extent of gating-related movements in site 1? In closed channels the NBD dimer
882 interface must disengage occasionally even around site 1 because, albeit slowly, the nucleotide in site 1
883 can be clearly exchanged (233), and that is most unlikely to happen while the interface is tight. But, to
884 what extent, and how frequently, does site 1 open up? The slow nucleotide exchange rate at site 1 is
885 affected by NBD2 signature sequence (S1347) mutations (233), suggesting that the NBD2 tail
886 continues to contribute to ATP binding even while the pore is closed. In apparent contradiction to these
887 findings, cysteines engineered into the signature sequence at either site 1 (S549C) or site 2 (S1347C) –
888 accessible to small hydrophilic methane-thiosulfonate (MTS) reagents in the closed but not in the open
889 state – were modified equally rapidly, at a rate approximating the rate of pore closure. Thus, upon pore

closure the NBD interface must open up around both ATP sites promptly, and sufficiently to accommodate reagents with a diameter up to ~8Å (37). A heterodimeric bacterial ABC transporter, Tm287-288, crystallized in the presence of AMPPNP, shows an inward-facing conformation (101), with nucleotide bound only at site 1, but both binding sites partially open (i.e., Walker A and signature sequences are separated, accessible to the solvent – and to relatively large reagents). Some contact across the site-1 interface is maintained through interactions between the Walker A loop of NBD1 and the D-loop of NBD2. In particular, the residues corresponding to CFTR's T460 in NBD1 and H1375 in NBD2 are seen to form hydrogen bonds. Maintained contact between these two residues, throughout CFTR's gating cycle, is supported by lack of gating-associated changes in energetic coupling (223). One possible interpretation, consistent with both MTS accessibility (37) and mutant cycle (223) studies, is that closing of the pore corresponds to a partial opening of site 1, as seen in the Tm287-288 AMPPNP-bound crystal. However, functional studies on Tm287-288 (230), as well as on SUR1/K_{ATP} (176) and CFTR (243) channels, suggest that binding of AMPPNP to heterodimeric ABC proteins has a poor efficacy in altering equilibria towards the NBD-dimerized conformations. Thus, bound MgATP might be more effective in maintaining the site-1 interface tightly dimerized, even immediately after pore closure, as the nucleotide exchange studies would suggest (233). One possible unifying interpretation could be that there is a rapid equilibrium between a tightly dimerized and a partially open conformation of site 1 in closed channels: whereas the impact of NBD2 signature sequence mutations on site-1 nucleotide exchange rate (233), depends on the *fraction of time* a closed channel spends with site 1 dimerized, the rate of MTS modification of site-1 cysteines upon pore closure (37) reflects the *rate of first passage* to the de-dimerized state. Thus, possibly, in a closed channel site 1 might remain in a dimerized state for most of the time, but nevertheless visit the de-dimerized state frequently enough to allow high-probability modification of site-1 cysteines within a single closed-channel (interburst) event. Understanding the precise range of gating-related movements in CFTR's site 1 will require a high-resolution structure of phosphorylated CFTR in a closed state with ATP bound at site 1.

What role does site 1 play in CFTR channel gating? Regardless of what the precise spatial arrangement of the most frequently populated closed-channel conformation is, significant rearrangements must occur in site 1 between that conformation and the open-channel conformation,

because site-1 structural perturbations clearly alter the free-energy difference between the ATP-saturated closed-pore (Fig. 2E, C_1) and the prehydrolytic open-pore (Fig. 2E, O_1) states (56, 185, 281). But, whereas in canonical site 2 the conformational changes upon pore opening are completed already in the transition state, as reported by its large Φ value of ~1 (Fig. 3A, *right*, *red numbers*), for degenerate site 1 the low Φ value of ~0.4 (Fig. 3A, *right*, *orange numbers*) reports some further motion between the transition state and the open state. ATP stabilizes the open-pore conformation by acting as a molecular glue that bonds the NBD dimer interface together. Comparison of gating kinetics of ATP hydrolysis deficient mutants in saturating ATP and of WT CFTR channels in the absence of ATP (spontaneous gating) indicates that the presence of bound ATP both speeds channel opening (Fig. 2E, step $C_1 \rightarrow O_1$) and slows non-hydrolytic closure (Fig. 2E, step $O_1 \rightarrow C_1$) (160). The effect on opening rate is readily explained by the bonding of the ATP glue in site 2, which is already completed in the transition state (Fig. 3B, *bottom site*, *red cups around ATP* in states T and O_1): that glue stabilizes state T (and O_1) relative to state C, thereby lowering the energetic barrier for opening. However, slowing of non-hydrolytic closure indicates that ATP binding also stabilizes the open state (O_1) relative to the transition state (T), i.e. ATP-bound channels, compared to spontaneously-opened channels, face a higher energetic barrier to closing by simple reversal of the opening step. Indeed, the movements in site 1 that occur between the transition state and the open state might reflect the bonding of the ATP glue in the degenerate site (Fig. 3B, *top site*, *red cups around ATP* in state O_1) which underlies this differential stabilization of O_1 compared to T. In the context of ATP-dependent gating of WT CFTR (Fig. 2E) that bonding effect of ATP in site 1 would explain the small value of rate $O_1 \rightarrow C_1$, which ensures strictly unidirectional, non-equilibrium cycling (Fig. 2E, *purple circular arrow*; cf., Fig. 5D). Consistent with such an interpretation, channel closure under non-hydrolytic conditions is affected by a number of structural perturbations in site 1: it is accelerated by the K464A mutation (56, 185, 243) or by deletion of the RI (54)), but slowed by the H1348A mutation (56), or by P-ATP bound in site 1 (56, 233).

G. The channel-transporter interface: CFTR viewed as a degraded active transporter

From an evolutionary perspective CFTR is most closely related to the exporter class of ABC proteins which extrude a variety of substrates, against their electrochemical gradients, out of cells. To

avoid instantaneous dissipation of the electrochemical gradient, built up at the expense of ATP hydrolysis, exporters must have two gates, and these must never be open at the same time (83). In the inward-facing conformation of ABC exporters a closed outer gate is formed by the converging external ends of the TM helices (8, 101, 212, 256), whereas in the outward-facing conformation tight bundling of the cytosolic ends of the TM helices forms a closed inner gate (46, 67, 256). The inward-facing conformation thus allows high-affinity substrate binding from the cytosolic side, whereas in the outward-facing conformation the substrate is released into the extracellular medium. The inward- to outward-facing conformational transition is driven by NBD dimerization following ATP binding (146). However, unidirectional uphill transport requires a source of external energy input. That energy source, the binding and hydrolysis of ATP, is harnessed to drive conformational changes unidirectionally, thus switching, in the loaded transporter, the substrate binding site from inward-facing high affinity to outward-facing low affinity, and allowing release of substrate even in the face of a high extracellular concentration (13).

Based on the common evolutionary origin of CFTR and ABC exporters, and on the finding that in CFTR dimerized NBDs are coupled to an open, but de-dimerized NBDs to a closed, pore (242), CFTR's TMDs were believed to adopt an inward-facing conformation in the closed (interburst), but an outward-facing conformation in the open (burst), state. Because the latter conformation forms a transmembrane aqueous pore permeable to anions, in CFTR the ABC protein internal gate was proposed to have become "leaky" to anions over the course of evolution. Supported by a line of functional evidence (12, 64, 107, 252), that proposal was finally proven to be correct by the recent structures of inward- and outward-facing CFTR ((145, 273, 274); Fig. 1E-F). These structures also identify the structural changes that implemented CFTR's evolution from a transporter to a channel: the appearance of a lateral opening between TM helices 4 and 6 (Fig. 1F, *right*, *red arrow*) provides an aqueous pathway between the cytosol and the internal vestibule, thus short-circuiting the ABC protein internal gate formed by the cytosolic TM helix bundle crossing (cf., (76, 77)). But why has the ATP hydrolysis-driven non-equilibrium gating cycle of CFTR been spared by evolution? The passive, electrochemically downhill chloride ion flow through CFTR could in principle be controlled by simple ATP binding (i.e., reversible $C_1 \leftrightarrow O_1$ transitions, see Fig. 2E), without any need for "wasteful" ATP

hydrolysis. A likely explanation is a lack of evolutionary pressure, given that ATP wasting by CFTR is negligible: whereas P-type ATPases like the ubiquitous Na^+-K^+-ATPase transport ≤5 cations, CFTR transports millions of chloride ions at the expense of hydrolysis of a single ATP molecule. Alternatively, in addition to serving as an anion channel, CFTR might also serve as an active transporter of some, as yet unidentified, substrate. Interestingly, CFTR was found to mediate efflux of large organic anions such as gluconate or lactobionate (142), or of reduced and oxidized gluthatione (143), from the cytosolic solution, but not influx of the same anions from the extracellular solution; this asymmetry was disrupted when ATP hydrolysis was prevented using PP_i or AMPPNP. However, the molecular mechanism of such ATP hydrolysis-dependent unidirectional export is still elusive: it is not a classical transporter-like process, as the estimated throughput rate for gluconate export (~40 fA, corresponding to ~$2.5 \cdot 10^5$ ions/s (142)) exceeds measured rates of ATP hydrolysis (~1/s (131, 145)) by five orders of magnitude.

H. Adenylate Kinase catalytic activity and gating regulation

Isolated, purified NBD1 and NBD2 of CFTR show measurable adenylate kinase (AK) activity, catalyzing reversible interconversion between ATP+AMP and 2 ADP molecules by direct phosphotransfer between the two nucleotides (93, 193, 194). Based on this finding, CFTR was suggested to catalyze preferentially AK, rather than ATPase reactions, in the presence of AMP levels found in living cells (195). Along these lines, partial inhibition of CFTR channel currents by ADP or the AK inhibitor P1,P5-di(adenosine-5')pentaphosphate (AP_5A), as well as subtle effects of AMP on currents evoked by low micromolar ATP, were all interpreted to reflect alterations in CFTR gating caused by modulation of its intrinsic AK activity (195, 197). However, unlike the purified isolated NBDs, full-length CFTR protein purified to homogeneity was shown to exhibit exclusively ATPase, but no significant AK activity (193). As the ATPase turnover rate of the same preparation was comparable with that of channel bursting rates (~0.2 s^{-1}), intrinsic AK activity of full-length CFTR, if any, would be expected to be orders of magnitude slower than channel gating rates; indeed, even for isolated NBDs reported AK turnover rates were in the range of 0.003-0.02 s^{-1} (193, 195); but, cf., (93)). Interestingly, recent studies demonstrated phosphoryl transfer between γ-^{32}P-GTP and 2-azido-AMP

(2-N_3-AMP) in membrane preparations of CFTR-overexpressing HeLa cells, and the resulting β-^{32}P-2-N_3-ADP product could be photo-crosslinked to CFTR; moreover, that signal was weakened by CFTR site-2 mutations S1248F (196) and Q1291F (70). These results could indeed reflect some intrinsic AK activity for CFTR, but they could also be explained by the activity of an endogenous AK associated with HeLa cell membranes: reduced labeling of the CFTR mutants could then reflect impaired binding to CFTR's site 2 of the labeled β-^{32}P-2-N_3-ADP produced by the associated AK. Indeed, AK1β contains a myristoylation domain and has been shown to strongly associate with membranes (49). AK also interacts with multiple enzymes involved in energy homeostasis, and at least two AK anchoring proteins have been identified (reviewed in (73)). Specifically, AK1 directly interacts with sarcolemmal ATP-sensitive potassium (K_{ATP}) channels, as demonstrated by mutual co-immunoprecipitation and AK-mediated regulation of K_{ATP} channel activity, implying strong structural and functional coupling between the two proteins (31). Thus, a definitive proof of intrinsic AK activity for CFTR will require demonstration of such activity for full-length CFTR protein under conditions that exclude the presence of associated cellular proteins.

Modulation of CFTR currents by various nucleotides and nucleotide analogs has been addressed by multiple studies, and is mostly consistent with competition with ATP for sites 1 and 2 (e.g., (24, 25, 195, 203, 258). At least the strong inhibitory effect of ADP, caused by a slowing of channel opening and an acceleration of channel closing (24, 203, 258), is readily explained by competition with ATP for sites 2 and 1, respectively (24, 25), and cannot be linked to AK activity of CFTR, as both effects are observed also for CFTR channels bearing site-2 mutations K1250A or D1370N (25) shown to abolish AK activity even for isolated NBD2 of CFTR (93, 195). Likewise, inhibition by AP_5A of ATP-induced CFTR currents cannot be attributable to inhibition of AK activity since it is observed in the absence of AMP, i.e., in inside-out patches continuously superfused with solutions that contain ATP but no AMP (195).

V. Regulation of CFTR gating by R-domain phosphorylation

A. Kinases and phosphatases involved in CFTR regulation

Cytosolic ATP is essential for CFTR channel gating, but ATP concentration cannot serve as a physiological regulator of channel activity: because the $K_{1/2}$ for stimulation of open probability by ATP is ~50 μM, CFTR channels are saturated by the millimolar ATP concentrations present in the cytosol of living cells. ATP-dependent gating is therefore regulated through phosphorylation/dephosphorylation of the CFTR protein. PKA, the key regulator of CFTR activity, phosphorylates multiple R-domain serines found in consensus motifs – a process essential for channel gating (9, 20). In addition, several other kinases have been identified that affect CFTR function. CFTR phosphorylation by protein kinase C (PKC) was shown to cause partial current activation (21, 225), and basal PKC phosphorylation of some CFTR residue(s) was claimed essential for subsequent full channel activation by PKA (35, 111). *In vitro* studies using an R-domain peptide identified R-domain serines 686 and 790 as the target sites for PKC phosphorylation (183). AMP-activated protein kinase (AMPK) binds to the C-terminus of CFTR and phosphorylates the CFTR protein *in vitro* (98), and co-expression of AMPK with CFTR in *Xenopus laevis* oocytes (98) or pharmacological activation of endogenous AMPK in a lung epithelial cell line (97) lower whole-cell CFTR currents. Tyrosine kinases, including p60c-Src and the proline-rich tyrosine kinase 2 (Pyk2) are both capable of activating CFTR currents (22, 81), and such activation is prevented by simultaneous mutation of two tyrosines at positions 625 and 627, implicating the latter residues as likely tyrosine kinase substrates (23). CaM kinase I was also found to phosphorylate a CFTR R-domain peptide *in vitro* (183), but no effects on channel activity have so far been demonstrated (21). Cyclic GMP-dependent protein kinase isoforms have also been found to phosphorylate CFTR, an activity that is likely to play a role in the action of heat-stable enterotoxins during secretory diarrheas (82), and possibly in CFTR current activation by S-Nitrosoglutathione in an airway cell line (41). In particular isoform II (cGKII), isolated from pig intestines was shown to phosphorylate the R-domain, with patterns of 2D-peptide mapping similar to PKA, and result in activation of CFTR channels in heterologous expression systems and in an intestinal cell line (82)

Several phosphatases have been tested for their effectiveness in dephosphorylating CFTR. Whereas phosphatases 1 (PP1) and 2B (PP2B, calcineurin) little affect currents of prephosphorylated CFTR (21, 149); but, cf., (80)), phosphatases 2A (PP2A; (21, 149) and 2C (PP2C; (149, 232)) have both been shown to efficiently deactivate CFTR channels in inside-out patches. The relative

contribution of these two phosphatases to CFTR regulation *in vivo* is likely cell-type specific. Among exogenous phosphatases frequently used for *in vitro* studies, alkaline phosphatase does not affect CFTR activity (21), whereas lambda phosphatase deactivates CFTR (81) and abolishes detectable phosphorylation of CFTR protein purified from resting cells (145).

B. Target sites of PKA

PKA phosphorylates serines and threonines of target proteins found in consensus motifs of the form R-R/K-X-S/T (dibasic sites) or R-X(-X)-S/T (monobasic sites), with a preference for dibasic motifs (116). The R domain sequence in CFTR (a.a.s ~640 to ~840) contains nine dibasic and several monobasic PKA consensus motifs; a further serine in a dibasic motif, S422, localizes to the RI segment of NBD1. Out of this pool of potentially phosphorylatable residues a large number of studies have identified at least nine positions that are phosphorylated by PKA either *in vivo* or *in vitro* (Table 1). Although found in a dibasic motif, serine 686 was not seen to be phosphorylated by PKA, but instead was found to be a substrate for PKC (183). To our knowledge, phosphorylation by PKA of threonine 788, located in a dibasic motif, has not yet been demonstrated.

Under *in vitro* conditions gradual phosphorylation of an R-domain peptide by PKA causes incremental electrophoretic mobility shifts, allowing visual discrimination of up to six distinct phosphoforms that appear with different kinetics (Fig. 6A). 2-D peptide mapping and mass spectrometric analysis of the phosphoforms revealed that phosphorylation of serine 737 causes the largest mobility shift, and identified serine 768 as being among the first to become phosphorylated (58, 183).

C. Stimulatory and inhibitory phosphorylation sites

In inside-out patches, in the presence of saturating ATP but various concentrations of the active catalytic subunit of PKA (Fig. 6B), the steady-state open probability of single CFTR channels shows a roughly hyperbolic dependence on PKA concentration ((58); Fig. 6C, *red symbols*). Because membrane-associated endogenous phosphatase activity is independent of the amount of applied kinase, at steady state the R domain is expected to become phosphorylated to a higher stoichiometry when the

applied PKA concentration is higher. The implication is that channel open probability is not regulated in an all-or-none fashion by PKA, but is rather roughly proportional to the degree (stoichiometry) of R-domain phosphorylation. Thus, most PKA target serines might be classified as "stimulatory PKA sites". Accordingly, mutation to alanine of four, eight (199) or ten (34) consensus serines substantially reduced channel open probability in the presence of ATP and PKA. Surprisingly, however, even channels lacking all ten serines located in dibasic PKA sites retain substantial phosphorylation-dependent channel activity, with a maximal open probability almost 50% of that of WT CFTR (154), implying large functional redundancy among PKA target serines. Just as different PKA target sites are phosphorylated with different kinetics, the rates of dephosphorylation of individual phosphoserines by membrane-associated endogenous phosphatases are likely diverse: in inside-out patches excised from various cell types (9, 55, 250) macroscopic CFTR currents decline with a biexponential time course following sudden removal (or inhibition) of PKA (Fig. 6D). An initial rapid partial current decline (within seconds) is followed by a much slower decay (over minutes), suggesting the existence of a relatively stable "partially phosphorylated" state of CFTR distinguishable from the "fully phosphorylated" state by ~2-3-fold shorter mean burst durations and ~2-fold longer interburst durations (55).

Whereas alanine replacement of most PKA target serines negatively affects channel activation, mutation of serines 737 and 768 were found to increase the sensitivity of whole-cell CFTR currents towards activation by 3-isobutyl-1-methylxanthine (IBMX), which activates endogenous PKA by elevating cellular cAMP levels (260). Classification of serines 737 and 768 as "inhibitory PKA sites" was further supported by slightly and robustly elevated open probabilities, respectively, of S737A and S768A CFTR channels in inside-out patches ((237); but, cf., (100)). The S768A mutation increases the sensitivity for channel activation by PKA, resulting in substantial CFTR currents already at the low endogenous PKA activity of resting, unstimulated cells, but also increases maximal open probability (Fig. 6C, *blue symbols*), mainly by lengthening mean burst durations. These effects appear to be direct effects on channel gating, as the kinetics and degree of phosphorylation of other PKA target serines remain largely unaffected in the mutant (58, 100)). The *in vivo* relevance of inhibitory CFTR regulation might be twofold. First, by shifting the PKA dose response curve to the right, phosphorylation of serine

768 by PKA, already detectable at basal PKA activity levels, might dampen the WT CFTR current response to low levels of PKA stimulation (Fig. 6C). Second, serine 768 was also identified as the target site for phosphorylation by inhibitory AMPK (119, 123), so its phosphorylation might represent a mechanism to adjust CFTR activity to the metabolic state of the cell.

D. Molecular mechanism of gating regulation by phosphorylation

PKA-dependent regulation of CFTR activity can be largely ascribed to an inhibitory influence of the unphosphorylated R domain on channel gating, which is relieved upon phosphorylation. Whereas unphosphorylated WT CFTR channels show negligible open probability, a construct in which a large part (a.a. 708-835) of the R domain is deleted (ΔR CFTR) is substantially active without phosphorylation (200). Similarly, deletion of the entire R domain (a.a. 634-836) by co-expression of CFTR segments 1-633 and 837-1480 (cut-ΔR CFTR) yields channels that are active prior to phosphorylation, whereas channels merely split in two, but still containing the R domain – obtained by co-expression of CFTR segments 1-633 and 634-1480 – remain strictly regulated by PKA (55).

In addition to loss of an inhibitory effect, a direct stimulation of channel gating by the phosphorylated R domain also seems to contribute to the full gating response of CFTR to PKA, as unphosphorylated ΔR CFTR is slightly stimulated by superfusion with a phosphorylated R-domain peptide (150, 262). Accordingly, open probability of unphosphorylated cut-ΔR CFTR is somewhat lower than that of fully phosphorylated split channels containing the R domain (55). Quantitative analysis suggests that disinhibition accounts for ~50-fold, whereas direct stimulation by the phosphorylated R domain accounts for an additional ~2-fold, increase in open probability, amounting to an ~100-fold total enhancement of WT CFTR channel currents by PKA (54).

In searches for the biophysical mechanism that underlies the regulatory effect of the R domain, a number of observations have been made. Pull-down assays documented phosphorylation-dependent interactions of the R domain with other parts of the channel (29, 36), including the lasso motif (Fig. 1E, *red*), which is located at CFTR's cytoplasmic N terminus (166) and has been shown to also act as an interaction hub for other proteins (167). Introduction of stable negative charges by replacement of up to eight R-domain PKA target serines with aspartates (199) or glutamates (4, 18) resulted in a small but

substantial activity prior to exposure to exogenous PKA, although some part of that small activity might have reflected basal phosphorylation of remaining serines by endogenous kinases. In any case, given the existence of both inhibitory and stimulatory sites, mere accumulation of negative charge in the R domain is unlikely to explain channel activation by phosphorylation: rather, conformational changes must also play a role.

Several mechanisms of phosphorylation-dependent regulation of CFTR gating had been proposed in the past. The unphosphorylated R domain was suggested to act as a plug that physically occludes the pore (199, 200). Phosphorylation was suggested to increase the affinity of ATP for binding to the NBDs (131, 154, 262). Prompted by their spatial positioning and high mobilities in the NBD1 structure, as well as their inclusion of phosphorylatable serines, the RI and RE segments were suggested to impede NBD dimerization while unphosphorylated (130). However, split ΔRI CFTR channels lacking residues 415-432, as well as split ΔRE channels lacking residues 634-667, and ΔRE channels with the only phosphorylatable serine in the RI mutated (ΔRE/S422A), all retained unaltered, strict PKA-dependence of channel activity (54). Moreover, even the low-level ATP-independent activity of CFTR channels with the entire NBD2 domain (a.a. 1198-1480) deleted (ΔNBD2) remains fully dependent on phosphorylation by PKA, suggesting that the R domain exerts its modulatory effect by acting directly on the TMD extensions (248). Finally, because phosphorylation little affected [α^{32}P]8-azido-ATP labeling of NBD1, or of NBD2 in the presence of V_i, phosphorylation was suggested to modulate coupling between ATP hydrolysis cycles and gating movements, similar to an automobile clutch (14).

A recent breakthrough toward a clear mechanistic picture has come with the first high-resolution structures of unphosphorylated CFTR (145, 273). Although in those structures the R domain is not well resolved, consistent with the suggested lack of a well defined structure, its clearly visible density is wedged in between the two NBDs and among the cytosolic extensions of the TM helices. Such an arrangement is sterically incompatible both with a transition to an outward-facing TMD conformation and with NBD dimerization, explaining the inhibitory effect of the unphosphorylated R domain on channel gating. A single resolvable α-helix wedged in between the TM helices, believed to correspond to residues 825-843 of the R domain (Fig. 1E, *yellow surface plot*), is likely important for

inhibition, as severing that helix by co-expression of CFTR segments 1-835 and 837-1480 results in channels that display substantial phosphorylation-independent channel activity (55). In light of the occluded localization of the unphosphorylated R domain (cartooned as a *red tongue* in Fig. 6E), how does PKA gain access to its target serines? Possibly, occasional spontaneous release of the unphosphorylated R-domain peptide from its occluded position (Fig. 6E, *left*; D="dephosphorylated") renders it accessible to the kinase (Fig. 6E, *center*; P="phosphorylatable") which, by phosphorylating its serines, traps the R domain in its released conformational ensemble (Fig. 6E, *right*; M="maximally phosphorylated"), no longer incompatible with an outward-facing (open-pore) TMD conformation. Consistent with occasional release of the unphosphorylated R domain, dephosphorylated CFTR protein displays a small but measurable ATPase activity (131, 145), and, also in the presence of ATP, unphosphorylated CFTR channels are seen to gate with a small but discernible open probability (Fig. 6D, *inset*; (145)): neither process is compatible with the wedged-in position of the R domain seen in the unphosphorylated structures. Moreover, the time course of macroscopic CFTR current activation upon exposure to PKA is clearly sigmoidal (Fig. 6D), and can be reasonably well fitted assuming two sequential slow steps in the activation process (Fig. 6D, *red curve*): the slowest step might reflect the spontaneous R-domain release (Fig. 6E, step D$\rightarrow$P, rate k_{a1}), and the subsequent step, R-domain phosphorylation (Fig. 6E, step P$\rightarrow$M, rate k_{a2}).

Open questions remain. It is still unclear whether in unphosphorylated CFTR ATP hydrolysis might happen without concomitant pore opening, as implied by the automobile clutch model. On the one hand, based on the available structures it is unclear how NBD dimerization (required for ATP hydrolysis) might occur without concomitant pore opening. But, on the other hand, although phosphorylation clearly robustly stimulates ATPase activity, the 8- (145) to 15-fold (131) difference in ATPase rates measured for PKA- vs. phosphatase-treated purified CFTR protein seems to fall short of explaining the ~100-fold stimulation of channel currents upon PKA exposure (Fig. 6D; (54)), unless specific gating changes are invoked. Possibly, some of the "basal" ATPase activity measured for dephosphorylated CFTR might reflect a minute contamination by some highly active ATPase: given the turnover rate of ~1 s^{-1} for CFTR, but up to ~1000 s^{-1} for many other ATPases, a 0.01% contamination of a CFTR protein preparation by such an ATPase might account for a "basal" activity

~10% of that of phosphorylated CFTR, possibly contributing to the much lower apparent stimulation of ATPase than of channel activity by phosphorylation. A further uncertainty is the mechanism of the ~2-fold stimulation of channel open probability by the phosphorylated R domain, an action apparently distinct from the ~50-fold stimulation that results from the disinhibitory effect of phosphorylating, or deleting, the R domain. Kinetic analysis suggests the ~2-fold stimulation reflects in part slowing of channel closure (55), but the absence of any density for the R domain in the cryo-EM structure of phosphorylated CFTR precludes speculation as to how that might occur.

VI. Targeting CFTR function to treat disease

While for decades the treatment of CF has largely focused on treating the symptoms of the disease, in recent years new drugs have emerged that directly bind to CFTR and so target the primary molecular defect. "Potentiators" are small molecules that enhance CFTR open probability, thus offering hope to restore channel activity decreased by Class III (and IV) CF mutations. In contrast, pharmacological agents aimed at amending the protein folding/processing defect caused by Class II CF mutations are called "correctors". Because the most common CF mutation, ΔF508, belongs to both classes, effective treatment of the majority of CF patients will likely require a viable combination of corrector and potentiator drugs. The following paragraphs provide a brief overview of what is known about how presently available potentiators work.

The feasibility of designing practically useful potentiators was signalled by early identification of a number of compounds that stimulate CFTR channel gating when applied *in vitro*. Replacement of ATP with various analogs such as P-ATP (280), 2'- and 3'-deoxy-ATP (3), 2'-deoxy-P-ATP (P-dATP) (161) increases open probability for WT CFTR, and even more so for mutants with low open probabilities. The structurally unrelated natural plant compounds genistein (105, 247), capsaicin (2), and curcumin (19, 248) were shown to increase CFTR activity with apparent affinities in the tens-of-micromolar range. All three compounds act by simultaneously speeding channel opening and delaying channel closure, and likely share overlapping binding sites, as the effects of genistein and capsaicin (2), or of genistein and curcumin (19), are competitive. The negatively charged voltage-dependent pore

blocker NPPB (276) was later found to strongly potentiate channel open probability, and this potentiator effect was retained, without pore block, in the uncharged amide analog NPPB-AM (250). NPPB similarly increases the rates of opening and of non-hydrolytic closure of WT CFTR (59), suggesting that it decreases the energetic barrier for the $C_1 \leftrightarrow O_1$ step (Fig. 2E): interestingly, thanks to CFTR's non-equilibrium gating cycle, such a catalyst effect might enhance opening rate without speeding normal (hydrolytic) closure. In fact, NPPB also slows hydrolytic channel closing rate by slowing the ATP hydrolysis step (Fig. 2E, step $O_1 \rightarrow O_2$; (59)). These two distinct kinetic effects can be ascribed, respectively, to the 3-nitrobenzoate, and 3-phenylpropylamine, moieties of the parent compound (60). In addition, NPPB also increases open probability of the G551D mutant (134) which opens preferentially with site 2 vacant (133), suggesting that it might either stabilize the monoliganded open state more than the transition state for the $C_1 \leftrightarrow O_1$ step, or stabilize only the monoliganded open state in the mutant.

The first potentiator evaluated in clinical trials was VX-770 (ivacaftor), identified by Vertex Pharmaceuticals using high-throughput screening. VX-770 very effectively stimulates CFTR channels carrying the common Class III mutation G551D (~2% of CF alleles), but was also found to enhance ΔF508 CFTR activity *in vitro* (238). Later work demonstrated the drug's efficacy on a number of other, less frequent, Class III (and Class IV) mutants (267). At present the drug is approved in most Western countries for the treatment of CF patients carrying G551D and some other rare mutant alleles, all of which strongly impact gating. *In vitro* mechanistic studies of VX-770 action revealed current stimulation for both WT CFTR and for non-hydrolytic mutants. Kinetically, VX-770 acts by increasing channel opening rate and by slowing both hydrolytic and non-hydrolytic closing rate (112, 125, 134). Although more complex mechanisms have been suggested (see Section IV. E, (112)), the simplest explanation of these kinetic effects is a stabilization of state O_1 (relative to both C_1 and O_2; Fig. 2E) by the drug: just as for the binding of ATP itself (see Section IV. F), VX-770 stabilizes the transition state (T, Fig 3B) for opening (modestly increasing rate k_{CO}), but stabilizes state O_1 even more (decreasing rate k_{-1}). Insofar as the rarely visited unliganded open state of CFTR is structurally similar to state O_1 (see Section IV. D, (160)), such a mechanism would also explain the observed stimulation by VX-770 of spontaneous channel activity in the absence of ATP (74, 112). Similar fold-potentiation of non-

hydrolytic mutants, K464A CFTR, and WT CFTR channels – which visit the posthydrolytic state O_2 in none, in a small proportion, or in all of the open-burst events, respectively – suggests that any effect on stability of the posthydrolytic state O_2 (112) is likely to be minor (126). Consistent with its extremely hydrophobic nature (logP~6.3) the binding site for VX-770 is believed to be located in the membrane-spanning region of CFTR (112).

The clinical success of administering VX-770 in combination with corrector compounds to treat patients carrying ΔF508 alleles has, so far, been limited (244). This disappointing result might be due to a demonstrated negative impact of VX-770 on ΔF508 CFTR biogenesis, and particularly on its stability at the plasma membrane. Thus the potentiator appears to effectively counteract the action of co-administered corrector drugs, VX-809 (lumacaftor), and VX-661 (45, 240). Surprisingly, a number of structurally diverse potentiators were found to cause a similar reduction in ΔF508 CFTR plasma membrane density (240). As mentioned above, F508 is positioned at the transmission interface that connects the TMDs and NBD1, on the outer side of the "socket" in which CH4 (the "ball" element of the joint, see Section II. C), fits. A conserved short α-helix completes the socket in most ABC protein NBDs (see Fig. 1B, *green helix* in NBD2) but is absent from CFTR's NBD1. It is possible that the reduced metabolic stability of potentiator-bound ΔF508 CFTR at the plasma membrane might result from the increased frequency of opening, and hence increased exposure of the fragile mutant, lacking the socket-completing phenylalanine, to the high molecular strain of the opening transition state ((6, 57, 155), see Section IV. C). Consistent with this interpretation, mutations, such as E1371S, that decrease the frequency of pore opening events by greatly prolonging burst duration, were seen to protect ΔF508 CFTR from VX-770-induced peripheral instability (240). These considerations suggest that potentiators that increase burst duration, and/or strongly reduce the strain in the opening transition state (59, 60), might be better suited for treatment of patients carrying the ΔF508 mutation. Given the very large number of CFTR mutations known to cause CF, this observation highlights how "precision" potentiator development might need to be tailored according to the CFTR genotype, as potentiators developed for potency/efficacy on ΔF508 CFTR might not provide maximal therapeutic benefit to all CF patients.

Recently, the potentiator GLPG1837, developed by Abbvie-Galapagos, has also entered clinical trials. Although GLPG1837 was found to be more effective on G551D and G1349D CFTR than VX-770, the mechanisms of action of the two drugs seem similar: indeed, GLPG1837 also potentiates both WT CFTR and non-hydrolytic mutants, and acts by speeding channel opening and by slowing both hydrolytic and non-hydrolytic pore closure (265). Thus, just as for VX-770, a plausible mechanism for GLPG1837 might be stabilization of state O_1 relative to C_1, O_2 (Fig. 2E) and T (Fig. 3B). In line with such an explanation, GLPG1837 also stimulates spontaneous CFTR opening (265). In contrast to NPPB, which acts synergistically with VX-770 suggesting distinct binding sites, GLPG1837 and VX-770 act competitively, suggesting that binding of these two drugs is mutually exclusive, i.e., that their binding sites might overlap (265).

Several additional laboratories are actively involved in CFTR potentiator development. Employing high-throughput screening, the Verkman group was the first to identify potentiators with low micromolar (84) or submicromolar (152, 180) affinities, based on a variety of structurally unrelated chemical scaffolds. Furthermore, some of their recently identified potentiators have been shown not to reduce plasma membrane density of ΔF508 CFTR or to interfere with the corrector effect of VX-809, and are therefore promising candidates for CF therapy of patients carrying ΔF508, or similar phenotype, alleles (182). Other groups have identified potential lead compounds capable of increasing CFTR open probability ((79, 127, 179), https://www.cff.org/Trials/Pipeline/details/91/QBW251). However, so far, the mechanisms of action of all these compounds have not been studied in detail.

The recognition that CFTR plays a vital physiological role in regulating transepithelial fluid movement has prompted researchers to start considering it as a pharmacological target for treatment of disorders other than CF. Potentiators might be useful for the treatment of other airway diseases sharing characteristics with CF, such as mucus stasis and CFTR dysfunction/inhibition. One such area of clinical interest is the treatment of Chronic Obstructive Pulmonary Disease (COPD) (191, 214). Focusing instead on CFTR expressed in intestinal epithelia, initial results suggest CFTR potentiators can outperform currently approved treatments for constipation (47, 217).

In contrast, CFTR inhibitors might provide benefit in diseases characterized by excessive transepithelial fluid movement. Such compounds could help prevent cyst formation in autosomal

dominant polycystic kidney disease (ADPKD) (132, 263), and could be crucial in preventing death by dehydration caused by secretory diarrhoeas (e.g. following cholera infection), especially in situations in which obtaining safe water for oral rehydration therapy is problematic (229). The voltage-dependent pore blocker GlyH-101 that acts from outside the cell has been described (Section III. D). $CFTR_{inh}$-172 (3-[(3-trifluoromethyl)phenyl]-5-[(4-carboxyphenyl)methylene]-2-thioxo-4-thiazolidinone), was identified by high-throughput screening as a membrane permeant compound which inhibits CFTR currents in a voltage-independent manner, with a K_I of ~300 nM (151). Studies addressing the mechanism of this inhibition concluded that $CFTR_{inh}$-172 does not act as a pore blocker, but rather as a gating modifier that delays pore opening and accelerates pore closure (124, 228). More recently, higher potency benzopyrimido-pyrrolo-oxazinedione compounds have been identified that bind at site 2, in competition with ATP, thus impeding channel opening (118). The nanomolar potency attained with these compounds might make such drugs specific enough to avoid short-term toxicity at non-target ATP binding sites.

VII. Concluding remarks

Almost three decades after the cloning of the CFTR gene our understanding of CFTR structure and function has seen tremendous progress, while high-throughput screening has led to the development of potentiator and corrector drugs that are finding their way to clinical application. There are undoubtedly still major gaps in our knowledge that need to be filled. These include unraveling what an open channel looks like and what state the outward-facing zebrafish CFTR structure represents, clarifying the existence and functional significance of reentry events, determining the extent of interface separation in the degenerate site of closed channels during gating, dissecting possible conformations of the R domain and their dependence on phosphorylation, and mapping protein-protein interactions of CFTR with scaffolding proteins and with other channels and transporters. That notwithstanding, with the recent breakthrough provided by the first high-resolution structures, CFTR research has transitioned into a new era, one that holds the promise of exploiting atomic-level structural information and advances in mechanistic understanding of CFTR molecular motions to guide drug

development. There is now well-grounded hope that decades of basic research could soon strongly impact human health, resulting in novel treatments for a variety of disorders, and an effective causative treatment for both common and rare forms of CF.

Acknowledgements

Supported by Cystic Fibrosis Trust CFT Project No SRC 005 and Sparks Grant Ref. No15UCL04 to P.V., and Hungarian Academy of Sciences Lendület grant LP2017-14/2017 and Cystic Fibrosis Foundation Research Grant CSANAD17G0 to L.C.

Tables and Figure legends

Table 1: CFTR positions phosphorylated by PKA in vivo or in vitro

	660	700	712	737		768	795	813	((43): CFTR in vitro)
	660			737			795	813	((43): CFTR in vivo)
	660	700		737		768	795	813	((183): CFTR in vitro)
					753*				((206): CFTR in vitro)
422	660	700	712	737		768	795	813	((231): NBD1-R in vitro)
	660	700	712	737	753*	768	795	813	((168), CFTR in vitro)
	660	700	712	737		768	795		((58), CFTR in vivo**)

*monobasic site
**resting *Xenopus laevis* oocytes

Fig. 1. CFTR domain topology and structure. *A*, CFTR domain topology. TMD1 (*light gray*), TMD2 (*dark gray*), intracellular loops (*light purple*), NBD1 (*blue*), NBD2 (*green*), R domain (*rose*), membrane (*yellow*). *B*, Ribbon representation of NBD1 (*left*) and NBD2 (*right*) from the cryo-EM structure of the phosphorylated, ATP-bound form of zebrafish CFTR (PDBID: 5W81). F1-like parallel β-sheet plus α-helices (*green*), ABC-specific antiparallel β-sheet (*cyan*), α-helical subdomain (*orange*), Walker A motif (*red*), Walker B motif (*marine*), signature motif (*magenta*), ATP (*yellow sticks*), Mg^{2+} ion (*slate sphere*). The numbering of the conserved residues shown in stick representation is based on the human CFTR sequence. An E-to-Q mutation of the catalytic glutamate in NBD2 was used to trap the protein in an ATP-bound form. In NBD1 *light magenta dotted lines* mark the locations in the primary sequence of the unresolved regulatory insertion (RI) and regulatory extension (RE). *C*, Organization of the ATP-bound head-to-tail NBD1-NBD2 heterodimer (from PDBID: 5W81). NBD1 (*blue*), NBD2 (*green*), ATP molecules (*yellow sticks*), Walker-A motifs (*red*), signature sequences (*magenta*). The conserved Walker-A lysines are shown as *red spheres*. *D*, Cartoon representation of residue asymmery in the CFTR NBD dimer, color coding of conserved residues as in *B*. The upper site (site 1, degenerate site) harbours all non-canonical substitutions, whereas in the lower site (site 2, canonical site) all catalytically important side chains are intact. *E*, Ribbon representation of the dephosphorylated human CFTR apo-structure (PDBID: 5UAK); domain color coding as in *A*. Lasso

motif (*red*), R-domain helix modeled into observed density (*yellow surface*), coupling helices (*magenta*), ATP (*yellow sticks*), membrane (*horizontal gray lines*). *F*, Ribbon representations of the structure of phosphorylated ATP-bound CFTR (PDBID: 5W81) viewed from two different orientations; left view, and domain color coding, as in *E*. The view to the right shows the cytoplasmic opening of the ion permeation pathway (*red arrow*, "lateral opening") flanked by TM helices 4 (*yellow*) and 6 (*orange*); positively charged residues lining the opening are shown as *blue spheres*. Outer segments of TM8 and TM12 are colored (*cyan* and *deep cyan*); TM7 is *pale green*; the lasso motif has been removed for clarity.

Fig. 2. Coupling of CFTR pore opening to NBD dimerization. *A*, An arginine-threonine (serine) or a lysine-asparagine side chain pair is optimally positioned to form a salt bridge between CFTR positions 555 and 1246. *B-C*, Single-channel outward current traces (*B*; V_m=+40 mV) and mean closed (interburst) durations (*C*) of pre-posphorylated WT, R555K, 1246N, and R555K/T1246N CFTR channels gating in 5 mM MgATP. *D*, Thermodynamic mutant cycle illustrating mutation-induced changes in $\Delta G^{\ddagger}_{T\text{-}C}$ (numbers next to arrows); $\Delta\Delta G_{int(opening)}$ is the difference between $\Delta\Delta G^{\ddagger}_{T\text{-}C}$ values along two parallel sides of the cycle. The four corners of the cycle are represented by the pairs of residues present at positions 555 and 1246, respectively. *E*, Cartoon gating cycle of phosphorylated CFTR. Color coding as in Fig. 1A, the R domain is not depicted. Site 1 (degenerate site), *upper site*; site 2 (canonical site), *lower site*; ATP, *yellow circles*, ADP, *orange crescent*; chloride ions, *dark red dots*. Panels *A-D* adapted with permission from (242).

Fig. 3: Cytosolic-to-extracellular Φ-value gradient, and asymmetry between sites 1 and 2. *A*, Cartoon representation of homology models (52) of phosphorylated closed- (*left*) and open-state (*right*) CFTR, with color coding as in Fig. 1A; the R domain is omitted. Target positions for REFER analysis are highlighted in colored spacefill (*left*), corresponding colored numbers illustrate estimated Φ values (*right*). *B*, Cartoon representation of approximate structural rearrangements during the pore opening transition, as the channel transits from an ATP-bound closed state (C_1) through the transition state (T) to the ATP-bound open state (O_1). Site 1 (degenerate site), *upper site*; site 2 (canonical site), *lower site*;

color coding as in Fig. 2E. *Vertical colored arrow* illustrates the direction of the spreading conformational wave. *Red arcs* in states T and O_1 represent tight bonding across the NBD interface. Adapted with permission from (219, 220).

Fig. 4: Spontaneous pore openings are also coupled to NBD dimerization. *A*, Microscopic inside-out patch recordings of CFTR background construct P355A-K978C, and of channels bearing mutations R555K, T1246N, and R555K-T1246N in that background; V_m=-80 mV. *B*, Open probabilities of the constructs in *A* (see *color coding*) during the last 4 minutes of each 5-minute ATP-free segment of recording. *C*, Thermodynamic mutant cycle illustrating mutation-induced changes in $\Delta G_{O\text{-}C}$ (numbers next to arrows); $\Delta\Delta G_{int(O\text{-}C)}$ is the difference beween $\Delta\Delta G_{O\text{-}C}$ values along two parallel sides of the cycle. The four corners of the cycle are represented by the pairs of residues present at positions 555 and 1246, respectively. *D*, Cartoon depicting mechanism of spontaneous openings. Color coding as in Fig. 1A; the R domain is not depicted. Adapted with permission from (160).

Fig. 5: Distributions of CFTR burst durations support non-equilibrium gating. *A-C*, Distributions of burst durations for prephosphorylated WT (*A*), D1370N (*B*), and K464A (*C*) CFTR channels gating in 2 mM ATP at 25°C. *Solid red lines* in *A* and *C* are maximum likelihood fits to the scheme in panel D; in *A* rate k_{-1} was fixed to zero. *Dotted blue lines* in *A-C* are maximum likelihood fits to a non-hydrolytic equilibrium $C_1 \leftrightarrow O_1$ scheme. Fitted rates are printed in the panels. *Insets* show 30-s segments of single-channel inward currents; V_m=-80 mV. *D*, Cartoon gating cycle illustrating coupling ratios. *Colored vertical* and *horizontal arrows* and *numbers* depict fractions of bursts terminated through ATP hydrolysis and non-hydrolytic NBD dimer dissociation, respectively, for WT (*blue*), K464A (*red*), and D1370N (*green*) CFTR. Adapted with permission from (61).

Fig. 6: Regulation of CFTR channel activity through phosphorylation by PKA. *A*, Time course of phosphorylation of an R-domain peptide (aa. 645-835) by PKA resolved by SDS-PAGE. Autoradiogram shows samples incubated for the indicated time intervals in 1 or 50 μM (as indicated) [γ^{32}P]-ATP and 0.2 μg/ml PKA catalytic subunit. Six distinct resolvable bands are numbered. *B*, Inside-

out patch recording showing activity of four WT CFTR channels exposed to 55 and then 550 nM PKA catalytic subunit in the presence of 2 mM MgATP; V_m=+40 mV. *C,* Steady-state open probability of WT (*red symbols*) and S768A (*blue symbols*) CFTR channels gating in 2 mM ATP and various concentrations of PKA catalytic subunit, plotted as a function of [PKA]. Solid lines are fits to the Hill equation; $P_{o,max}$=0.34±0.06, $K_{0.5}$=149±46 nM, n_H=1.5± 0.5 for WT, and $P_{o,max}$=0.51±0.05, $K_{0.5}$=71±12 nM, n_H=1.8±0.5 for S768A. *D,* Macroscopic CFTR current elicited in an inside-out patch by exposure to 2 mM MgATP (*gray bar*) and 300 nM PKA catalytic subunit (*black bar*); V_m=-80 mV. Activation time course is fitted (*red line*) to a sequential two-step mechanism of the form closed→closed→active. *E,* Cartoon model of two-step channel activation; color coding as in Fig. 2E; R domain, *red tongue*; "D", dephosphorylated, "P", phosphorylatable, "M", maximally phosphorylated. Occasional spontaneous release of the unphosphorylated R domain (step D→P) allows its phosphorylation by PKA (step P→M). Adapted with permission from (58) (panels *A*-*C*) and (145) (panels *D*-*E*).

References

1. Ai, T., Bompadre, S. G., Sohma, Y., Wang, X., Li, M. & Hwang, T. C. Direct effects of 9-anthracene compounds on cystic fibrosis transmembrane conductance regulator gating. *Pflugers Arch* **449**, 88-95, 2004.

2. Ai, T., Bompadre, S. G., Wang, X., Hu, S., Li, M. & Hwang, T. C. Capsaicin potentiates wild-type and mutant cystic fibrosis transmembrane conductance regulator chloride-channel currents. *Mol Pharmacol* **65**, 1415-1426, 2004.

3. Aleksandrov, A. A., Aleksandrov, L. & Riordan, J. R. Nucleoside triphosphate pentose ring impact on CFTR gating and hydrolysis. *FEBS Lett* **518**, 183-188, 2002.

4. Aleksandrov, A. A., Chang, X., Aleksandrov, L. & Riordan, J. R. The non-hydrolytic pathway of cystic fibrosis transmembrane conductance regulator ion channel gating. *J Physiol* **528 Pt 2**, 259-265, 2000.

5. Aleksandrov, A. A., Cui, L. & Riordan, J. R. Relationship between nucleotide binding and ion channel gating in cystic fibrosis transmembrane conductance regulator. *J Physiol* **587**, 2875-2886, 2009.

6. Aleksandrov, A. A. & Riordan, J. R. Regulation of CFTR ion channel gating by MgATP. *FEBS Lett* **431**, 97-101, 1998.

7. Aleksandrov, L., Aleksandrov, A. A., Chang, X. B. & Riordan, J. R. The First Nucleotide Binding Domain of Cystic Fibrosis Transmembrane Conductance Regulator Is a Site of Stable Nucleotide Interaction, whereas the Second Is a Site of Rapid Turnover. *J Biol Chem* **277**, 15419-15425, 2002.

8. Aller, S. G., Yu, J., Ward, A., Weng, Y., Chittaboina, S., Zhuo, R. P., Harrell, P. M., Trinh, Y. T., Zhang, Q. H., Urbatsch, I. L. *et al.* Structure of P-Glycoprotein Reveals a Molecular Basis for Poly-Specific Drug Binding. *Science* **323**, 1718-1722, 2009.

9. Anderson, M. P., Berger, H. A., Rich, D. P., Gregory, R. J., Smith, A. E. & Welsh, M. J. Nucleoside triphosphates are required to open the CFTR chloride channel. *Cell* **67**, 775-784, 1991.

10. Auerbach, A. How to turn the reaction coordinate into time. *J Gen Physiol* **130**, 543-546, 2007.

11. Bai, Y. H., Li, M. & Hwang, T. C. Dual roles of the sixth transmembrane segment of the CFTR chloride channel in gating and permeation. *J Gen Physiol* **136**, 293-309, 2010.

12. Bai, Y. H., Li, M. & Hwang, T. C. Structural basis for the channel function of a degraded ABC transporter, CFTR (ABCC7). *J Gen Physiol* **138**, 495-507, 2011.

13. Barsony, O., Szaloki, G., Turk, D., Tarapcsak, S., Gutay-Toth, Z., Bacso, Z., Holb, I. J., Szekvolgyi, L., Szabo, G., Csanady, L. *et al.* A single active catalytic site is sufficient to promote transport in P-glycoprotein. *Sci Rep* **6**, 24810, 2016.

14. Basso, C., Vergani, P., Nairn, A. C. & Gadsby, D. C. Prolonged nonhydrolytic interaction of nucleotide with CFTR's NH2-terminal nucleotide binding domain and its role in channel gating. *J Gen Physiol* **122**, 333-348, 2003.

15. Baukrowitz, T., Hwang, T. C., Nairn, A. C. & Gadsby, D. C. Coupling of CFTR Cl- channel gating to an ATP hydrolysis cycle. *Neuron* **12**, 473-482, 1994.

16. Bear, C. E., Li, C. H., Kartner, N., Bridges, R. J., Jensen, T. J., Ramjeesingh, M. & Riordan, J. R. Purification and functional reconstitution of the cystic fibrosis transmembrane conductance regulator (CFTR). *Cell* **68**, 809-818, 1992.

17. Beck, E. J., Yang, Y., Yaemsiri, S. & Raghuram, V. Conformational changes in a pore-lining helix coupled to cystic fibrosis transmembrane conductance regulator channel gating. *J Biol Chem* **283**, 4957-4966, 2008.

18. Becq, F., Verrier, B., Chang, X. B., Riordan, J. R. & Hanrahan, J. W. cAMP- and Ca2+-independent activation of cystic fibrosis transmembrane conductance regulator channels by phenylimidazothiazole drugs. *J Biol Chem* **271**, 16171-16179, 1996.

19. Berger, A. L., Randak, C. O., Ostedgaard, L. S., Karp, P. H., Vermeer, D. W. & Welsh, M. J. Curcumin stimulates cystic fibrosis transmembrane conductance regulator Cl- channel activity. *J Biol Chem* **280**, 5221-5226, 2005.

20. Berger, H. A., Anderson, M. P., Gregory, R. J., Thompson, S., Howard, P. W., Maurer, R. A., Mulligan, R., Smith, A. E. & Welsh, M. J. Identification and regulation of the cystic fibrosis transmembrane conductance regulator-generated chloride channel. *J Clin Invest* **88**, 1422-1431, 1991.

21. Berger, H. A., Travis, S. M. & Welsh, M. J. Regulation of the cystic fibrosis transmembrane conductance regulator Cl- channel by specific protein kinases and protein phosphatases. *J Biol Chem* **268**, 2037-2047, 1993.

22. Billet, A., Jia, Y., Jensen, T., Riordan, J. R. & Hanrahan, J. W. Regulation of the cystic fibrosis transmembrane conductance regulator anion channel by tyrosine phosphorylation. *FASEB J* **29**, 3945-3953, 2015.

23. Billet, A., Jia, Y., Jensen, T. J., Hou, Y. X., Chang, X. B., Riordan, J. R. & Hanrahan, J. W. Potential sites of CFTR activation by tyrosine kinases. *Channels (Austin)* **10**, 247-251, 2016.

24. Bompadre, S. G., Ai, T., Cho, J. H., Wang, X., Sohma, Y., Li, M. & Hwang, T. C. CFTR gating I: Characterization of the ATP-dependent gating of a phosphorylation-independent CFTR channel (DeltaR-CFTR). *J Gen Physiol* **125**, 361-375, 2005.

25. Bompadre, S. G., Cho, J. H., Wang, X., Zou, X., Sohma, Y., Li, M. & Hwang, T. C. CFTR gating II: Effects of nucleotide binding on the stability of open states. *J Gen Physiol* **125**, 377-394, 2005.

26. Bompadre, S. G., Sohma, Y., Li, M. & Hwang, T. C. G551D and G1349D, two CF-associated mutations in the signature sequences of CFTR, exhibit distinct gating defects. *J Gen Physiol* **129**, 285-298, 2007.

27. Boucher, R. C. Regulation of airway surface liquid volume by human airway epithelia. *Pflugers Arch* **445**, 495-498, 2003.

28. Boucher, R. C., Stutts, M. J., Knowles, M. R., Cantley, L. & Gatzy, J. T. Na+ transport in cystic fibrosis respiratory epithelia. Abnormal basal rate and response to adenylate cyclase activation. *J Clin Invest* **78**, 1245-1252, 1986.

29. Bozoky, Z., Krzeminski, M., Muhandiram, R., Birtley, J. R., Al Zahrani, A., Thomas, P. J., Frizzell, R. A., Ford, R. C. & Forman-Kay, J. D. Regulatory R region of the CFTR chloride channel is a dynamic integrator of phospho-dependent intra- and intermolecular interactions. *Proc Natl Acad Sci U S A* **110**, E4427-E4436, 2013.

30. Cai, Z., Scott-Ward, T. S. & Sheppard, D. N. Voltage-dependent gating of the cystic fibrosis transmembrane conductance regulator Cl- channel. *J Gen Physiol* **122**, 605-620, 2003.

31. Carrasco, A. J., Dzeja, P. P., Alekseev, A. E., Pucar, D., Zingman, L. V., Abraham, M. R., Hodgson, D., Bienengraeber, M., Puceat, M., Janssen, E. *et al.* Adenylate kinase phosphotransfer communicates cellular energetic signals to ATP-sensitive potassium channels. *Proc Natl Acad Sci U S A* **98**, 7623-7628, 2001.

32. Carson, M. R., Travis, S. M. & Welsh, M. J. The two nucleotide-binding domains of cystic fibrosis transmembrane conductance regulator (CFTR) have distinct functions in controlling channel activity. *J Biol Chem* **270**, 1711-1717, 1995.

33. Chan, K. W., Csanády, L., Seto-Young, D., Nairn, A. C. & Gadsby, D. C. Severed molecules functionally define the boundaries of the cystic fibrosis transmembrane conductance regulator's NH(2)-terminal nucleotide binding domain. *J Gen Physiol* **116**, 163-180, 2000.

34. Chang, X. B., Tabcharani, J. A., Hou, Y. X., Jensen, T. J., Kartner, N., Alon, N., Hanrahan, J. W. & Riordan, J. R. Protein kinase A (PKA) still activates CFTR chloride channel after mutagenesis of all 10 PKA consensus phosphorylation sites. *J Biol Chem* **268**, 11304-11311, 1993.

35. Chappe, V., Hinkson, D. A., Zhu, T., Chang, X. B., Riordan, J. R. & Hanrahan, J. W. Phosphorylation of protein kinase C sites in NBD1 and the R domain control CFTR channel activation by PKA. *J Physiol* **548**, 39-52, 2003.

36. Chappe, V., Irvine, T., Liao, J., Evagelidis, A. & Hanrahan, J. W. Phosphorylation of CFTR by PKA promotes binding of the regulatory domain. *EMBO J* **24**, 2730-2740, 2005.

37. Chaves, L. A. P. & Gadsby, D. C. Cysteine accessibility probes timing and extent of NBD separation along the dimer interface in gating CFTR channels. *J Gen Physiol* **145**, 261-283, 2015.

38. Chen, J., Lu, G., Lin, J., Davidson, A. L. & Quiocho, F. A. A tweezers-like motion of the ATP-binding cassette dimer in an ABC transport cycle. *Mol Cell* **12**, 651-661, 2003.

39. Chen, J. H., Stoltz, D. A., Karp, P. H., Ernst, S. E., Pezzulo, A. A., Moninger, T. O., Rector, M. V., Reznikov, L. R., Launspach, J. L., Chaloner, K. *et al.* Loss of anion transport without

increased sodium absorption characterizes newborn porcine cystic fibrosis airway epithelia. *Cell* **143**, 911-923, 2010.

40. Chen, J. H., Xu, W. & Sheppard, D. N. Altering intracellular pH reveals the kinetic basis of intraburst gating in the CFTR Cl- channel. *J Physiol* **595**, 1059-1076, 2017.

41. Chen, L., Patel, R. P., Teng, X., Bosworth, C. A., Lancaster, J. R., Jr. & Matalon, S. Mechanisms of cystic fibrosis transmembrane conductance regulator activation by S-nitrosoglutathione. *J Biol Chem* **281**, 9190-9199, 2006.

42. Cheng, S. H., Gregory, R. J., Marshall, J., Paul, S., Souza, D. W., White, G. A., Oriordan, C. R. & Smith, A. E. Defective Intracellular-Transport and Processing of Cftr Is the Molecular-Basis of Most Cystic-Fibrosis. *Cell* **63**, 827-834, 1990.

43. Cheng, S. H., Rich, D. P., Marshall, J., Gregory, R. J., Welsh, M. J. & Smith, A. E. Phosphorylation of the R domain by cAMP-dependent protein kinase regulates the CFTR chloride channel. *Cell* **66**, 1027-1036, 1991.

44. Chinet, T. C., Fullton, J. M., Yankaskas, J. R., Boucher, R. C. & Stutts, M. J. Mechanism of sodium hyperabsorption in cultured cystic fibrosis nasal epithelium: a patch-clamp study. *Am J Physiol* **266**, C1061-C1068, 1994.

45. Cholon, D. M., Quinney, N. L., Fulcher, M. L., Esther Jr, C. R., Das, J., Dokholyan, N. V., Randell, S. H., Boucher, R. C. & Gentzsch, M. Potentiator ivacaftor abrogates pharmacological correction of ΔF508 CFTR in cystic fibrosis. *Sci Transl Med* **6**, 246ra96, 2014.

46. Choudhury, H. G., Tong, Z., Mathavan, I., Li, Y., Iwata, S., Zirah, S., Rebuffat, S., van Veen, H. W. & Beis, K. Structure of an antibacterial peptide ATP-binding cassette transporter in a novel outward occluded state. *Proc Natl Acad Sci U S A* **111**, 9145-9150, 2014.

47. Cil, O., Phuan, P. W., Son, J. H., Zhu, J. S., Ku, C. K., Tabib, N. A., Teuthorn, A. P., Ferrera, L., Zachos, N. C., Lin, R. *et al.* Phenylquinoxalinone CFTR activator as potential prosecretory therapy for constipation. *Transl Res* **182**, 14-26, 2017.

48. Cohn, J. A., Nairn, A. C., Marino, C. R., Melhus, O. & Kole, J. Characterization of the cystic fibrosis transmembrane conductance regulator in a colonocyte cell line. *Proc Natl Acad Sci U S A* **89**, 2340-2344, 1992.

49. Collavin, L., Lazarevic, D., Utrera, R., Marzinotto, S., Monte, M. & Schneider, C. wt p53 dependent expression of a membrane-associated isoform of adenylate kinase. *Oncogene* **18**, 5879-5888, 1999.

50. Colquhoun, D. & Sigworth, F. J. (1995) in *Single channel recording*, eds. Sakmann, B. & Neher, E. (*Plenum Press*, New York).

51. Corradi, V., Gu, R. X., Vergani, P. & Tieleman, D. P. Structure of Transmembrane Helix 8 and Possible Membrane Defects in CFTR. *Biophys J* **114**, 1751-1754, 2018.

52. Corradi, V., Vergani, P. & Tieleman, D. P. Cystic fibrosis transmembrane conductance regulator (CFTR): closed and open state channel models. *J Biol Chem* **290**, 22891-22906, 2015.

53. Csanády, L. Application of rate-equilibrium free energy relationship analysis to nonequilibrium ion channel gating mechanisms. *J Gen Physiol* **134**, 129-136, 2009.

54. Csanády, L., Chan, K. W., Nairn, A. C. & Gadsby, D. C. Functional roles of nonconserved structural segments in CFTR's NH2-terminal nucleotide binding domain. *J Gen Physiol* **125**, 43-55, 2005.

55. Csanády, L., Chan, K. W., Seto-Young, D., Kopsco, D. C., Nairn, A. C. & Gadsby, D. C. Severed channels probe regulation of gating of cystic fibrosis transmembrane conductance regulator by its cytoplasmic domains. *J Gen Physiol* **116**, 477-500, 2000.

56. Csanády, L., Mihályi, C., Szollosi, A., Torocsik, B. & Vergani, P. Conformational changes in the catalytically inactive nucleotide binding site of CFTR. *J Gen Physiol* **142**, 61-73, 2013.

57. Csanády, L., Nairn, A. C. & Gadsby, D. C. Thermodynamics of CFTR channel gating: a spreading conformational change initiates an irreversible gating cycle. *J Gen Physiol* **128**, 523-533, 2006.

58. Csanády, L., Seto-Young, D., Chan, K. W., Cenciarelli, C., Angel, B. B., Qin, J., McLachlin, D. T., Krutchinsky, A. N., Chait, B. T., Nairn, A. C. *et al.* Preferential phosphorylation of R-domain Serine 768 dampens activation of CFTR channels by PKA. *J Gen Physiol* **125**, 171-186, 2005.

59. Csanády, L. & Torocsik, B. Catalyst-like modulation of transition states for CFTR channel opening and closing: New stimulation strategy exploits nonequilibrium gating. *J Gen Physiol* **143**, 269-287, 2014.

60. Csanády, L. & Torocsik, B. Structure-activity analysis of a CFTR channel potentiator: Distinct molecular parts underlie dual gating effects. *J Gen Physiol* **144**, 321-336, 2014.

61. Csanády, L., Vergani, P. & Gadsby, D. C. Strict coupling between CFTR's catalytic cycle and gating of its Cl- ion pore revealed by distributions of open channel burst durations. *Proc Natl Acad Sci U S A* **107**, 1241-1246, 2010.

62. Cui, G. & McCarty, N. A. Murine and human CFTR exhibit different sensitivities to CFTR potentiators. *Am J Physiol Lung Cell Mol Physiol* **309**, L687-L699, 2015.

63. Cui, G., Song, B., Turki, H. W. & McCarty, N. A. Differential contribution of TM6 and TM12 to the pore of CFTR identified by three sulfonylurea-based blockers. *Pflugers Arch* **463**, 405-418, 2012.

64. Cui, G. Y., Rahman, K. S., Infield, D. T., Kuang, C., Prince, C. Z. & McCarty, N. A. Three charged amino acids in extracellular loop 1 are involved in maintaining the outer pore architecture of CFTR. *J Gen Physiol* **144**, 159-179, 2014.

65. Cui, L., Aleksandrov, L., Chang, X. B., Hou, Y. X., He, L., Hegedus, T., Gentzsch, M., Aleksandrov, A., Balch, W. E. & Riordan, J. R. Domain interdependence in the biosynthetic assembly of CFTR. *J Mol Biol* **365**, 981-994, 2007.

66. Dalemans, W., Barbry, P., Champigny, G., Jallat, S., Dott, K., Dreyer, D., Crystal, R. G., Pavirani, A., Lecocq, J. P. & Lazdunski, M. Altered chloride ion channel kinetics associated with the delta F508 cystic fibrosis mutation. *Nature* **354**, 526-528, 1991.

67. Dawson, R. J. P. & Locher, K. P. Structure of a bacterial multidrug ABC transporter. *Nature* **443**, 180-185, 2006.

68. De Boeck, K. & Amaral, M. D. Progress in therapies for cystic fibrosis. *Lancet Respir Med* **4**, 662-674, 2016.

69. Dean, M. & Annilo, T. Evolution of the ATP-binding cassette (ABC) transporter superfamily in vertebrates. *Annu Rev Genomics Hum Genet* **6**, 123-142, 2005.

70. Dong, Q., Ernst, S. E., Ostedgaard, L. S., Shah, V. S., Ver Heul, A. R., Welsh, M. J. & Randak, C. O. Mutating the Conserved Q-loop Glutamine 1291 Selectively Disrupts Adenylate Kinase-dependent Channel Gating of the ATP-binding Cassette (ABC) Adenylate Kinase Cystic Fibrosis Transmembrane Conductance Regulator (CFTR) and Reduces Channel Function in Primary Human Airway Epithelia. *J Biol Chem* **290**, 14140-14153, 2015.

71. Dousmanis, A. G., Nairn, A. C. & Gadsby, D. C. Distinct Mg(2+)-dependent steps rate limit opening and closing of a single CFTR Cl(-) channel. *J Gen Physiol* **119**, 545-559, 2002.

72. Dulhanty, A. M. & Riordan, J. R. Phosphorylation by cAMP-dependent protein kinase causes a conformational change in the R domain of the cystic fibrosis transmembrane conductance regulator. *Biochemistry* **33**, 4072-4079, 1994.

73. Dzeja, P. & Terzic, A. Adenylate kinase and AMP signaling networks: metabolic monitoring, signal communication and body energy sensing. *Int J Mol Sci* **10**, 1729-1772, 2009.

74. Eckford, P. D., Li, C., Ramjeesingh, M. & Bear, C. E. Cystic fibrosis transmembrane conductance regulator (CFTR) potentiator VX-770 (ivacaftor) opens the defective channel gate of mutant CFTR in a phosphorylation-dependent but ATP-independent manner. *J Biol Chem* **287**, 36639-36649, 2012.

75. El Hiani, Y. & Linsdell, P. Changes in Accessibility of Cytoplasmic Substances to the Pore Associated with Activation of the Cystic Fibrosis Transmembrane Conductance Regulator Chloride Channel. *J Biol Chem* **285**, 32126-32140, 2010.

76. El Hiani, Y. & Linsdell, P. Functional Architecture of the Cytoplasmic Entrance to the Cystic Fibrosis Transmembrane Conductance Regulator Chloride Channel Pore. *J Biol Chem* **290**, 15855-15865, 2015.

77. El Hiani, Y., Negoda, A. & Linsdell, P. Cytoplasmic pathway followed by chloride ions to enter the CFTR channel pore. *Cell Mol Life Sci* **73**, 1917-1925, 2016.

78. Fatehi, M. & Linsdell, P. Novel Residues Lining the CFTR Chloride Channel Pore Identified by Functional Modification of Introduced Cysteines. *J Membr Biol* **228**, 151-164, 2009.

79. Favia, M., Mancini, M. T., Bezzerri, V., Guerra, L., Laselva, O., Abbattiscianni, A. C., Debellis, L., Reshkin, S. J., Gambari, R., Cabrini, G. *et al.* Trimethylangelicin promotes the

functional rescue of mutant F508del CFTR protein in cystic fibrosis airway cells. *Am J Physiol Lung Cell Mol Physiol* **307**, L48-L61, 2014.

80. Fischer, H., Illek, B. & Machen, T. E. Regulation of CFTR by protein phosphatase 2B and protein kinase C. *Pflugers Arch* **436**, 175-181, 1998.

81. Fischer, H. & Machen, T. E. The tyrosine kinase p60c-src regulates the fast gate of the cystic fibrosis transmembrane conductance regulator chloride channel. *Biophys J* **71**, 3073-3082, 1996.

82. French, P. J., Bijman, J., Edixhoven, M., Vaandrager, A. B., Scholte, B. J., Lohmann, S. M., Nairn, A. C. & de Jonge, H. R. Isotype-specific activation of cystic fibrosis transmembrane conductance regulator-chloride channels by cGMP-dependent protein kinase II. *J Biol Chem* **270**, 26626-26631, 1995.

83. Gadsby, D. C. Ion channels versus ion pumps: the principal difference, in principle. *Nat Rev Mol Cell Biol* **10**, 344-352, 2009.

84. Galietta, L. J., Springsteel, M. F., Eda, M., Niedzinski, E. J., By, K., Haddadin, M. J., Kurth, M. J., Nantz, M. H. & Verkman, A. S. Novel CFTR chloride channel activators identified by screening of combinatorial libraries based on flavone and benzoquinolizinium lead compounds. *J Biol Chem* **276**, 19723-19728, 2001.

85. Gao, X., Bai, Y. & Hwang, T. C. Cysteine Scanning of CFTR's First Transmembrane Segment Reveals Its Plausible Roles in Gating and Permeation. *Biophys J* **104**, 786-797, 2013.

86. Gao, X. & Hwang, T. C. Spatial positioning of CFTR's pore-lining residues affirms an asymmetrical contribution of transmembrane segments to the anion permeation pathway. *J Gen Physiol* **147**, 407-422, 2016.

87. Gao, X. L. & Hwang, T. C. Localizing a gate in CFTR. *Proc Natl Acad Sci U S A* **112**, 2461-2466, 2015.

88. Ge, N., Muise, C. N., Gong, X. & Linsdell, P. Direct comparison of the functional roles played by different transmembrane regions in the cystic fibrosis transmembrane conductance regulator chloride channel pore. *J Biol Chem* **279**, 55283-55289, 2004.

89. Gentzsch, M., Dang, H., Dang, Y., Garcia-Caballero, A., Suchindran, H., Boucher, R. C. & Stutts, M. J. The cystic fibrosis transmembrane conductance regulator impedes proteolytic stimulation of the epithelial Na+ channel. *J Biol Chem* **285**, 32227-32232, 2010.

90. Gong, X., Burbridge, S. M., Cowley, E. A. & Linsdell, P. Molecular determinants of Au(CN)(2)(-) binding and permeability within the cystic fibrosis transmembrane conductance regulator Cl(-) channel pore. *J Physiol* **540**, 39-47, 2002.

91. Gray, M. A., Pollard, C. E., Harris, A., Coleman, L., Greenwell, J. R. & Argent, B. E. Anion selectivity and block of the small-conductance chloride channel on pancreatic duct cells. *Am J Physiol* **259**, C752-C761, 1990.

92. Grosman, C. & Auerbach, A. The dissociation of acetylcholine from open nicotinic receptor channels. *Proc Natl Acad Sci U S A* **98**, 14102-14107, 2001.

93. Gross, C. H., Abdul-Manan, N., Fulghum, J., Lippke, J., Liu, X., Prabhakar, P., Brennan, D., Willis, M. S., Faerman, C., Connelly, P. *et al.* Nucleotide-binding domains of cystic fibrosis transmembrane conductance regulator, an ABC transporter, catalyze adenylate kinase activity but not ATP hydrolysis. *J Biol Chem* **281**, 4058-4068, 2006.

94. Grunwald, E. Structure-Energy Relations, Reaction Mechanism, and Disparity of Progress of Concerted Reaction Events. *J Am Chem Soc* **107**, 125-133, 1985.

95. Gunderson, K. L. & Kopito, R. R. Effects of pyrophosphate and nucleotide analogs suggest a role for ATP hydrolysis in cystic fibrosis transmembrane regulator channel gating. *J Biol Chem* **269**, 19349-19353, 1994.

96. Gunderson, K. L. & Kopito, R. R. Conformational states of CFTR associated with channel gating: the role ATP binding and hydrolysis. *Cell* **82**, 231-239, 1995.

97. Hallows, K. R., McCane, J. E., Kemp, B. E., Witters, L. A. & Foskett, J. K. Regulation of channel gating by AMP-activated protein kinase modulates cystic fibrosis transmembrane conductance regulator activity in lung submucosal cells. *J Biol Chem* **278**, 998-1004, 2003.

98. Hallows, K. R., Raghuram, V., Kemp, B. E., Witters, L. A. & Foskett, J. K. Inhibition of cystic fibrosis transmembrane conductance regulator by novel interaction with the metabolic sensor AMP-activated protein kinase. *J Clin Invest* **105**, 1711-1721, 2000.

99. He, L. H., Aleksandrov, A. A., Serohijos, A. W. R., Hegedus, T., Aleksandrov, L. A., Cui, L., Dokholyan, N. V. & Riordan, J. R. Multiple membrane-cytoplasmic domain contacts in the cystic fibrosis transmembrane conductance regulator (CFTR) mediate regulation of channel gating. *J Biol Chem* **283**, 26383-26390, 2008.

100. Hegedus, T., Aleksandrov, A., Mengos, A., Cui, L., Jensen, T. J. & Riordan, J. R. Role of individual R domain phosphorylation sites in CFTR regulation by protein kinase A. *Biochim Biophys Acta* **1788**, 1341-1349, 2009.

101. Hohl, M., Briand, C., Grutter, M. G. & Seeger, M. A. Crystal structure of a heterodimeric ABC transporter in its inward-facing conformation. *Nat Struct Mol Biol* **19**, 395-402, 2012.

102. Hou, Y., Cui, L., Riordan, J. R. & Chang, X. Allosteric interactions between the two non-equivalent nucleotide binding domains of multidrug resistance protein MRP1. *J Biol Chem* **275**, 20280-20287, 2000.

103. Hwang, T. C., Nagel, G., Nairn, A. C. & Gadsby, D. C. Regulation of the gating of cystic fibrosis transmembrane conductance regulator C1 channels by phosphorylation and ATP hydrolysis. *Proc Natl Acad Sci U S A* **91**, 4698-4702, 1994.

104. Hwang, T. C., Yeh, J. T., Zhang, J., Yu, Y. C., Yeh, H. I. & Destefano, S. Structural mechanisms of CFTR function and dysfunction. *J Gen Physiol* **150**, 539-570, 2018.

105. Illek, B., Fischer, H., Santos, G. F., Widdicombe, J. H., Machen, T. E. & Reenstra, W. W. cAMP-independent activation of CFTR Cl channels by the tyrosine kinase inhibitor genistein. *Am J Physiol* **268**, C886-C893, 1995.

106. Illek, B., Tam, A. W., Fischer, H. & Machen, T. E. Anion selectivity of apical membrane conductance of Calu 3 human airway epithelium. *Pflugers Arch* **437**, 812-822, 1999.

107. Infield, D. T., Cui, G., Kuang, C. & McCarty, N. A. Positioning of extracellular loop 1 affects pore gating of the cystic fibrosis transmembrane conductance regulator. *Am J Physiol Lung Cell Mol Physiol* **310**, L403-L414, 2016.

108. Ishiguro, H., Steward, M. C., Naruse, S., Ko, S. B., Goto, H., Case, R. M., Kondo, T. & Yamamoto, A. CFTR functions as a bicarbonate channel in pancreatic duct cells. *J Gen Physiol* **133**, 315-326, 2009.

109. Ishihara, H. & Welsh, M. J. Block by MOPS reveals a conformation change in the CFTR pore produced by ATP hydrolysis. *Am J Physiol* **273**, C1278-C1289, 1997.

110. Itani, O. A., Chen, J. H., Karp, P. H., Ernst, S., Keshavjee, S., Parekh, K., Klesney-Tait, J., Zabner, J. & Welsh, M. J. Human cystic fibrosis airway epithelia have reduced Cl- conductance but not increased Na+ conductance. *Proc Natl Acad Sci U S A* **108**, 10260-10265, 2011.

111. Jia, Y., Mathews, C. J. & Hanrahan, J. W. Phosphorylation by protein kinase C is required for acute activation of cystic fibrosis transmembrane conductance regulator by protein kinase A. *J Biol Chem* **272**, 4978-4984, 1997.

112. Jih, K. Y. & Hwang, T. C. Vx-770 potentiates CFTR function by promoting decoupling between the gating cycle and ATP hydrolysis cycle. *Proc Natl Acad Sci U S A* **110**, 4404-4409, 2013.

113. Jih, K. Y., Sohma, Y. & Hwang, T. C. Nonintegral stoichiometry in CFTR gating revealed by a pore-lining mutation. *J Gen Physiol* **140**, 347-359, 2012.

114. Jih, K. Y., Sohma, Y., Li, M. & Hwang, T. C. Identification of a novel post-hydrolytic state in CFTR gating. *J Gen Physiol* **139**, 359-370, 2012.

115. Karpowich, N., Martsinkevich, O., Millen, L., Yuan, Y. R., Dai, P. L., MacVey, K., Thomas, P. J. & Hunt, J. F. Crystal structures of the MJ1267 ATP binding cassette reveal an induced-fit effect at the ATPase active site of an ABC transporter. *Structure (Camb)* **9**, 571-586, 2001.

116. Kennelly, P. J. & Krebs, E. G. Consensus sequences as substrate specificity determinants for protein kinases and protein phosphatases. *J Biol Chem* **266**, 15555-15558, 1991.

117. Kijima, S. & Kijima, H. Statistical analysis of channel current from a membrane patch. I. Some stochastic properties of ion channels or molecular systems in equilibrium. *J Theor Biol* **128**, 423-434, 1987.

118. Kim, Y., Anderson, M. O., Park, J., Lee, M. G., Namkung, W. & Verkman, A. S. Benzopyrimido-pyrrolo-oxazine-dione (R)-BPO-27 Inhibits CFTR Chloride Channel Gating by Competition with ATP. *Mol Pharmacol* **88**, 689-696, 2015.

119. King, J. D., Jr., Fitch, A. C., Lee, J. K., McCane, J. E., Mak, D. O., Foskett, J. K. & Hallows, K. R. AMP-activated protein kinase phosphorylation of the R domain inhibits PKA stimulation of CFTR. *Am J Physiol Cell Physiol* **297**, C94-101, 2009.

120. Kirk, K. L. & Wang, W. A Unified View of Cystic Fibrosis Transmembrane Conductance Regulator (CFTR) Gating: Combining the Allosterism of a Ligand-gated Channel with the Enzymatic Activity of an ATP-binding Cassette (ABC) Transporter. *J Biol Chem* **286**, 12813-12819, 2011.

121. Knowles, M., Gatzy, J. & Boucher, R. Relative ion permeability of normal and cystic fibrosis nasal epithelium. *J Clin Invest* **71**, 1410-1417, 1983.

122. Knowles, M. R., Stutts, M. J., Spock, A., Fischer, N., Gatzy, J. T. & Boucher, R. C. Abnormal ion permeation through cystic fibrosis respiratory epithelium. *Science* **221**, 1067-1070, 1983.

123. Kongsuphol, P., Cassidy, D., Hieke, B., Treharne, K. J., Schreiber, R., Mehta, A. & Kunzelmann, K. Mechanistic insight into control of CFTR by AMPK. *J Biol Chem* **284**, 5645-5653, 2009.

124. Kopeikin, Z., Sohma, Y., Li, M. & Hwang, T. C. On the mechanism of CFTR inhibition by a thiazolidinone derivative. *J Gen Physiol* **136**, 659-671, 2010.

125. Kopeikin, Z., Yuksek, Z., Yang, H. Y. & Bompadre, S. G. Combined effects of VX-770 and VX-809 on several functional abnormalities of F508del-CFTR channels. *J Cyst Fibros* **http://dx.doi.org/10.1016/j.jcf.2014.04.003**, 2014.

126. Langron, E. & Vergani, P. VX-770 potentiation of CFTR gating involves stabilisation of the pre-hydrolytic O1 open state. https://www.ecfs.eu/news/abstract-book-14th-ecfs-basic-science-conference. 2017.

127. Laselva, O., Molinski, S., Casavola, V. & Bear, C. E. The investigational Cystic Fibrosis drug Trimethylangelicin directly modulates CFTR by stabilizing the first membrane-spanning domain. *Biochem Pharmacol* **119**, 85-92, 2016.

128. Lazrak, A., Jurkuvenaite, A., Chen, L., Keeling, K. M., Collawn, J. F., Bedwell, D. M. & Matalon, S. Enhancement of alveolar epithelial sodium channel activity with decreased cystic fibrosis transmembrane conductance regulator expression in mouse lung. *Am J Physiol Lung Cell Mol Physiol* **301**, L557-L567, 2011.

129. Lee, M. G., Ohana, E., Park, H. W., Yang, D. & Muallem, S. Molecular mechanism of pancreatic and salivary gland fluid and HCO3 secretion. *Physiol Rev* **92**, 39-74, 2012.

130. Lewis, H. A., Buchanan, S. G., Burley, S. K., Conners, K., Dickey, M., Dorwart, M., Fowler, R., Gao, X., Guggino, W. B., Hendrickson, W. A. *et al.* Structure of nucleotide-binding domain 1 of the cystic fibrosis transmembrane conductance regulator. *EMBO J* **23**, 282-293, 2004.

131. Li, C., Ramjeesingh, M., Wang, W., Garami, E., Hewryk, M., Lee, D., Rommens, J. M., Galley, K. & Bear, C. E. ATPase activity of the cystic fibrosis transmembrane conductance regulator. *J Biol Chem* **271**, 28463-28468, 1996.

132. Li, H., Yang, W., Mendes, F., Amaral, M. D. & Sheppard, D. N. Impact of the cystic fibrosis mutation F508del-CFTR on renal cyst formation and growth. *Am J Physiol Renal Physiol* **303**, F1176-F1186, 2012.

133. Lin, W. Y., Jih, K. Y. & Hwang, T. C. A single amino acid substitution in CFTR converts ATP to an inhibitory ligand. *J Gen Physiol* **144**, 311-320, 2014.

134. Lin, W. Y., Sohma, Y. & Hwang, T. C. Synergistic Potentiation of Cystic Fibrosis Transmembrane Conductance Regulator Gating by Two Chemically Distinct Potentiators, Ivacaftor (VX-770) and 5-Nitro-2-(3-Phenylpropylamino) Benzoate. *Mol Pharmacol* **90**, 275-285, 2016.

135. Linsdell, P. Relationship between anion binding and anion permeability revealed by mutagenesis within the cystic fibrosis transmembrane conductance regulator chloride channel pore. *J Physiol* **531**, 51-66, 2001.

136. Linsdell, P. Thiocyanate as a probe of the cystic fibrosis transmembrane conductance regulator chloride channel pore. *Can J Physiol Pharmacol* **79**, 573-579, 2001.

137. Linsdell, P. Location of a common inhibitor binding site in the cytoplasmic vestibule of the cystic fibrosis transmembrane conductance regulator chloride channel pore. *J Biol Chem* **280**, 8945-8950, 2005.

138. Linsdell, P. Interactions between permeant and blocking anions inside the CFTR chloride channel pore. *Biochim Biophys Acta* **1848**, 1573-1590, 2015.

139. Linsdell, P. Anion conductance selectivity mechanism of the CFTR chloride channel. *Biochim Biophys Acta* **1858**, 740-747, 2016.

140. Linsdell, P., Evagelidis, A. & Hanrahan, J. W. Molecular determinants of anion selectivity in the cystic fibrosis transmembrane conductance regulator chloride channel pore. *Biophys J* **78**, 2973-2982, 2000.

141. Linsdell, P. & Hanrahan, J. W. Disulphonic stilbene block of cystic fibrosis transmembrane conductance regulator Cl- channels expressed in a mammalian cell line and its regulation by a critical pore residue. *J Physiol* **496 (Pt 3)**, 687-693, 1996.

142. Linsdell, P. & Hanrahan, J. W. Adenosine triphosphate-dependent asymmetry of anion permeation in the cystic fibrosis transmembrane conductance regulator chloride channel. *J Gen Physiol* **111**, 601-614, 1998.

143. Linsdell, P. & Hanrahan, J. W. Glutathione permeability of CFTR. *Am J Physiol* **275**, C323-C326, 1998.

144. Linsdell, P., Tabcharani, J. A., Rommens, J. M., Hou, Y. X., Chang, X. B., Tsui, L. C., Riordan, J. R. & Hanrahan, J. W. Permeability of wild-type and mutant cystic fibrosis transmembrane conductance regulator chloride channels to polyatomic anions. *J Gen Physiol* **110**, 355-364, 1997.

145. Liu, F., Zhang, Z., Csanády, L., Gadsby, D. C. & Chen, J. Molecular Structure of the Human CFTR Ion Channel. *Cell* **169**, 85-95, 2017.

146. Locher, K. P. Structure and mechanism of ATP-binding cassette transporters. *Phil Trans Roy Soc B* **364**, 239-245, 2009.

147. Locher, K. P. Mechanistic diversity in ATP-binding cassette (ABC) transporters. *Nat Struct Mol Biol* **23**, 487-493, 2016.

148. Lukacs, G. L. & Verkman, A. S. CFTR: folding, misfolding and correcting the DeltaF508 conformational defect. *Trends Mol Med* **18**, 81-91, 2012.

149. Luo, J., Pato, M. D., Riordan, J. R. & Hanrahan, J. W. Differential regulation of single CFTR channels by PP2C, PP2A, and other phosphatases. *Am J Physiol* **274**, C1397-C1410, 1998.

150. Ma, J., Zhao, J., Drumm, M. L., Xie, J. & Davis, P. B. Function of the R domain in the cystic fibrosis transmembrane conductance regulator chloride channel. *J Biol Chem* **272**, 28133-28141, 1997.

151. Ma, T., Thiagarajah, J. R., Yang, H., Sonawane, N. D., Folli, C., Galietta, L. J. & Verkman, A. S. Thiazolidinone CFTR inhibitor identified by high-throughput screening blocks cholera toxin-induced intestinal fluid secretion. *J Clin Invest* **110**, 1651-1658, 2002.

152. Ma, T., Vetrivel, L., Yang, H., Pedemonte, N., Zegarra-Moran, O., Galietta, L. J. & Verkman, A. S. High-affinity activators of cystic fibrosis transmembrane conductance regulator (CFTR) chloride conductance identified by high-throughput screening. *J Biol Chem* **277**, 37235-37241, 2002.

153. Marcus, R. A. Theoretical Relations among Rate Constants, Barriers, and Bronsted Slopes of Chemical Reactions. *J Phys Chem* **72**, 891-899, 1968.

154. Mathews, C. J., Tabcharani, J. A., Chang, X. B., Jensen, T. J., Riordan, J. R. & Hanrahan, J. W. Dibasic protein kinase A sites regulate bursting rate and nucleotide sensitivity of the cystic fibrosis transmembrane conductance regulator chloride channel. *J Physiol* **508 (Pt 2)**, 365-377, 1998.

155. Mathews, C. J., Tabcharani, J. A. & Hanrahan, J. W. The CFTR chloride channel: nucleotide interactions and temperature-dependent gating. *J Membr Biol* **163**, 55-66, 1998.

156. McCarty, N. A., McDonough, S., Cohen, B. N., Riordan, J. R., Davidson, N. & Lester, H. A. Voltage-dependent block of the cystic fibrosis transmembrane conductance regulator Cl-channel by two closely related arylaminobenzoates. *J Gen Physiol* **102**, 1-23, 1993.

157. McCarty, N. A. & Zhang, Z. R. Identification of a region of strong discrimination in the pore of CFTR. *Am J Physiol Lung Cell Mol Physiol* **281**, L852-L867, 2001.

158. McDonough, S., Davidson, N., Lester, H. A. & McCarty, N. A. Novel Pore-Lining Residues in Cftr That Govern Permeation and Open-Channel Block. *Neuron* **13**, 623-634, 1994.

159. Mense, M., Vergani, P., White, D. M., Altberg, G., Nairn, A. C. & Gadsby, D. C. In vivo phosphorylation of CFTR promotes formation of a nucleotide-binding domain heterodimer. *EMBO J* **25**, 4728-4739, 2006.

160. Mihályi, C., Torocsik, B. & Csanády, L. Obligate coupling of CFTR pore opening to tight nucleotide-binding domain dimerization. *Elife* **5. pii: e18164. doi: 10.7554/eLife.18164.**, e18164, 2016.

161. Miki, H., Zhou, Z., Li, M., Hwang, T. C. & Bompadre, S. G. Potentiation of Disease-associated Cystic Fibrosis Transmembrane Conductance Regulator Mutants by Hydrolyzable ATP Analogs. *J Biol Chem* **285**, 19967-19975, 2010.

162. Moody, J. E., Millen, L., Binns, D., Hunt, J. F. & Thomas, P. J. Cooperative, ATP-dependent association of the nucleotide binding cassettes during the catalytic cycle of ATP-binding cassette transporters. *J Biol Chem* **277**, 21111-21114, 2002.

163. Mornon, J. P., Hoffmann, B., Jonic, S., Lehn, P. & Callebaut, I. Full-open and closed CFTR channels, with lateral tunnels from the cytoplasm and an alternative position of the F508 region, as revealed by molecular dynamics. *Cell Mol Life Sci* **72**, 1377-1403, 2015.

164. Muanprasat, C., Sonawane, N. D., Salinas, D., Taddei, A., Galietta, L. J. & Verkman, A. S. Discovery of glycine hydrazide pore-occluding CFTR inhibitors: mechanism, structure-activity analysis, and in vivo efficacy. *J Gen Physiol* **124**, 125-137, 2004.

165. Nagel, G., Barbry, P., Chabot, H., Brochiero, E., Hartung, K. & Grygorczyk, R. CFTR fails to inhibit the epithelial sodium channel ENaC expressed in Xenopus laevis oocytes. *J Physiol* **564**, 671-682, 2005.

166. Naren, A. P., Cormet-Boyaka, E., Fu, J., Villain, M., Blalock, J. E., Quick, M. W. & Kirk, K. L. CFTR chloride channel regulation by an interdomain interaction. *Science* **286**, 544-548, 1999.

167. Naren, A. P., Quick, M. W., Collawn, J. F., Nelson, D. J. & Kirk, K. L. Syntaxin 1A inhibits CFTR chloride channels by means of domain-specific protein-protein interactions. *Proc Natl Acad Sci U S A* **95**, 10972-10977, 1998.

168. Neville, D. C., Rozanas, C. R., Price, E. M., Gruis, D. B., Verkman, A. S. & Townsend, R. R. Evidence for phosphorylation of serine 753 in CFTR using a novel metal-ion affinity resin and matrix-assisted laser desorption mass spectrometry. *Protein Sci* **6**, 2436-2445, 1997.

169. Norimatsu, Y., Ivetac, A., Alexander, C., O'Donnell, N., Frye, L., Sansom, M. S. P. & Dawson, D. C. Locating a Plausible Binding Site for an Open-Channel Blocker, GlyH-101, in the Pore of the Cystic Fibrosis Transmembrane Conductance Regulator. *Mol Pharmacol* **82**, 1042-1055, 2012.

170. O'Donoghue, D. L., Dua, V., Moss, G. W. & Vergani, P. Increased apical Na+ permeability in cystic fibrosis is supported by a quantitative model of epithelial ion transport. *J Physiol* **591**, 3681-3692, 2013.

171. O'Sullivan, B. P. & Freedman, S. D. Cystic fibrosis. *Lancet* **373**, 1891-1904, 2009.

172. Okeyo, G., Wang, W., Wei, S. & Kirk, K. L. Converting nonhydrolyzable nucleotides to strong cystic fibrosis transmembrane conductance regulator (CFTR) agonists by gain of function (GOF) mutations. *J Biol Chem* **288**, 17122-17133, 2013.

173. Okiyoneda, T., Barriere, H., Bagdany, M., Rabeh, W. M., Du, K., Hohfeld, J., Young, J. C. & Lukacs, G. L. Peripheral Protein Quality Control Removes Unfolded CFTR from the Plasma Membrane. *Science* **329**, 805-810, 2010.

174. Oldham, M. L. & Chen, J. Snapshots of the maltose transporter during ATP hydrolysis. *Proc Natl Acad Sci U S A* **108**, 15152-15156, 2011.

175. Orelle, C., Dalmas, O., Gros, P., Di Pietro, A. & Jault, J. M. The conserved glutamate residue adjacent to the Walker-B motif is the catalytic base for ATP hydrolysis in the ATP-binding cassette transporter BmrA. *J Biol Chem* **278**, 47002-47008, 2003.

176. Ortiz, D., Gossack, L., Quast, U. & Bryan, J. Reinterpreting the action of ATP analogs on K(ATP) channels. *J Biol Chem* **288**, 18894-18902, 2013.

177. Ostedgaard, L. S., Baldursson, O., Vermeer, D. W., Welsh, M. J. & Robertson, A. D. A functional R domain from cystic fibrosis transmembrane conductance regulator is predominantly unstructured in solution. *Proc Natl Acad Sci U S A* **97**, 5657-5662, 2000.

178. Park, H. W., Nam, J. H., Kim, J. Y., Namkung, W., Yoon, J. S., Lee, J. S., Kim, K. S., Venglovecz, V., Gray, M. A., Kim, K. H. *et al.* Dynamic regulation of CFTR bicarbonate permeability by [Cl-]i and its role in pancreatic bicarbonate secretion. *Gastroenterology* **139**, 620-631, 2010.

179. Park, J., Khloya, P., Seo, Y., Kumar, S., Lee, H. K., Jeon, D. K., Jo, S., Sharma, P. K. & Namkung, W. Potentiation of Delta. *PLoS One* **11**, e0149131, 2016.

180. Pedemonte, N., Sonawane, N. D., Taddei, A., Hu, J., Zegarra-Moran, O., Suen, Y. F., Robins, L. I., Dicus, C. W., Willenbring, D., Nantz, M. H. *et al.* Phenylglycine and sulfonamide correctors of defective Delta F508 and G551D cystic fibrosis transmembrane conductance regulator chloride-channel gating. *Mol Pharmacol* **67**, 1797-1807, 2005.

181. Pezzulo, A. A., Tang, X. X., Hoegger, M. J., Abou Alaiwa, M. H., Ramachandran, S., Moninger, T. O., Karp, P. H., Wohlford-Lenane, C. L., Haagsman, H. P., van Eijk, M. *et al.* Reduced airway surface pH impairs bacterial killing in the porcine cystic fibrosis lung. *Nature* **487**, 109-113, 2012.

182. Phuan, P. W., Veit, G., Tan, J. A., Finkbeiner, W. E., Lukacs, G. L. & Verkman, A. S. Potentiators of Defective DeltaF508-CFTR Gating that Do Not Interfere with Corrector Action. *Mol Pharmacol* **88**, 791-799, 2015.

183. Picciotto, M. R., Cohn, J. A., Bertuzzi, G., Greengard, P. & Nairn, A. C. Phosphorylation of the cystic fibrosis transmembrane conductance regulator. *J Biol Chem* **267**, 12742-12752, 1992.

184. Poulsen, J. H., Fischer, H., Illek, B. & Machen, T. E. Bicarbonate conductance and pH regulatory capability of cystic fibrosis transmembrane conductance regulator. *Proc Natl Acad Sci U S A* **91**, 5340-5344, 1994.

185. Powe, A. C., Jr., Al Nakkash, L., Li, M. & Hwang, T. C. Mutation of Walker-A lysine 464 in cystic fibrosis transmembrane conductance regulator reveals functional interaction between its nucleotide-binding domains. *J Physiol* **539**, 333-346, 2002.

186. Procko, E., Ferrin-O'Connell, I., Ng, S. L. & Gaudet, R. Distinct structural and functional properties of the ATPase sites in an asymmetric ABC transporter. *Mol Cell* **24**, 51-62, 2006.

187. Procko, E., O'Mara, M. L., Bennett, W. F. D., Tieleman, D. P. & Gaudet, R. The mechanism of ABC transporters: general lessons from structural and functional studies of an antigenic peptide transporter. *FASEB J* **23**, 1287-1302, 2009.

188. Qian, F., El Hiani, Y. & Linsdell, P. Functional arrangement of the 12th transmembrane region in the CFTR chloride channel pore based on functional investigation of a cysteine-less CFTR variant. *Pflugers Arch* **462**, 559-571, 2011.

189. Quinton, P. M. The neglected ion: HCO3-. *Nat Med* **7**, 292-293, 2001.

190. Quinton, P. M. & Bijman, J. Higher bioelectric potentials due to decreased chloride absorption in the sweat glands of patients with cystic fibrosis. *N Engl J Med* **308**, 1185-1189, 1983.

191. Raju, S. V., Lin, V. Y., Liu, L., McNicholas, C. M., Karki, S., Sloane, P. A., Tang, L., Jackson, P. L., Wang, W., Wilson, L. *et al.* The Cystic Fibrosis Transmembrane Conductance Regulator Potentiator Ivacaftor Augments Mucociliary Clearance Abrogating Cystic Fibrosis Transmembrane Conductance Regulator Inhibition by Cigarette Smoke. *Am J Respir Cell Mol Biol* **56**, 99-108, 2017.

192. Ramjeesingh, M., Li, C., Garami, E., Huan, L. J., Galley, K., Wang, Y. & Bear, C. E. Walker mutations reveal loose relationship between catalytic and channel-gating activities of purified CFTR (cystic fibrosis transmembrane conductance regulator). *Biochemistry* **38**, 1463-1468, 1999.

193. Ramjeesingh, M., Ugwu, F., Stratford, F. L., Huan, L. J., Li, C. & Bear, C. E. The intact CFTR protein mediates ATPase rather than adenylate kinase activity. *Biochem J* **412**, 315-321, 2008.

194. Randak, C., Neth, P., Auerswald, E. A., Eckerskorn, C., Assfalg-Machleidt, I. & Machleidt, W. A recombinant polypeptide model of the second nucleotide-binding fold of the cystic fibrosis transmembrane conductance regulator functions as an active ATPase, GTPase and adenylate kinase. *FEBS Lett* **410**, 180-186, 1997.

195. Randak, C. & Welsh, M. J. An intrinsic adenylate kinase activity regulates gating of the ABC transporter CFTR. *Cell* **115**, 837-850, 2003.

196. Randak, C. O., Ver Heul, A. R. & Welsh, M. J. Demonstration of phosphoryl group transfer indicates that the ATP-binding cassette (ABC) transporter cystic fibrosis transmembrane conductance regulator (CFTR) exhibits adenylate kinase activity. *J Biol Chem* **287**, 36105-36110, 2012.

197. Randak, C. O. & Welsh, M. J. ADP inhibits function of the ABC transporter cystic fibrosis transmembrane conductance regulator via its adenylate kinase activity. *Proc Natl Acad Sci U S A* **102**, 2216-2220, 2005.

198. Reddy, M. M. & Quinton, P. M. Control of dynamic CFTR selectivity by glutamate and ATP in epithelial cells. *Nature* **423**, 756-760, 2003.

199. Rich, D. P., Berger, H. A., Cheng, S. H., Travis, S. M., Saxena, M., Smith, A. E. & Welsh, M. J. Regulation of the cystic fibrosis transmembrane conductance regulator Cl- channel by negative charge in the R domain. *J Biol Chem* **268**, 20259-20267, 1993.

200. Rich, D. P., Gregory, R. J., Anderson, M. P., Manavalan, P., Smith, A. E. & Welsh, M. J. Effect of deleting the R domain on CFTR-generated chloride channels. *Science* **253**, 205-207, 1991.

201. Riordan, J. R., Rommens, J. M., Kerem, B., Alon, N., Rozmahel, R., Grzelczak, Z., Zielenski, J., Lok, S., Plavsic, N., Chou, J. L. *et al.* Identification of the cystic fibrosis gene: cloning and characterization of complementary DNA. *Science* **245**, 1066-1073, 1989.

202. Saint-Criq, V. & Gray, M. A. Role of CFTR in epithelial physiology. *Cell Mol Life Sci* **74**, 93-115, 2017.

203. Schultz, B. D., Venglarik, C. J., Bridges, R. J. & Frizzell, R. A. Regulation of CFTR Cl- channel gating by ADP and ATP analogues. *J Gen Physiol* **105**, 329-361, 1995.

204. Scott-Ward, T. S., Cai, Z., Dawson, E. S., Doherty, A., Da Paula, A. C., Davidson, H., Porteous, D. J., Wainwright, B. J., Amaral, M. D., Sheppard, D. N. *et al.* Chimeric constructs endow the human CFTR Cl- channel with the gating behavior of murine CFTR. *Proc Natl Acad Sci U S A* **104**, 16365-16370, 2007.

205. Sebastian, A., Rishishwar, L., Wang, J., Bernard, K. F., Conley, A. B., McCarty, N. A. & Jordan, I. K. Origin and evolution of the cystic fibrosis transmembrane regulator protein R domain. *Gene* **523**, 137-146, 2013.

206. Seibert, F. S., Tabcharani, J. A., Chang, X. B., Dulhanty, A. M., Mathews, C., Hanrahan, J. W. & Riordan, J. R. cAMP-dependent protein kinase-mediated phosphorylation of cystic fibrosis transmembrane conductance regulator residue Ser-753 and its role in channel activation. *J Biol Chem* **270**, 2158-2162, 1995.

207. Serohijos, A. W. R., Hegedus, T., Aleksandrov, A. A., He, L., Cui, L., Dokholyan, N. V. & Riordan, J. R. Phenylalanine-508 mediates a cytoplasmic-membrane domain contact in the CFTR 3D structure crucial to assembly and channel function. *Proc Natl Acad Sci U S A* **105**, 3256-3261, 2008.

208. Shah, V. S., Ernst, S., Tang, X. X., Karp, P. H., Parker, C. P., Ostedgaard, L. S. & Welsh, M. J. Relationships among CFTR expression. *Proc Natl Acad Sci U S A* **113**, 5382-5387, 2016.

209. Shah, V. S., Ernst, S., Tang, X. X., Karp, P. H., Parker, C. P., Ostedgaard, L. S. & Welsh, M. J. Relationships among CFTR expression, HCO3- secretion, and host defense may inform gene- and cell-based cystic fibrosis therapies. *Proc Natl Acad Sci U S A* **113**, 5382-5387, 2016.

210. Shah, V. S., Meyerholz, D. K., Tang, X. X., Reznikov, L., Abou, A. M., Ernst, S. E., Karp, P. H., Wohlford-Lenane, C. L., Heilmann, K. P., Leidinger, M. R. *et al.* Airway acidification initiates host defense abnormalities in cystic fibrosis mice. *Science* **351**, 503-507, 2016.

211. Sheppard, D. N. & Robinson, K. A. Mechanism of glibenclamide inhibition of cystic fibrosis transmembrane conductance regulator Cl- channels expressed in a murine cell line. *J Physiol* **503 (Pt 2)**, 333-346, 1997.

212. Shintre, C. A., Pike, A. C., Li, Q., Kim, J. I., Barr, A. J., Goubin, S., Shrestha, L., Yang, J., Berridge, G., Ross, J. *et al.* Structures of ABCB10, a human ATP-binding cassette transporter in apo- and nucleotide-bound states. *Proc Natl Acad Sci U S A* **110**, 9710-9715, 2013.

213. Siarheyeva, A., Liu, R. & Sharom, F. J. Characterization of an asymmetric occluded state of P-glycoprotein with two bound nucleotides: implications for catalysis. *J Biol Chem* **285**, 7575-7586, 2010.

214. Sloane, P. A., Shastry, S., Wilhelm, A., Courville, C., Tang, L. P., Backer, K., Levin, E., Raju, S. V., Li, Y., Mazur, M. *et al.* A pharmacologic approach to acquired cystic fibrosis transmembrane conductance regulator dysfunction in smoking related lung disease. *PLoS One* **7**, e39809, 2012.

215. Smith, P. C., Karpowich, N., Millen, L., Moody, J. E., Rosen, J., Thomas, P. J. & Hunt, J. F. ATP binding to the motor domain from an ABC transporter drives formation of a nucleotide sandwich dimer. *Mol Cell* **10**, 139-149, 2002.

216. Smith, S. S., Steinle, E. D., Meyerhoff, M. E. & Dawson, D. C. Cystic fibrosis transmembrane conductance regulator. Physical basis for lyotropic anion selectivity patterns. *J Gen Physiol* **114**, 799-818, 1999.

217. Son, J. H., Zhu, J. S., Phuan, P. W., Cil, O., Teuthorn, A. P., Ku, C. K., Lee, S., Verkman, A. S. & Kurth, M. J. High-Potency Phenylquinoxalinone Cystic Fibrosis Transmembrane Conductance Regulator (CFTR) Activators. *J Med Chem* **60**, 2401-2410, 2017.

218. Sonawane, N. D., Zhao, D., Zegarra-Moran, O., Galietta, L. J. & Verkman, A. S. Nanomolar CFTR inhibition by pore-occluding divalent polyethylene glycol-malonic acid hydrazides. *Chem Biol* **15**, 718-728, 2008.

219. Sorum, B., Czege, D. & Csanády, L. Timing of CFTR pore opening and structure of its transition state. *Cell* **163**, 724-733, 2015.

220. Sorum, B., Torocsik, B. & Csanády, L. Asymmetry of movements in CFTR's two ATP sites during pore opening serves their distinct functions. *Elife* **6. pii: e29013. doi: 10.7554/eLife.29013**, e29013, 2017.

221. St Aubin, C. N., Zhou, J. J. & Linsdell, P. Identification of a second blocker binding site at the cytoplasmic mouth of the cystic fibrosis transmembrane conductance regulator chloride channel pore. *Mol Pharmacol* **71**, 1360-1368, 2007.

222. Szakacs, G., Ozvegy, C., Bakos, E., Sarkadi, B. & Varadi, A. Transition-state formation in ATPase-negative mutants of human MDR1 protein. *Biochem Biophys Res Commun* **276**, 1314-1319, 2000.

223. Szollosi, A., Muallem, D. R., Csanády, L. & Vergani, P. Mutant cycles at CFTR's non-canonical ATP-binding site support little interface separation during gating. *J Gen Physiol* **137**, 549-562, 2011.

224. Szollosi, A., Vergani, P. & Csanády, L. Involvement of F1296 and N1303 of CFTR in induced-fit conformational change in response to ATP binding at NBD2. *J Gen Physiol* **136**, 407-423, 2010.

225. Tabcharani, J. A., Chang, X. B., Riordan, J. R. & Hanrahan, J. W. Phosphorylation-regulated Cl- channel in CHO cells stably expressing the cystic fibrosis gene. *Nature* **352**, 628-631, 1991.

226. Tabcharani, J. A., Linsdell, P. & Hanrahan, J. W. Halide permeation in wild-type and mutant cystic fibrosis transmembrane conductance regulator chloride channels. *J Gen Physiol* **110**, 341-354, 1997.

227. Tabcharani, J. A., Rommens, J. M., Hou, Y. X., Chang, X. B., Tsui, L. C., Riordan, J. R. & Hanrahan, J. W. Multi-ion pore behaviour in the CFTR chloride channel. *Nature* **366**, 79-82, 1993.

228. Taddei, A., Folli, C., Zegarra-Moran, O., Fanen, P., Verkman, A. S. & Galietta, L. J. Altered channel gating mechanism for CFTR inhibition by a high-affinity thiazolidinone blocker. *FEBS Lett* **558**, 52-56, 2004.

229. Thiagarajah, J. R., Donowitz, M. & Verkman, A. S. Secretory diarrhoea: mechanisms and emerging therapies. *Nat Rev Gastroenterol Hepatol* **12**, 446-457, 2015.

230. Timachi, M. H., Hutter, C. A., Hohl, M., Assafa, T., Bohm, S., Mittal, A., Seeger, M. A. & Bordignon, E. Exploring conformational equilibria of a heterodimeric ABC transporter. *Elife* **6. pii: e20236. doi: 10.7554/eLife.20236.**, e20236, 2017.

231. Townsend, R. R., Lipniunas, P. H., Tulk, B. M. & Verkman, A. S. Identification of protein kinase A phosphorylation sites on NBD1 and R domains of CFTR using electrospray mass spectrometry with selective phosphate ion monitoring. *Protein Sci* **5**, 1865-1873, 1996.

232. Travis, S. M., Berger, H. A. & Welsh, M. J. Protein phosphatase 2C dephosphorylates and inactivates cystic fibrosis transmembrane conductance regulator. *Proc Natl Acad Sci U S A* **94**, 11055-11060, 1997.

233. Tsai, M. F., Li, M. & Hwang, T. C. Stable ATP binding mediated by a partial NBD dimer of the CFTR chloride channel. *J Gen Physiol* **135**, 399-414, 2010.

234. Tsai, M. F., Shimizu, H., Sohma, Y., Li, M. & Hwang, T. C. State-dependent modulation of CFTR gating by pyrophosphate. *J Gen Physiol* **133**, 405-419, 2009.

235. Ueda, K., Inagaki, N. & Seino, S. MgADP antagonism to Mg2+-independent ATP binding of the sulfonylurea receptor SUR1. *J Biol Chem* **272**, 22983-22986, 1997.

236. Urbatsch, I. L., Julien, M., Carrier, I., Rousseau, M. E., Cayrol, R. & Gros, P. Mutational analysis of conserved carboxylate residues in the nucleotide binding sites of P-glycoprotein. *Biochemistry* **39**, 14138-14149, 2000.

237. Vais, H., Zhang, R. & Reenstra, W. W. Dibasic phosphorylation sites in the R domain of CFTR have stimulatory and inhibitory effects on channel activation. *Am J Physiol Cell Physiol* **287**, C737-C745, 2004.

238. Van Goor, F., Hadida, S., Grootenhuis, P. D. J., Burton, B., Cao, D., Neuberger, T., Turnbull, A., Singh, A., Joubran, J., Hazlewood, A. *et al.* Rescue of CF airway epithelial cell function in vitro by a CFTR potentiator, VX-770. *Proc Natl Acad Sci U S A* **106**, 18825-18830, 2009.

239. Van Goor, F., Hadida, S., Grootenhuis, P. D. J., Burton, B., Stack, J. H., Straley, K. S., Decker, C. J., Miller, M., McCartney, J., Olson, E. R. *et al.* Correction of the F508del-CFTR protein processing defect in vitro by the investigational drug VX-809. *Proc Natl Acad Sci U S A* **108**, 18843-18848, 2011.

240. Veit, G., Avramescu, R. G., Perdomo, D., Phuan, P. W., Bagdany, M., Apaja, P. M., Borot, F., Szollosi, D., Wu, Y. S., Finkbeiner, W. E. *et al.* Some gating potentiators, including VX-770, diminish ΔF508-CFTR functional expression. *Sci Transl Med* **6**, 246ra97, 2014.

241. Venglarik, C. J., Schultz, B. D., Frizzell, R. A. & Bridges, R. J. ATP alters current fluctuations of cystic fibrosis transmembrane conductance regulator: evidence for a three-state activation mechanism. *J Gen Physiol* **104**, 123-146, 1994.

242. Vergani, P., Lockless, S. W., Nairn, A. C. & Gadsby, D. C. CFTR channel opening by ATP-driven tight dimerization of its nucleotide-binding domains. *Nature* **433**, 876-880, 2005.

243. Vergani, P., Nairn, A. C. & Gadsby, D. C. On the mechanism of MgATP-dependent gating of CFTR Cl- channels. *J Gen Physiol* **121**, 17-36, 2003.

244. Wainwright, C. E., Elborn, J. S., Ramsey, B. W., Marigowda, G., Huang, X., Cipolli, M., Colombo, C., Davies, J. C., De Boeck, K., Flume, P. A. *et al.* Lumacaftor-Ivacaftor in Patients with Cystic Fibrosis Homozygous for Phe508del CFTR. *N Engl J Med* **373**, 220-231, 2015.

245. Walker, J. E., Saraste, M., Runswick, M. J. & Gay, N. J. Distantly related sequences in the alpha- and beta-subunits of ATP synthase, myosin, kinases and other ATP-requiring enzymes and a common nucleotide binding fold. *EMBO J* **1**, 945-951, 1982.

246. Wang, F., Zeltwanger, S., Hu, S. & Hwang, T. C. Deletion of phenylalanine 508 causes attenuated phosphorylation-dependent activation of CFTR chloride channels. *J Physiol* **524 Pt 3**, 637-648, 2000.

247. Wang, F., Zeltwanger, S., Yang, I. C., Nairn, A. C. & Hwang, T. C. Actions of genistein on cystic fibrosis transmembrane conductance regulator channel gating. Evidence for two binding sites with opposite effects. *J Gen Physiol* **111**, 477-490, 1998.

248. Wang, W., Bernard, K., Li, G. & Kirk, K. L. Curcumin opens cystic fibrosis transmembrane conductance regulator channels by a novel mechanism that requires neither ATP binding nor dimerization of the nucleotide-binding domains. *J Biol Chem* **282**, 4533-4544, 2007.

249. Wang, W., He, Z., O'Shaughnessy, T. J., Rux, J. & Reenstra, W. W. Domain-domain associations in cystic fibrosis transmembrane conductance regulator. *Am J Physiol Cell Physiol* **282**, C1170-C1180, 2002.

250. Wang, W., Li, G., Clancy, J. P. & Kirk, K. L. Activating cystic fibrosis transmembrane conductance regulator channels with pore blocker analogs. *J Biol Chem* **280**, 23622-23630, 2005.

251. Wang, W., Okeyo, G. O., Tao, B. L., Hong, J. S. & Kirk, K. L. Thermally Unstable Gating of the Most Common Cystic Fibrosis Mutant Channel (Delta F508) "RESCUE" BY SUPPRESSOR MUTATIONS IN NUCLEOTIDE BINDING DOMAIN 1 AND BY CONSTITUTIVE MUTATIONS IN THE CYTOSOLIC LOOPS. *J Biol Chem* **286**, 41937-41948, 2011.

252. Wang, W., Roessler, B. C. & Kirk, K. L. An Electrostatic Interaction at the Tetrahelix Bundle Promotes Phosphorylation-dependent Cystic Fibrosis Transmembrane Conductance Regulator (CFTR) Channel Opening. *J Biol Chem* **289**, 30364-30378, 2014.

253. Wang, W., Wu, J. P., Bernard, K., Li, G., Wang, G. Y., Bevensee, M. O. & Kirk, K. L. ATP-independent CFTR channel gating and allosteric modulation by phosphorylation. *Proc Natl Acad Sci U S A* **107**, 3888-3893, 2010.

254. Wang, W. Y., El Hiani, Y. & Linsdell, P. Alignment of transmembrane regions in the cystic fibrosis transmembrane conductance regulator chloride channel pore. *J Gen Physiol* **138**, 165-178, 2011.

255. Wang, W. Y., El Hiani, Y., Rubaiy, H. N. & Linsdell, P. Relative contribution of different transmembrane segments to the CFTR chloride channel pore. *Pflugers Arch* **466**, 477-490, 2014.

256. Ward, A., Reyes, C. L., Yu, J., Roth, C. B. & Chang, G. Flexibility in the ABC transporter MsbA: Alternating access with a twist. *Proc Natl Acad Sci U S A* **104**, 19005-19010, 2007.

257. Wei, S., Roessler, B. C., Chauvet, S., Guo, J., Hartman, J. L. & Kirk, K. L. Conserved allosteric hot spots in the transmembrane domains of cystic fibrosis transmembrane conductance regulator (CFTR) channels and multidrug resistance protein (MRP) pumps. *J Biol Chem* **289**, 19942-19957, 2014.

258. Weinreich, F., Riordan, J. R. & Nagel, G. Dual effects of ADP and adenylylimidodiphosphate on CFTR channel kinetics show binding to two different nucleotide binding sites. *J Gen Physiol* **114**, 55-70, 1999.

259. Widdicombe, J. H., Welsh, M. J. & Finkbeiner, W. E. Cystic fibrosis decreases the apical membrane chloride permeability of monolayers cultured from cells of tracheal epithelium. *Proc Natl Acad Sci U S A* **82**, 6167-6171, 1985.

260. Wilkinson, D. J., Strong, T. V., Mansoura, M. K., Wood, D. L., Smith, S. S., Collins, F. S. & Dawson, D. C. CFTR activation: additive effects of stimulatory and inhibitory phosphorylation sites in the R domain. *Am J Physiol* **273**, L127-L133, 1997.

261. Winter, M. C., Sheppard, D. N., Carson, M. R. & Welsh, M. J. Effect of ATP concentration on CFTR Cl- channels: a kinetic analysis of channel regulation. *Biophys J* **66**, 1398-1403, 1994.

262. Winter, M. C. & Welsh, M. J. Stimulation of CFTR activity by its phosphorylated R domain. *Nature* **389**, 294-296, 1997.

263. Yang, B., Sonawane, N. D., Zhao, D., Somlo, S. & Verkman, A. S. Small-molecule CFTR inhibitors slow cyst growth in polycystic kidney disease. *J Am Soc Nephrol* **19**, 1300-1310, 2008.

264. Yasuda, R., Noji, H., Yoshida, M., Kinosita, K., Jr. & Itoh, H. Resolution of distinct rotational substeps by submillisecond kinetic analysis of F1-ATPase. *Nature* **410**, 898-904, 2001.

265. Yeh, H. I., Sohma, Y., Conrath, K. & Hwang, T. C. A common mechanism for CFTR potentiators. *J Gen Physiol* **149**, 1105-1118, 2017.

266. Yeh, H. I., Yeh, J. T. & Hwang, T. C. Modulation of CFTR gating by permeant ions. *J Gen Physiol* **145**, 47-60, 2015.

267. Yu, H., Burton, B., Huang, C. J., Worley, J., Cao, D., Johnson, J. P., Jr., Urrutia, A., Joubran, J., Seepersaud, S., Sussky, K. *et al.* Ivacaftor potentiation of multiple CFTR channels with gating mutations. *J Cyst Fibros* **11**, 237-245, 2012.

268. Yuan, Y. R., Blecker, S., Martsinkevich, O., Millen, L., Thomas, P. J. & Hunt, J. F. The crystal structure of the MJ0796 ATP-binding cassette. Implications for the structural consequences of ATP hydrolysis in the active site of an ABC transporter. *J Biol Chem* **276**, 32313-32321, 2001.

269. Zaitseva, J., Jenewein, S., Jumpertz, T., Holland, I. B. & Schmitt, L. H662 is the linchpin of ATP hydrolysis in the nucleotide-binding domain of the ABC transporter HlyB. *EMBO J* **24**, 1901-1910, 2005.

270. Zeltwanger, S., Wang, F., Wang, G. T., Gillis, K. D. & Hwang, T. C. Gating of cystic fibrosis transmembrane conductance regulator chloride channels by adenosine triphosphate hydrolysis. Quantitative analysis of a cyclic gating scheme. *J Gen Physiol* **113**, 541-554, 1999.

271. Zhang, J. & Hwang, T. C. The Fifth Transmembrane Segment of Cystic Fibrosis Transmembrane Conductance Regulator Contributes to Its Anion Permeation Pathway. *Biochemistry* **54**, 3839-3850, 2015.

272. Zhang, J. & Hwang, T. C. Electrostatic tuning of the pre- and post-hydrolytic open states in CFTR. *J Gen Physiol* **149**, 355-372, 2017.

273. Zhang, Z. & Chen, J. Atomic Structure of the Cystic Fibrosis Transmembrane Conductance Regulator. *Cell* **167**, 1586-1597, 2016.

274. Zhang, Z., Liu, F. & Chen, J. Conformational Changes of CFTR upon Phosphorylation and ATP Binding. *Cell* **170**, 483-491, 2017.

275. Zhang, Z. R., McDonough, S. I. & McCarty, N. A. Interaction between permeation and gating in a putative pore domain mutant in the cystic fibrosis transmembrane conductance regulator. *Biophys J* **79**, 298-313, 2000.

276. Zhang, Z. R., Zeltwanger, S. & McCarty, N. A. Direct comparison of NPPB and DPC as probes of CFTR expressed in Xenopus oocytes. *J Membr Biol* **175**, 35-52, 2000.

277. Zhou, Y., Pearson, J. E. & Auerbach, A. Phi-value analysis of a linear, sequential reaction mechanism: theory and application to ion channel gating. *Biophys J* **89**, 3680-3685, 2005.

278. Zhou, Z., Hu, S. & Hwang, T. C. Voltage-dependent flickery block of an open cystic fibrosis transmembrane conductance regulator (CFTR) channel pore. *J Physiol* **532**, 435-448, 2001.

279. Zhou, Z., Hu, S. & Hwang, T. C. Probing an open CFTR pore with organic anion blockers. *J Gen Physiol* **120**, 647-662, 2002.

280. Zhou, Z., Wang, X., Li, M., Sohma, Y., Zou, X. & Hwang, T. C. High affinity ATP/ADP analogues as new tools for studying CFTR gating. *J Physiol* **569**, 447-457, 2005.

281. Zhou, Z., Wang, X., Liu, H. Y., Zou, X., Li, M. & Hwang, T. C. The two ATP binding sites of cystic fibrosis transmembrane conductance regulator (CFTR) play distinct roles in gating kinetics and energetics. *J Gen Physiol* **128**, 413-422, 2006.

282. Zielenski, J. & Tsui, L. C. Cystic fibrosis: genotypic and phenotypic variations. *Annu Rev Genet* **29**, 777-807, 1995.

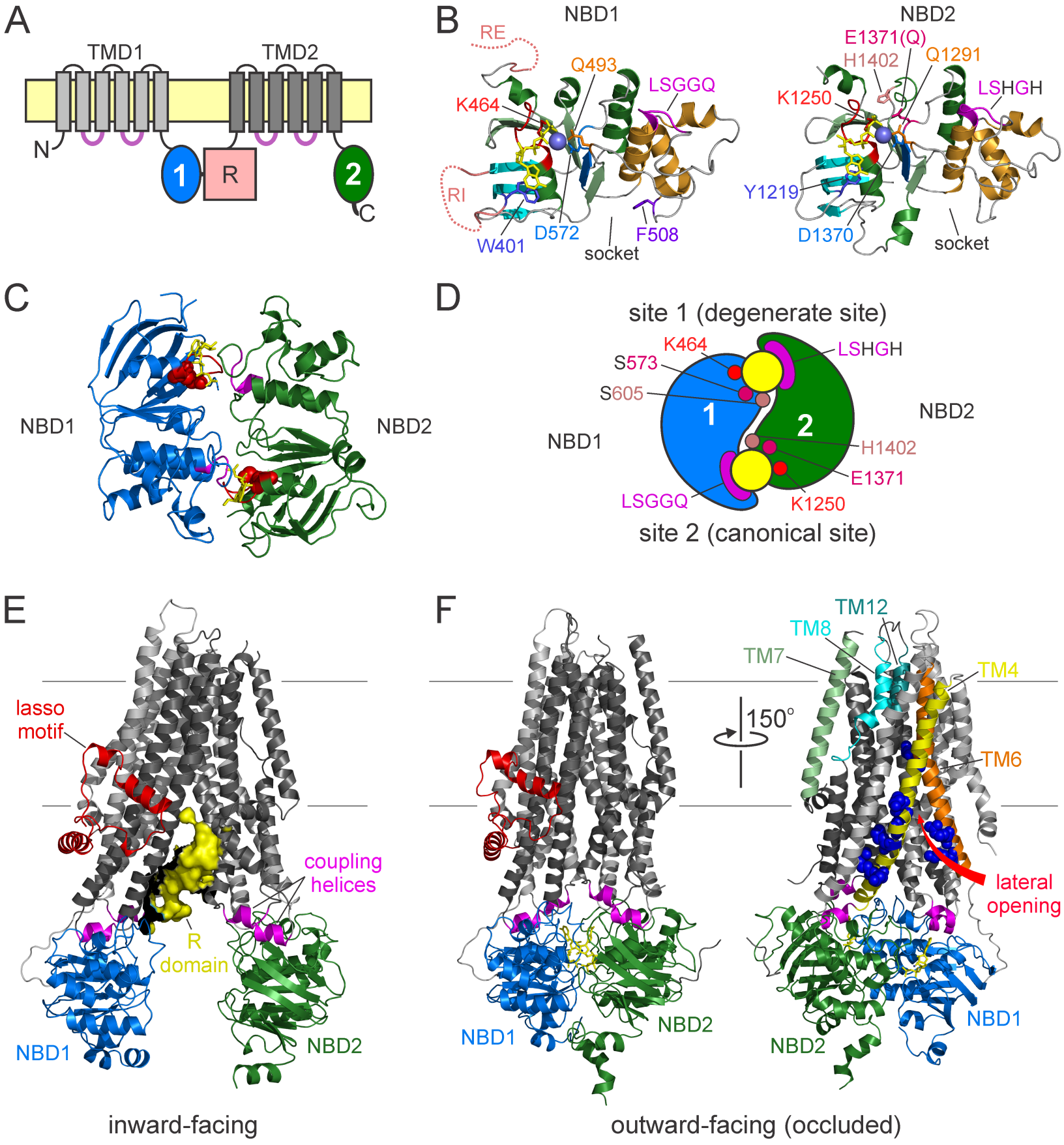
A
TMD1
TMD2
N
1
R
2
C
B
NBD1
RE
Q493
LSGGQ
K464
RI
W401
D572
F508
socket
NBD2
E1371(Q)
H1402
Q1291
LSHGH
K1250
Y1219
D1370
socket
C
NBD1
NBD2
D
site 1 (degenerate site)
K464
LSHGH
S573
S605
1
2
NBD1
NBD2
H1402
E1371
LSGGQ
K1250
site 2 (canonical site)
E
lasso motif
coupling helices
R domain
NBD1
NBD2
inward-facing
F
TM12
TM8
TM7
TM4
150°
TM6
lateral opening
NBD1
NBD2
NBD2
NBD1
outward-facing (occluded)

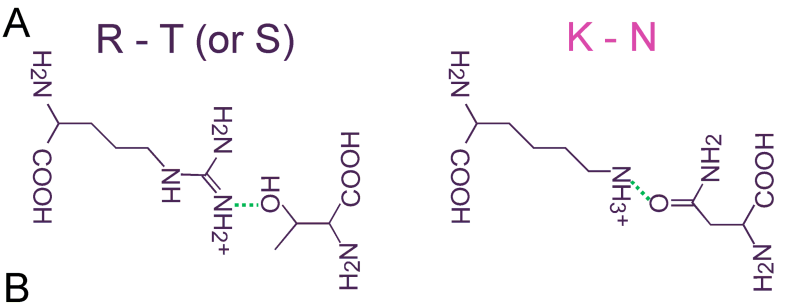
A
R - T (or S)
K - N

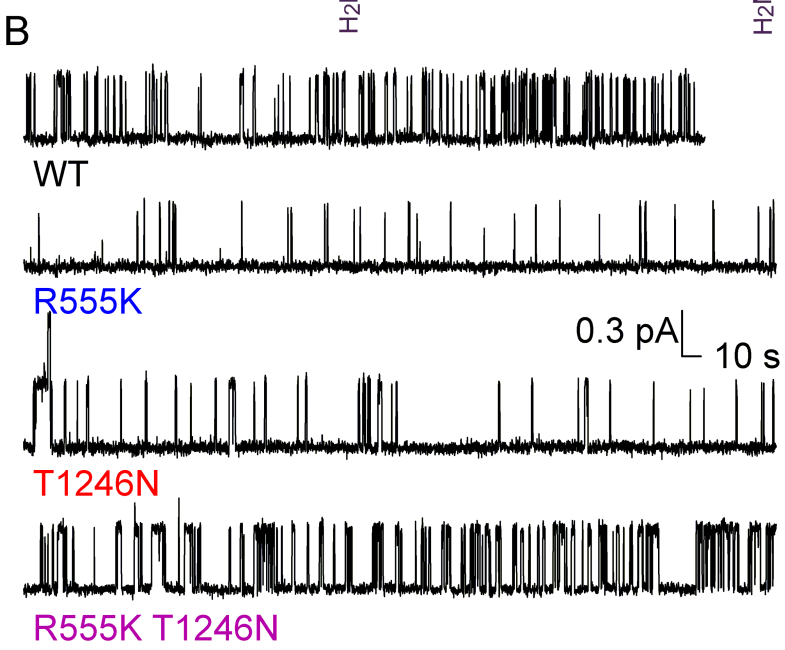
B
WT
R555K
0.3 pA
10 s
T1246N
R555K T1246N

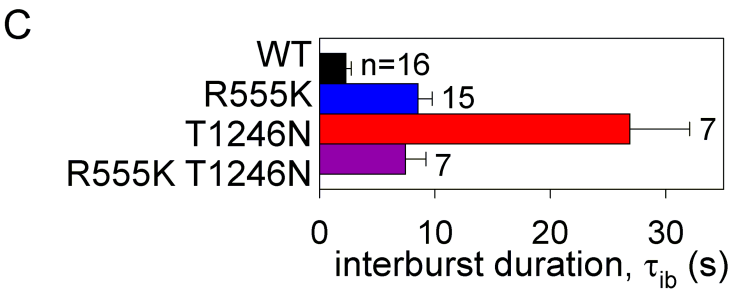
C
WT
R555K
T1246N
R555K T1246N
n=16
15
7
7
0
10
20
30
interburst duration, τib (s)

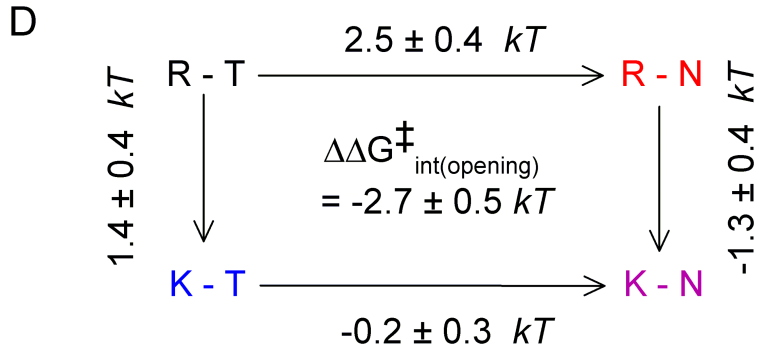
D
2.5 ± 0.4 kT
R - T
R - N
1.4 ± 0.4 kT
ΔΔG‡int(opening)
= -2.7 ± 0.5 kT
-1.3 ± 0.4 kT
K - T
K - N
-0.2 ± 0.3 kT

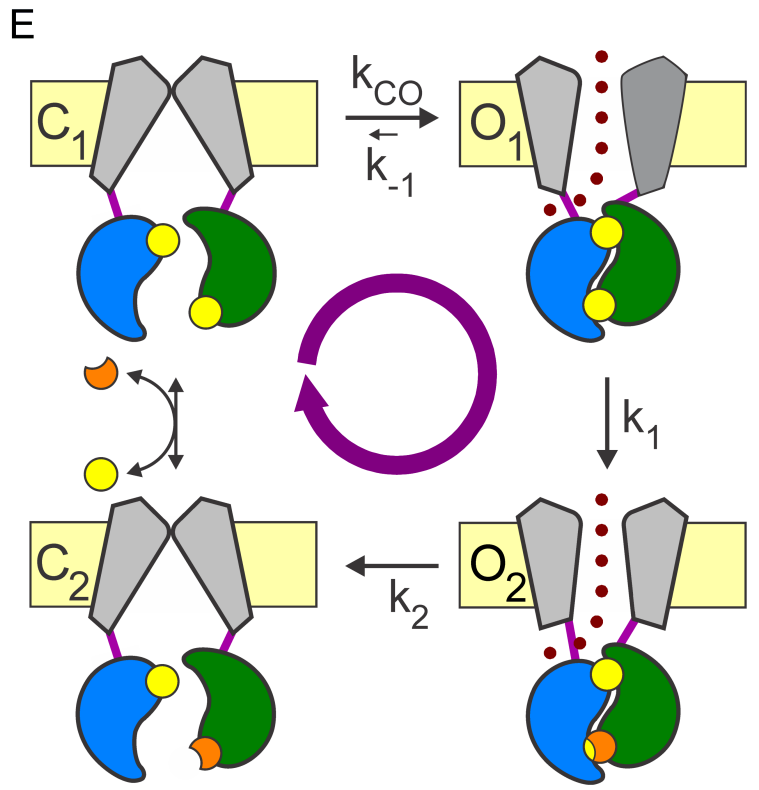
E
C1
kCO
k-1
O1
k1
C2
k2
O2

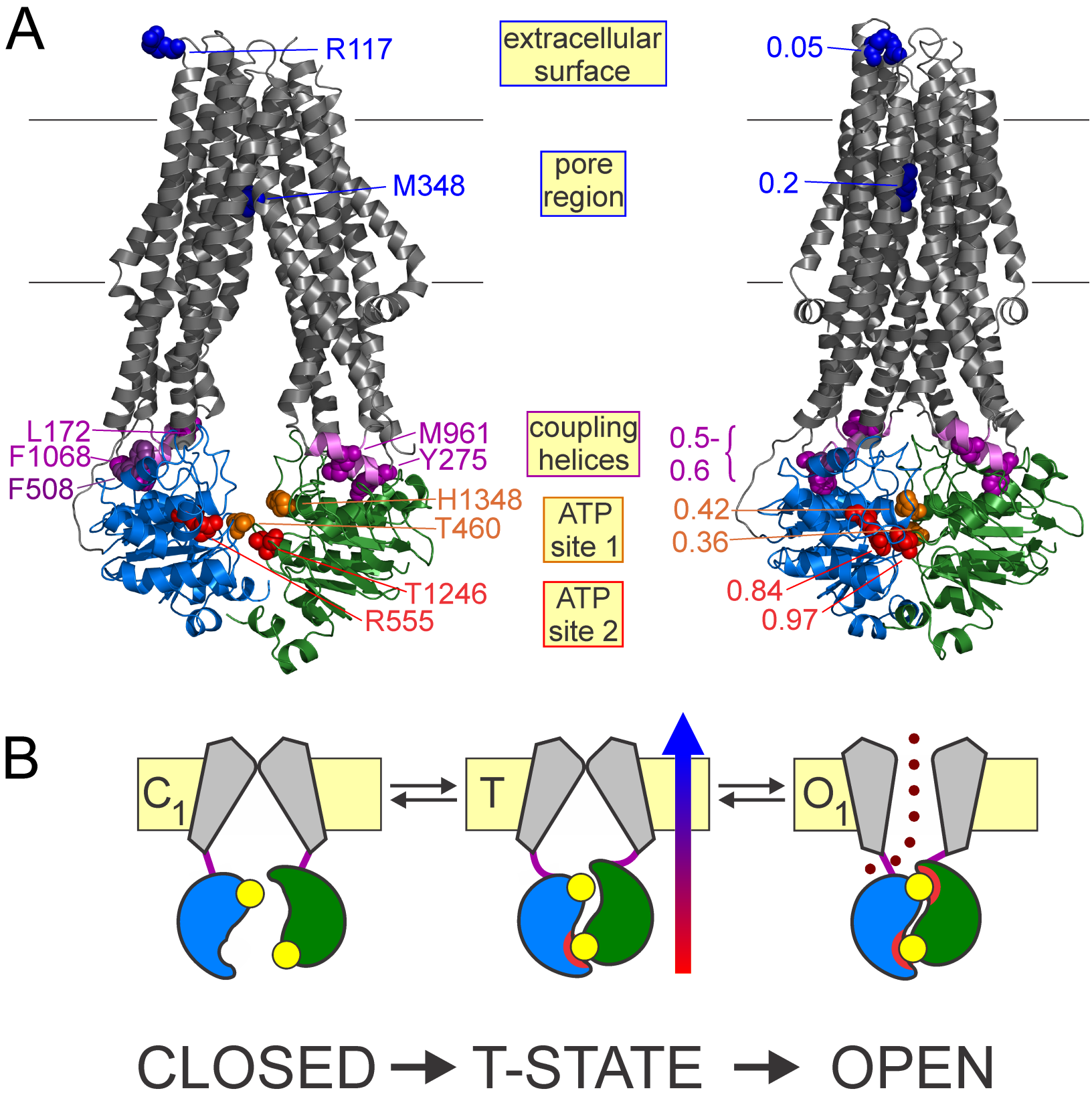
A
R117
M348
L172
F1068
F508
M961
Y275
H1348
T460
T1246
R555
extracellular surface
pore region
coupling helices
ATP site 1
ATP site 2
0.05
0.2
0.5-0.6
0.42
0.36
0.84
0.97
B
C1
T
O1
CLOSED → T-STATE → OPEN

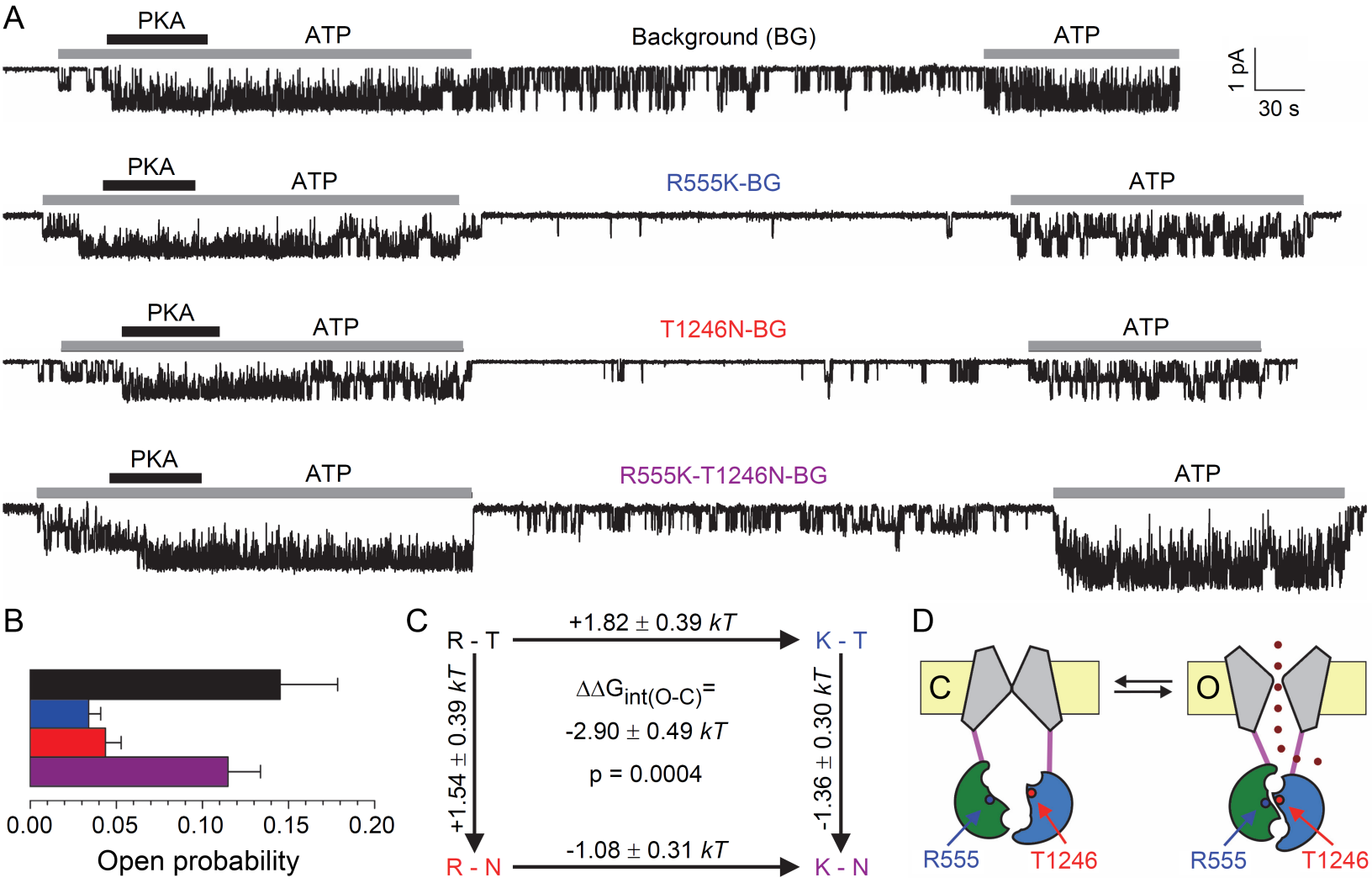
A
PKA
ATP
Background (BG)
ATP
1 pA
30 s
PKA
ATP
R555K-BG
ATP
PKA
ATP
T1246N-BG
ATP
PKA
ATP
R555K-T1246N-BG
ATP
B
0.00
0.05
0.10
0.15
0.20
Open probability
C
R - T
+1.82 ± 0.39 kT
K - T
ΔΔG int(O-C)=
-2.90 ± 0.49 kT
p = 0.0004
+1.54 ± 0.39 kT
-1.36 ± 0.30 kT
R - N
-1.08 ± 0.31 kT
K - N
D
C
O
R555
T1246
R555
T1246

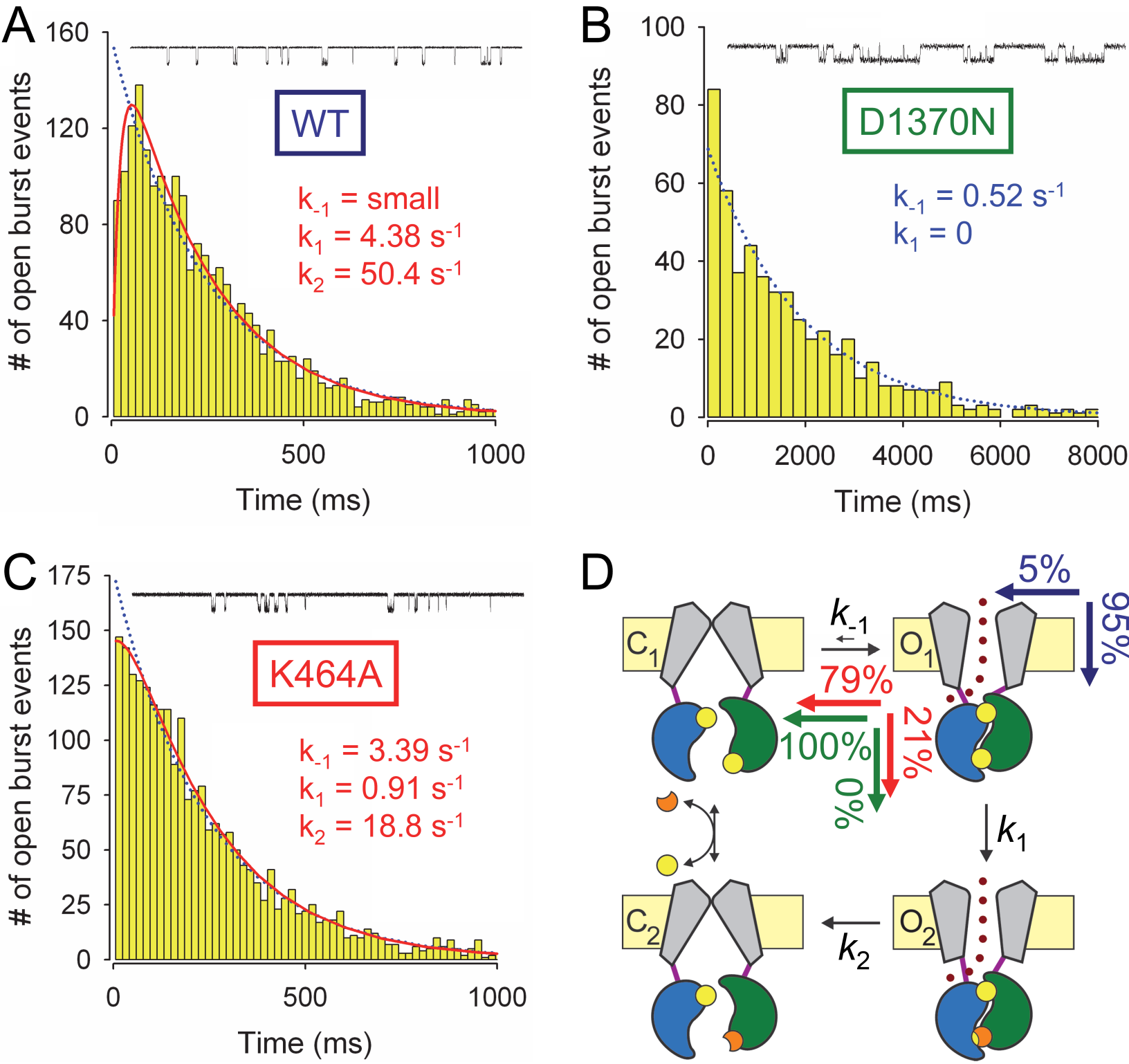
A
# of open burst events
160
120
80
40
0
WT
k-1 = small
k1 = 4.38 s-1
k2 = 50.4 s-1
0
500
1000
Time (ms)
B
# of open burst events
100
80
60
40
20
0
D1370N
k-1 = 0.52 s-1
k1 = 0
0
2000
4000
6000
8000
Time (ms)
C
# of open burst events
175
150
125
100
75
50
25
0
K464A
k-1 = 3.39 s-1
k1 = 0.91 s-1
k2 = 18.8 s-1
0
500
1000
Time (ms)
D
C1
O1
C2
O2
k-1
k1
k2
5%
95%
79%
100%
21%
0%

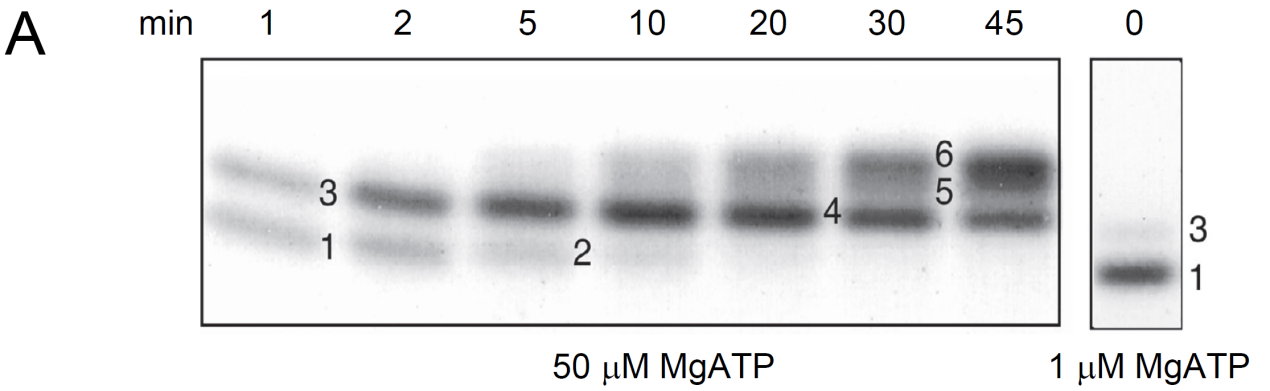
A
min
1
2
5
10
20
30
45
0
3
1
2
4
6
5
3
1
50 μM MgATP
1 μM MgATP

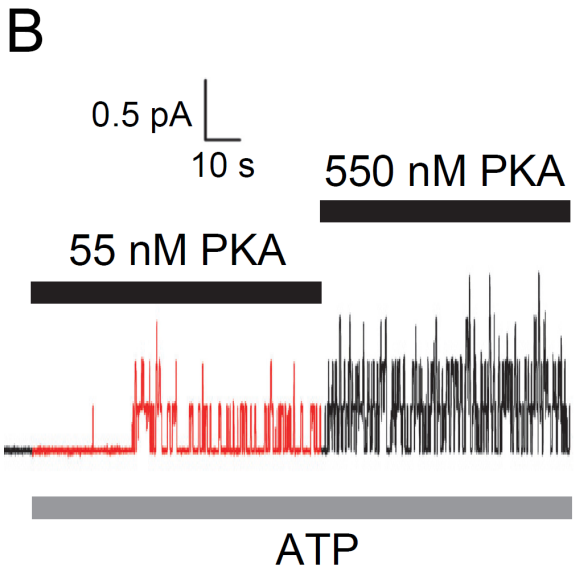
B
0.5 pA
10 s
550 nM PKA
55 nM PKA
ATP

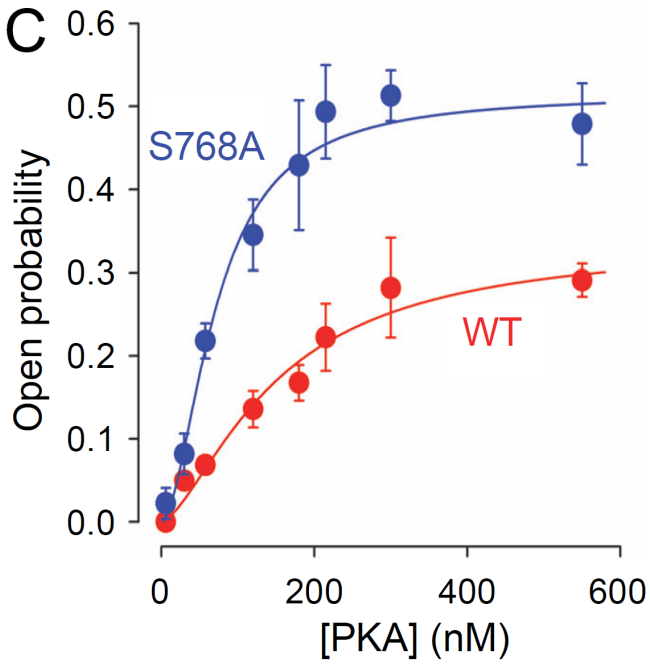
C
Open probability
0.6
0.5
0.4
0.3
0.2
0.1
0.0
S768A
WT
0
200
400
600
[PKA] (nM)

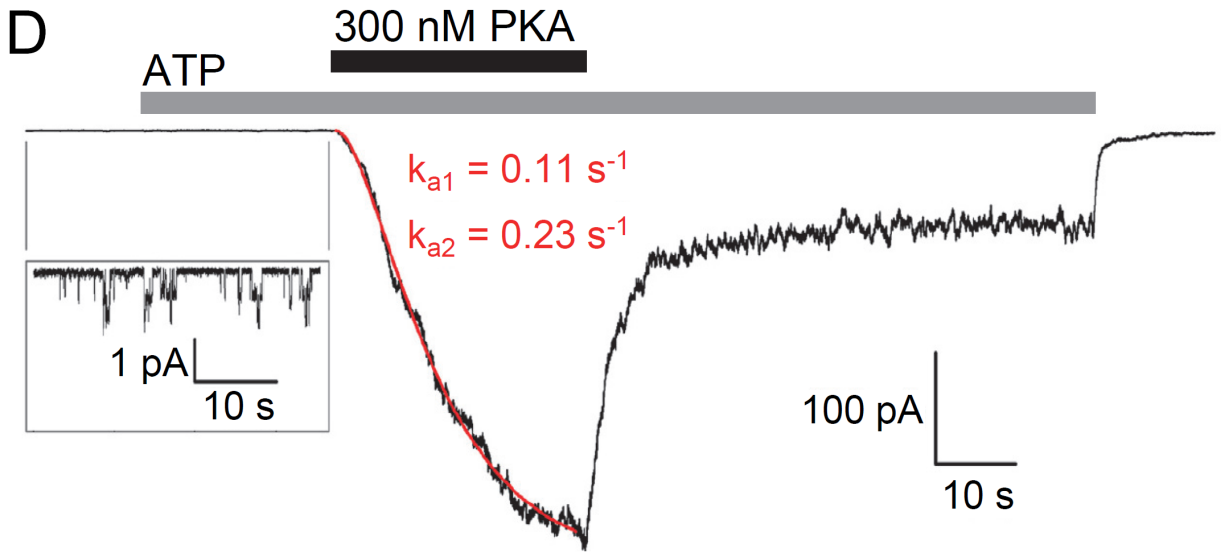
D
300 nM PKA
ATP
k_{a1} = 0.11 s^{-1}
k_{a2} = 0.23 s^{-1}
1 pA
10 s
100 pA
10 s

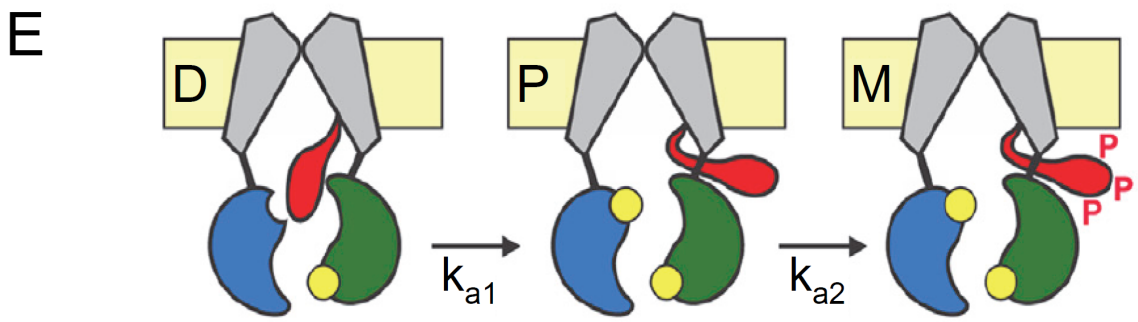
E
D
P
M
P
P
P
k_{a1}
k_{a2}